UNIVERSITY OF MINES AND TECHNOLOGY

TARKWA

FACULTY OF MINERAL RESOURCES TECHNOLOGY

DEPARPMENT OF GEOLOGICAL ENGINEERING

A THESIS REPORT ENTITLED

CORRELATION BETWEEN GEOMECHANICAL AND PETROPHYSICAL
PROPERTIES OF THE SEKONDIAN GROUP

BY

DASMANI ABDULAI

SUBMITTED IN FULFILMENT OF THE REQUIREMENT FOR THE AWARD OF
THE DEGREE OF THE MASTER OF PHILOSOHPY IN GEOLOGICAL
ENGINEERING

THESIS SUPERVISOR

………………………………………….

ASSOC. PROF. MICHAEL AFFAM

TARKWA, GHANA

MAY, 2019.

DECLARATION

I declare that this thesis is my own work. It is being submitted for the degree of master of philosophy in Geological Engineering in the University of Mines and Technology (UMaT), Tarkwa. It has not been submitted for any degree or examination in any other University.

………………………………………..

……… day of ……………………….(year)……….....

ABSTRACT

Instability issues have been a challenge in the Sekondian Group in Sekondi-Takoradi in the Western Region of Ghana, with regards to civil works and underground excarvations over the years. Uniaxial compressive strength, which is essential in stability analysis in engineering projects, requires high quality core samples of appropriate standards for its test, which cannot easily be obtained except at deeper depth strata. However, it could be inferred from physical properties of rocks. This research examined some geomechanical and petrophysical properties of Efia Nkwanta Sandstone, Elmina Sandstone and Takoradi Sandstone by correlation and regression analyses and obtained models for stability inference. The correlation and regression analyses were carried out with *t*- and *F*-tests using Minitab programming language. The analyses were based on results obtained from laboratory investigations of uniaxial compressive strength, porosity and particle density of samples. The laboratory investigations were respectively performed by uniaxial compressive test, saturation test and density test. For correlation, results were interpreted based on correlation coefficients and *p*-values whereas regression analyses were based on *R* squares, *p*-values and residual standard deviations. From the results, it was observed that linear association only exists between UCS and porosity in sandstones with well sorted grains and connected pores. Thus, the compressive strength of the sandstones is highly dependent on the degree of pore connectivity. Hence, the prediction of geomechanical and petrophysical properties of the Sekondian Group is only possible for UCS and porosity in the Efia Nkwanta beds.

DEDICATION

I dedicate this thesis to almighty Allah for providing life, protection, guidance and direction throughout the study period. Allah I am much grateful to your infinite provisions.

To my parents, there is no much words that could describe your indefatigable parental support in this study. I therefore dedicate this thesis to you. Finally, I dedicate this thesis to my lovely grandmother, Hajia Alimah Moligou, for her support in all endeavours.
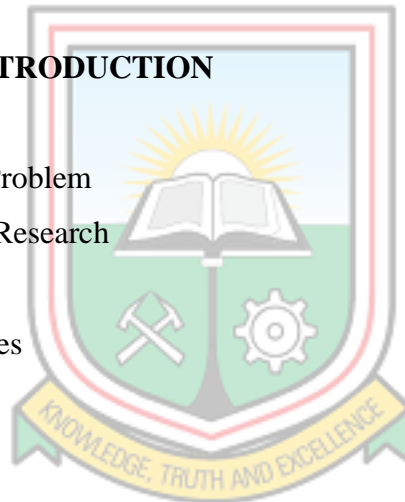
ACKNOWLEDGEMENT

TABLE OF CONTENTS

Contents   **Page**

LIST OF FIGURES

LIST OF TABLES

CHAPTER 1

INTRODUCTION

1.1   Statement of the Problem

Instability issues in civil, reservoirs and underground excavations are challenges to professionals and researchers all over the globe. According to Asef and Farrokhrouz (2010), knowledge of unconfined compressive strength, UCS, is essential in rock mass classification and stability analysis of almost every engineering project. However, according to the standards (e.g. ISRM, 1979; 1999), the test requires high quality core samples of appropriate geometry which cannot easily be extracted from many sedimentary rocks. Unconfined compressive strength therefore has to be estimated from physical properties of rocks for stability analysis. In reservoirs and related industries, instability may occur due to subsidence, hydraulic fracturing and changes in stress conditions. Similarly, intact rock may fail due to changes in in-situ stresses as a result of tectonic activity, changes in pore water pressure and reduction in rock strength (Daneshy, 2017). Ideally, knowledge of geomechanical properties such as the unconfined compressive strength is essential in stability analysis of formation rocks. Al-Maamori *et al.* (2014) therefore indicated that the first step in the design process of underground structures in rocks is to define the strength and deformation parameters of the rock unit. Knowledge and accurate acquisition of geomechanical properties of rocks is therefore essential in geotechnical investigation.

Liang *et al*. (2007) indicated that rocks react with deformation to changes in stress condition, that causes elastic deformation as described by Hook's law, brittle failure of the rock mass, or ductile, time dependent deformation called creep. Sekondi-Takoradi has many stress related projects: in civil and quarry activities that involve rocks as construction or foundation materials; in reservoir production in which large quantities of petroleum fields have been discovered and in environmental mitigation such as underground waste disposal. Geomechanical and petrophysical assessment of rocks in the basin is crucial in mitigating problems associated with these projects in the twin-city and its environs. As geomechanical study is aimed at assessing the mechanical stability of the

rocks, petrophysical study is aimed at assessing the physical properties of the host rocks in relation to fluid flow. According to Azizi and Memariam (2006), stability of civil, mining, underground excavations, environmental and related industries involve laboratory measurement of geomechanical properties of rocks by the use of cores and acoustic wireline log as in the petroleum industry.

However, engineering solutions to civil, mining, and environmental issues relating to underground waste disposal require good analytical and numerical estimates of geomechanical information. Also, reliable estimates of the strength and deformation characteristics of rock masses are required for almost any form of analysis used for the design of slopes, foundations and underground excavations (Hoek and Brown, 1988). Likewise, Aryal (2006) stated that the primary aim of stability analysis is to contribute to the safe and economic design of excavation, embankment and earth dams, which may face great challenge due to unstable ground. Similarly, failure may cost lives and dollars due to collapse of petroleum wells and infrastructures.

Meanwhile, laboratory determination of strength and deformability characteristics of intact rocks is time consuming and costly, and do not give the true representative of rock mass strength. In this regard, the primary motivation of the geomechanical model is to save time, offset risks to human lives and property, and reduce cost. One of the factors that affect rock strength is porosity. According to Chatterjee *et al.* (2013) and Glover (2017), microstructural parameters that affect porosity are grain size, grain packing, particle shape, and the distribution of grain sizes. Likewise, Sun *et al.* (2017) indicated that textural characteristics of rocks are influenced by mineral composition, size, shape, and spatial distribution of mineral grains, porosity, and inherent microcracks. Porosity and grain characteristics are therefore invariably interconnected and considered as petrophysical properties. Hence, there is interplay between geomechanical and petrophysical properties of rocks.

This research examines rock samples of the Sekondian Group in Sekondi-Takoradi in order to assess the relationship that exists between geomechanical and petrophysical properties of the rocks. In this respect, the relationship between these properties would be established for evaluation of unconfined compressive strength of the rocks in order to mitigate the risks associated with civil, environmental, and petroleum reservoirs.

1.2   Objectives of the Research

The aim of the study is to fulfill four (4) main objectives. They include:

i.   Correlation between geomechanical and petrophysical properties of the Sekondian Group.

ii.   Establishing implications of the correlation coefficients in the Group.

iii.   Determination of regression models that exist between geomechanical and petrophysical properties in the Group.

iv.   Establishing implications of the regression models in the Group.

1.3 Scope

The most common and important geomechanical property used for rock mass classification and stability analysis is the unconfined compressive strength (UCS). The UCS was considered and correlated with important petrophysical properties such as porosity and particle density of disaggregated samples from the Efia Nkwanta beds, Elmina sandstone and Takoradi sandstone. The correlation analyses were carried out with *t*-statistic using Minitab 16 statistical programmable package.

Simple and multiple regression analyses were considered and used to model the unconfined compressive strength as response variable as against the predictor variables of porosity and particle density with input parameters also from Efia Nkwanta beds, Elmina sandstone and Takoradi sandstone. The modeling was done with *t*- and *F*-statistics using Minitab 16 statistical computer programmable package.

1.4   Expected Outcomes

At the end of the thesis, it is expected that:

i.   Correlation coefficients between geomechanical and petrophysical properties in the Sekondian Group would be determined.

ii.   The implications of the correlation coefficients between geomechanical and petrophysical properties in the Series would also be established.

iii.   Regression models as well as its implications would also be established.

1.5   Methods Used

The methods used to achieve the objectives of the research are presented in the various Sections below.

1.5.1 Rock Sampling

Fresh rocks were sampled using simple random sampling technique. Simple random sampling was used for sample selection in each lithological unit since each lithological unit was assumed to be homogeneous and fresh samples were required.

1.5.2 Sample Preparations

UCS samples were prepared using the rock cutting machine according to the International Society of Rock Mechanics (ISRM) standard. Thin sections were also prepared for petrographic analysis. Disaggregated samples were however prepared using the laboratory crusher machine and the hammer mill.

1.5.3 Geomechanical Measurements

Rock samples were tested using the UCS servo hydraulic console machine in UMaT geotechnical laboratory, Tarkwa.

1.5.4 Petrophysical Measurements

Porosity and particle density measurements were performed by saturation and density tests respectively according to the British Standard (BS).

1.5.5 Sieve Analysis

Sieve analysis was performed to determine the particle size distribution of the disaggregated samples from the Efia Nkwanta beds, Elmina sandstone and Takoradi sandstone with different sieve sizes according to the BS standard.

1.5.6 Petrographic Analysis

Petrographic analysis was performed using the electron microscope to investigate the mineralogy and grain characteristics of rock samples in the petrology laboratory.

1.5.7 Statistical Analysis

Minitab 16 programmable language was used for statistical analysis of the rock properties.

1.5.8 Test of Models

The models obtained were statistically tested. The correlation coefficients and regression models were tested based on hypotheses with t- and f- statistics.

1.6 Facilities Used

The facilities used to conduct the research were:
   i. GPS and geological hammer;
   ii. UCS machine, rock cutting machine, sieves and density bottles in geotechnical laboratory;
   iii. Rock crushing machine and hammer mill in mineral engineering department, UMaT, Tarkwa;
   iv. Electron microscope and hand lens in petrology laboratory;
   v. Books, research journals, internet in UMaT library, and
   vi. Minitab 16 computer programmable language software, word and excel.

1.7 Organisation of the Thesis

Presentation of this thesis is organized into Chapters and Appendices.

Chapter 1 looks into the general introduction of the thesis where the background was presented that leads to the development of the problem. This Chapter focuses on the importance of the problem to the study area and the international community, its goal and

objectives, to be achieved. Also, the scope, justification, methods and facilities used to achieve the research are presented.

Chapter 2 describes the location and accessibility, relief and drainage, and climate and vegetation of the area which are relevant to the study. Furthermore, the regional geology of southwestern Ghana and the geology of the study area are captured .Moreover, detail geology of the Takoradi sandstone, Efia Nkwanta beds and the Elmina sandstone are also presented in the Chapter.

Chapter 3 details the literature review on geomechanical and petrophysical properties of rocks. The review focuses on the principles of unconfined compressive tests of intact rocks. The principles of porosity and particle size density tests are also highlighted in this Chapter. More so, the theory of statistical correlation and regression are well captured in the Chapter. The Chapter examines into detail the hypotheses tests for the various statistical parameters, correlation coefficients and regression models. Finally, review on correlation and regression analyses of geomechanical and petrophysical properties of rocks are presented.

Chapter 4 details the methods used for data collection, data organization and analysis. Also, the materials used for the data collection are highlighted in the Chapter.

In Chapter 5, results and discussions, and comments from the various methods used are presented. The emphasis is on UCS correlated with porosity and particle density. Simple and multiple regression relations between UCS and porosity and particle density are presented in the Chapter. Also, hypotheses tests of the models are captured in the Chapter. Additionally, discussions with regards to the objectives of the study and the theoretical background in Chapter 2 and Chapter 3 are included in the Chapter.

Finally, the main findings on the statistical analysis from the study are summarized in Chapter 6 including recommendations for further research.

CHAPTER 2

RELEVANT INFORMATION OF THE STUDY AREA

2.1 Introduction of the Study Area

The study with lots of civil works, quarry activities, underground excavations, offshore and onshore development projects was taken from Sekondi-Takoradi, the Western Region of Ghana. The offshore fields and the onshore projects such as the Deep Water Tano (DWT) block, West Cape three points, Takoradi Port, Takoradi railways, Sekondi sports stadium, Justmoh Quarry in Essipon and Aboadze Thermal plant, whose location map are given in Figure 2.1 are now in the developed and developing stage and contribute significantly to the socio-economic development of Ghana.

Three lithological units in the Group in the study area were considered for detailed geomechanical and petrophysical analyses: the Efia Nkwanta beds taken from Essipon (see Figure 2.2), Elmina sandstone from Aboadze (see Figure 2.3) and the Takoradi sandstone from Monkey hill (see Figure 2.4) where many construction works are ongoing and others are in the planning stage. An example is the expansion of the Takoradi port to increase its facilities and durability, construction of the Sekondi sports stadium and the Aboadze thermal plant. Details of the study area geomechanical and petrophysical analyses are presented in Chapter 5.

The geomechanical models obtained from the geomechanical and petrophysical analyses of the study would contribute to the understanding of stability analysis in Sekondi-Takoradi and other areas with similar geological and climatic environment.
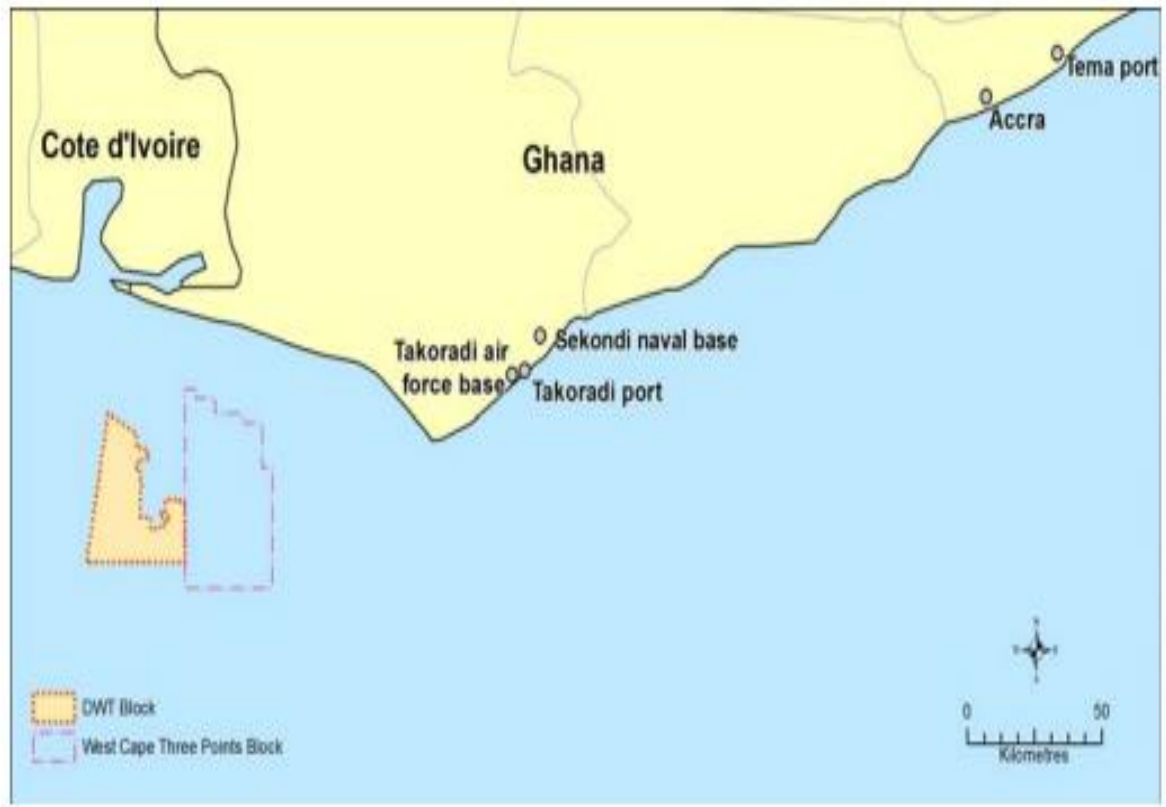
Figure 2.1 Topographic Map Showing Onshore and Offshore Projects in Sekondi-Takoradi (After Camp *et al.*, 2012)

Figure 2.2: Efia Nkwanta Beds in Essipon Showing Dark to Gray Coloration

Figure 2.3: Elmina Sandstone in Aboadze Showing Chocolate to Purple Coloration

Figure 2.4: Takoradi Sandstone in Monkey Hill Showing, Thin Bedding and Micaceous Formation

2.2 Relief and Drainage System

The study area is of varied landscape; the coast line has capes and bays, which have been largely eroded. The central portion of the study area is low lying with an altitude of about 6 meters below sea level. Otherwise, the area is undulating with ridges and hills (Anon, 2010). According to Anon (2010) the surface of the area is fairly watered, with the drainage pattern being largely trellis in nature with minor dendrite forms. The two main rivers flowing through the Metropolis are the Whin and the Kansawora rivers, while the lagoons are the Essei and the Butre that drain into the Atlantic Ocean.

Both surface and sub-surface drainage systems have also been constructed in the area. Surface drainage systems are however abundant in the area than the sub-surface systems. Trees have been planted in certain parts of the area to prevent surface erosion and to maintain the environment.

2.3 Climate and Vegetation

The climate of the Metropolis is equatorial, with an average annual temperature of about 22^0C, experienced between January and March. Rainfall is bi-modal, with the major season occurring between March and July and the minor season occurring between August and November. The mean annual rainfall is about 1,380 mm, covering an average of 122 rainy days (Anon, 2010).

According to Anon (2010), the study area has three main vegetation types, namely, mangrove, savannah woodland and tropical forest. The tropical forest is predominately found around the northern parts of the area and stretches to the east covering a large part. Savannah woodland is dotted around the middle belt and Mangrove vegetation is found along the southern portion of the area.

2.4 Regional Geology

According to Kesse (1985) the Sekondian Group is composed mainly of shales and sandstones with conglomerates, pebble beds and mudstones resting unconformably on a

complex of granites (Figure 2.5). Yendaw (2012) indicated that the sedimentary basin granitoids (see Figure 2.5) called the Cape Coast type are well foliated, often migmatic, potash rich granitoids which take the form of muscovite-biotite granite, granodiorite, porphyroblastic biotite gneiss, aplites and pegmatites. The granites are characterized by the presence of many enclaves of schists and gneisses. Yendaw (2012) likewise characterized the volcanic-belt granitoids that is the Dixcove type as consisting of hornblende granite or granodiorite grading locally into quartz diorite and hornblende diorite. This complex forms non-foliated discordant and semi-discordant bodies in the enclosing country rocks. Atubrah (2013) also indicated that the Dixcove Granite is found along the coast whilst the Cape Coast granite is found further inland.

Along the coast in Ghana also, are Phanerozoic sediments in numerous offshore basins which include: Keta basin, Accraian series, Amissian formation, Sekondian series and Tano basin (Kesse, 1985).

According to Kesse (1985), the Keta basin lies at the extreme southeastern corner of Ghana adjoining Togo comprising mainly of sands, gravels, siltstones, shales, and clays with layers of fossiliferous limestone. Also, the Accraian series covers an area in the vicinity of Accra and unconformably overlies the Dahomeyan basement complex consisting of quartz-grits, gentle folded sandstone, shale and mudstones. Kesse (1985) also stated that, the Amisian formation outcrops at a number of places along the coast near the mouth of the Amisa river consisting of interbedded, soft pebbly grits, conglomerates, micaceous sandstones, arkose and greenish grey clay.

Kesse (1985) further indicated that, the Sekondian Series occur as several disconnected outcrops along the coast between Cape Coast and the mouth of the Butre river near Dixcove consisting of sandstones, shale with conglomerates, pebble beds, grits and mudstones resting with a major unconformity on a complex of granites, gneisses and schists. Meanwhile, the Tano basin which is Cretaceous-Eocene marine sedimentary rocks covers between the mouths of the Ankobra river in the east and the Tano river in the west consisting of alternating sands, clays and limestones.

2.5 Geologic Setting and Description of the Study Area

The Study area geology, Sekondian Group, forms part of the coastal sedimentary basins in southwestern Ghana (see Figure 2.5 and Figure 2.6). According to Asiedu *et al*. (2010), sediments in the Sekondian Group were deposited in non-marine to coastal marine environments, and ranges in age from the Late Ordovician to Early Cretaceous that crop out along the western and central coast of Ghana (see Figure 2.5 and Figure 2.6). Likewise, Kesse (1985) indicated that the Series consist of sandstones and shales with conglomerates, pebble beds, grits and mudstones resting with major unconformity on a complex of granites, gneisses and schists that occur as several disconnected outcrops along the coast between Cape Coast and the mouth of Butre river near Dixcove. It extends inland for a distance, varying from 3 to 6 km and covering a total area of 200 km^2 having a total thickness of about 1245 to 1325 m (Kesse, 1985). Asiedu *et al*. (2010) also indicated that the Series is about 1.2 km-thick sandstone and shale dominated succession, but also includes coarse breccias and conglomerates which are extensively faulted and virtually unmetamorphosed.
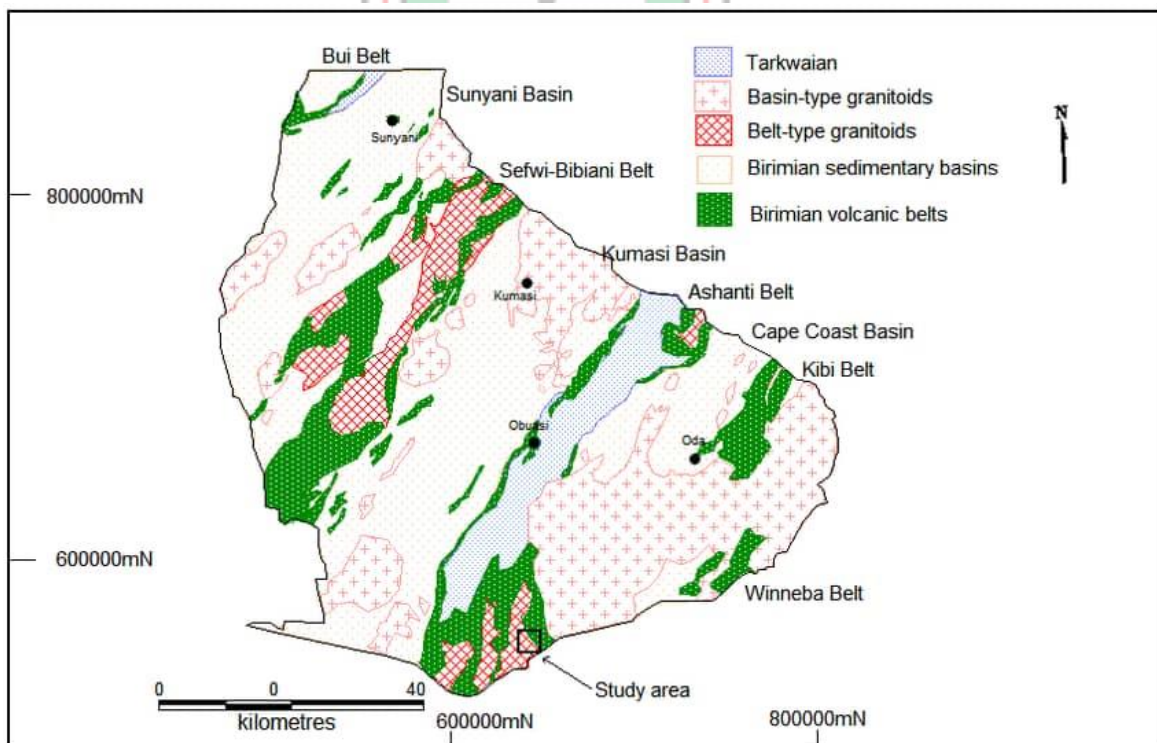
Figure 2.5: Geologic Map of Southern Ghana (Anon, 2017)
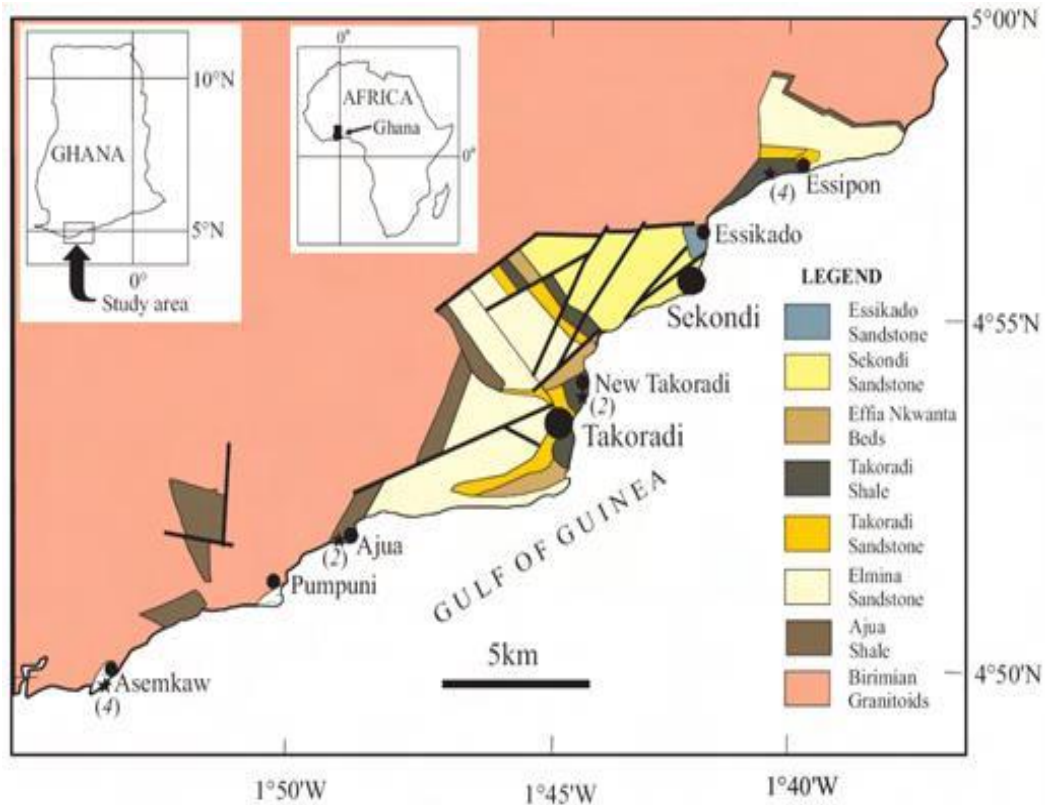
Figure 2.6: Geologic Map of the Sekondian Group Showing Various Stratigraphic Units (After Asiedu *et al*., 2010).

According to Kesse (1985), previous studies subdivided the Group lithologically as:

  i.   Upper pebbly argillaceous sandstones
  ii.   Alternating sandstone and shale with bands of chalcedony
  iii.   Carbonaceous shale
  iv.   Highly friable sandstone
  v.   Chocolate-coloured arkose.

The Group stratigraphically consists of six (6) recognized units as shown in Figure 2.6 above (Kesse, 1985) which also contains the lithological units that were sampled for this study (that is Elmina sandstone, Efia Nkwanta beds and Takoradi sandstone). These lithological units according to Kesse (1985) are symbolized S_1-S_6 based on the occurrence of the Series from Sekondi-Takoradi as indicated below.

Sekondi sandstone (S$_6$): This consists of upper-pebbly argillaceous and feldspathic sandstones and conglemerates, and lower-massive quartzose sandstones and grits with subordinate shales and mudstones having a thickness of about 304,8 m.

Efia Nkwanta beds (S$_5$): These consists of upper-thin bedded siltstone, shale, shaly sandstone, and some coarse sandstone, with nodules, bands and lenses of chert having a thickness of about 26 m; middle friable sandstone, well bedded and massive, with interbedded mudstone and shale having a thickness of about 96 m and a lower-cross bedded, soft, fine-grained, pale purple, pink, grey, green and cream sandstone having a thickness of about 91 m.

Takoradi shales (S$_4$): This formation consists of black and grey carbonaceous shales, sandy shales, and shaly sandstone, with ineterbedded grit and fine-grained sandstone with nodules of siderite and pyrite having a thickness of about 198 m.

Takoradi sandstone (S$_3$): Consists of massive and bedded friable ferruginous sandstone with coarse-grained beds, breccia-conglomerate, and inter-bedded shales having a thickness of about 152 m and a thin-bedded, brittle, micaceous sandstone with sandy shale and some clay shale having a thickness of about 30 m.

Elmina sandstone (S$_2$): This consists of chocolate and purple feldspathic, micaceous sandstone, with coarse sandstone, conglomerate, shale and mudstone near its base having a thickness of about 304-366 m.

Ajua shales (S$_1$): Consist of varved shales, sandy shales, and sandstone containing scattered boulders and pebbles with a coarse boulder bed at the base. Its thickness is about 43-60 m.

According to Asiedu *et al.* (2005), provenance studies suggested that the sedimentary rocks of the Sekondian Group were largely derived from the Birimian granitoids whose environment of deposition is non-marine to coastal marine. The detailed geology of the sampled area of the Sekondian Series is presented in the various Sections below.

2.5.1 Takoradi Sandstone

The Takoradi sandstone forms part of the Sekondian Group which is believed to be formed during the Devonian period (Asiedu *et al*., 2005). It forms contact with the underlying Elmina sandstone at Tanokrom and outcrops at Monkey hill (Atubrah, 2013).

Kesse (1985) generally characterised of the Takoradi sandstone as fresh and massive, micaceous, cream coloured, dark and rusty brown dominated by well sorted angular quartz grain minerals with perfect subaqueous cross-bedding (see Figure 2.7). Its base is however described as fossiliferous yielding poorly preserved brachiopods, lamellibranchs and fish remains. Generally, the Takoradi sandstone is composed primarily of angular well sorted quartz grains with total thickness of about 183 m.
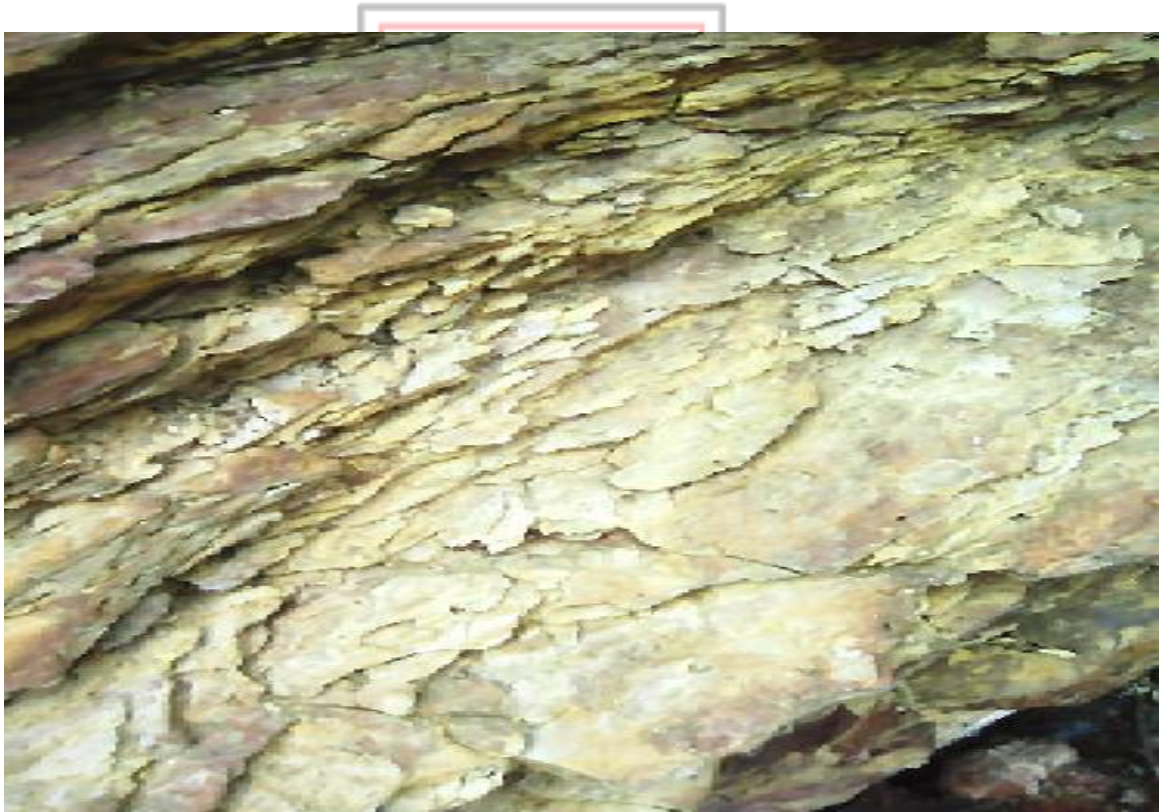
Figure 2.7: Takoradi Sandstone in Monkey Hill Showing Cream to Rusty Coloration

2.5.2 Efia Nkwanta Beds

According to Kesse (1985), the upper portion of the Beds consists of thin bedded siltstone, shale, shaly sandstone, and some coarse sandstone, with nodules, bands and lenses of chert

15

having a thickness of about 26 m. The middle portion consists of friable sandstone, well bedded and massive, with interbedded mudstone and shale having a thickness of about 96 m. Kesse (1985) further characterized the lower-portion of the Efia Nkwanta beds as consisting of cross bedded, soft, fine-grained, pale purple, pink, grey, green and cream sandstone having a thickness of about 91 m as shown in Figure 2.8.
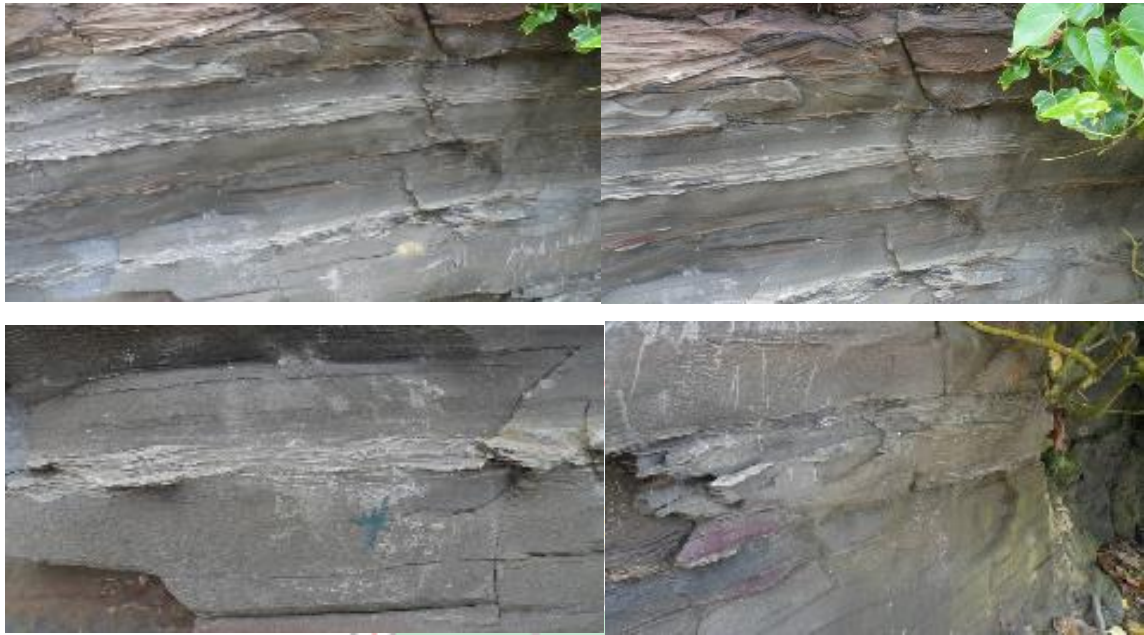
Figure 2.8: Fresh Efia Nkwanta Beds in Essipon Beach Showing Dark Gray Coloration
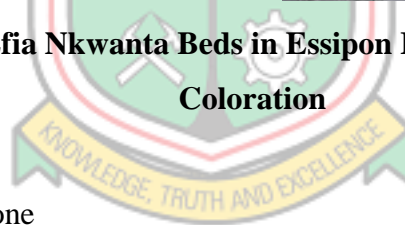
2.5.3 The Elmina Sandstone

According to Kesse (1985), the Elmina sandstone is a uniform, hard, massive, medium-grained sandstone with characteristic chocolate or chocolate-purple colour due to the pink feldspars and the dark brown limonitic cement as shown in Figure 2.9, which is believed to be formed around the Late Ordovician-Early Silurian. It is poorly bedded, well jointed and strongly cross-bedded. It becomes coarse-grained towards the base of the formation while it is thin-bedded and shaly at its top. Likewise, Asiedu *et al*. (2013) indicated that the Elmina sandstone also contains biotite and quartz and described it as being arkosic, micaceous, poorly bedded, well jointed, uniformly hard, massive and medium grained (seen Figure 2.9).

Figure 2.9: Fresh Elmina Sandstone in Aboadze Showing Chocolate-Purple Coloration
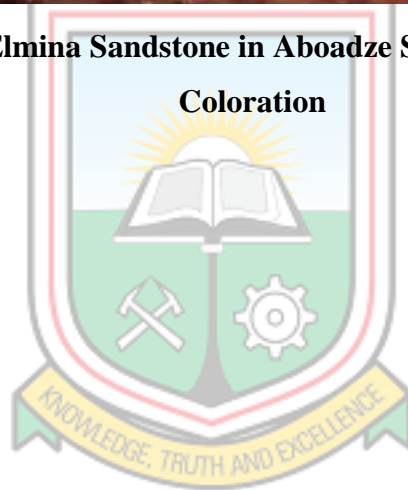
CHAPTER 3

REVIEW OF LITERATURE

3.1 Geomechanical Properties of Rocks

Geomechanics study deformation of earth materials in response to changes in stress, pressure, temperature and other environmental parameters (Cook, 2015). According to Cook *et al*. (2007) and Liang *et al*. (2007), stress plays a major role in rock deformation. Rock deformation takes various forms depending on the stress condition and the rock type that could result in elastic or permanent deformation.

Benz and Schwab (2008) indicated that critical stress is a representative of the rock strength. Various types of rock strength are obtained depending on the mode of the acting stresses on the rock. In this regard, compressive strength, tensile strength and shear strength are obtained as rock strength. With regards to the factors affecting the strength of rock masses, Hoek (1966) stated that rock anisotropy, influence of fluid pressure, and the influence of environment (temperature and moisture), time (weathering and time dependent mechanical behavior) and specimen size affect rock strength. Likewise, Parterson (1978) listed rock type and composition, grain size, weathering, density and porosity, rate of loading, confining stresses, geometry, size and shape of test specimen, rock anisotropy, pore water pressure and saturation, testing apparatus (end effects, stiffness), temperature and time as factors affecting rock strength. Bell *et al*. (1999) however summarized mineral composition and constitution thus its structural and textural features affecting rock strength.

According to Romana and Vásárhely (2007), porosity affects rock strength in which compressive failure is caused by the growth of cracks from the border of existing micro pores which coalesce and results in failure. Vásárhely and Bobet (2000) earlier indicated that maximum tangential stress, maximum energy release rate and minimum energy density are phenomena for crack initiation which could be used to predict tensile crack initiation, both in tension and/or compression, but not in shear. Also, as stated by Romana and Vásárhely (2007) the energy terms associated with crack initiation are change in

potential energy due to the applied forces, change in strain energy due to the existence of the crack and change in surface energy. There is a decrease in surface energy of the crack borders when the pore is full of water which facilitates micro-cracks propagation by decreasing the elastic limit and the peak strength of the rock (Vásárhely and Ledniczky, 1999).

In terms of rock availability and importance, Rutter *et al.* (2017) suggested that sedimentary rocks are common and serve as the source rock for oil and gas, and are frequently encountered in excavations and foundations. Therefore, there is an increased interest in the understanding of its geomechanical and petrophysical properties. Rutter *et al.* (2017) further indicated that geomechanical and microstructural studies on shales are demanding owing to their fine grain size, complex mineral assemblage, microstructure, friability, foliation, sensitivity to wetting and desiccation. In addition to their review, mineralogical characteristics, cohesion, plasticity, ductility, brittleness and elasticity are likely to exert great influence on the geomechanical and petrophysical properties of shales.

Considering the role of clay minerals, Wilson *et al.* (2017) indicated that the presence of certain clay minerals in shale could be a primary cause of mechanical instability. In relation to the mechanical behavior of clay and organic carbon-rich shales, over a range of confining pressures and temperatures, Rybacki *et al.* (2015) stated that increasing confining pressure around high porosity and higher clay content rocks favoured ductile deformation and a lower strength. Rybacki *et al.* (2016) moreover indicated that brittle rocks are strong, stiff and creep-resistant. Sandstones house oil and gas, and frequently used for civil works and encountered during excavations and foundations also have complex mechanical behavior. Its geomechanical and petrophysical properties equally need to be understood.

3.1.1 Unconfined Compression Strength (UCS)

The strength of a material is its ability to resist imposed forces and is measured as the maximum stress the material could sustain under specified loading and boundary conditions. According to Esmailzadeh *et al.* (2017), unconfined compressive strength is the most common strength parameter measured for engineering designs and decreases with

increasing water content (Romana and Vásárhelyi, 2007). Unconfined compressive strength is however determined in the laboratory by standards. Anon (1979, 1999) suggested that a right cylindrical core sample of height to diameter ratio of 2.5-3.0, a diameter preferably not less than 54 mm and at least 10 times the size of the largest grain in the rock should be used for compression testing. Anon (1985) rather specified the height to diameter ratio of 2.0-2.5 as standard for compression tests. Additionally, Anon (1979) recommends that the ends of the specimen should be flat to within 0.02 mm and should not depart from perpendicularity to the axis of the specimen by more than 0.001 rad or 0.05 mm in 50 mm sample and be tested in the natural water content condition as far as possible at a constant stress rate of 0.5 -1.0 MPas^{-1}. Adherence to these geometric standards for cores from sedimentary strata is difficult.

Additionally, whilst Anon (1979, 1999) suggested a conversion of the axial load to axial stress and plotting against axial and radial strains, Brady and Brown (2005) suggest that where post-peak deformations are recorded, the cross sectional area may change considerably as the specimen progressively breaks up; hence it is preferably to present the experimental data as force-displacement curves. Also, Brady and Brown (2005) described the stress-strain or load-deformation curve in unconfined compression test responses as exhibiting four stages. These are initial bedding down and crack closure stage followed by a stage of elastic deformation until an axial stress of crack initiation threshold is reached at which stable crack propagation is initiated. This continues until the axial stress reaches crack damage threshold when unstable crack growth and irrecoverable deformations begin and continues until the peak or unconfined compressive strength is reached. Accurate data in UCS test is therefore difficult to be obtained.

According to Hawkes and Mellor (1970), Vutukuri *et al*. (1974) and Paterson (1978), varying the conditions of the unconfined compression test will influence the observed response of the specimen. In this light, Brady and Brown (2005) suggested that the test arrangement should subject the specimen to uniform uniaxial stress and displacement to minimize end effect. With regards to this effect, Hawkes and Mellor (1970), Jaeger and Cook (1979) and Anon (1979) earlier suggested that the sample should be machined instead of treating its ends to avoid end effect. Hawkes and Mellor (1970) also are of the view, in their earlier work, that accurate flatness and parallelism should be maintained for minimization of 'bedding-down' effect. Brady and Brown (2005) also mentioned the

effect of specimen size. Hoek (1966) attributed the size effect to discontinuity spacing in the specimen, but Griffith (1921) however identified surface energy which is a material property as the controlling factor for the size effect. During unconfined compression test, Anon (1979) also recommended a loading rate of 0.5-1.0 MPas[-1]. Finally, according to Wawersik and Fairhurst (1970), loading and unloading cycles affect UCS. Anon (1979) recommends for a few loading and unloading cycles to be performed for rock specimens in UCS test. The standard conditions in UCS tests are therefore tedious to achieve.

With regards to environmental conditions affecting UCS, Romana and Vásárhelyi (2007) identified the decreasing effect of humidity on UCS. Likewise, Hsu and Nelson (1993); Lashkaripour and Passaris (1993) demonstrated the decreasing effect of water content on UCS. Vutukuri (1974) and Ballivy and Colin (1999) also showed the effect of changing the fluid saturating the rock on UCS due to changes in the dielectric constant of the fluid. Fluids with higher dielectric constant such as water decrease elastic limits of rocks whilst those with smaller dielectric constant increase the elastic limits of rocks. These environmental conditions therefore affect UCS.

In order to overcome some of the problems associating UCS test, Broch and Franklin (1972) proposed an indirect testing method called the point load test.

Point load testing consists of squeezing pieces of rock diametrally between two hardened steel cones having a length of at least 1.4 times its diameter (Anon, 1985). The rock sample develops tensile cracks parallel to the loading direction. Anon (1985) further specified that in point load tests, rock specimens in the form of a core (diametral and axial tests), cut blocks (block test) and irregular lumps (irregular lump test) are broken by a concentrated load applied through a pair of spherically truncated, conical platens. Anon (1985) further indicated that in diametral test, the load should be applied at least half the diameter from the ends of the platens. From the measured value of the force, P, at which the test specimen breaks, an uncorrected point load index, I_s, is calculated based on the Equation 3.1 below.

$$I_s = \frac{P}{D_e{}^2}$$ (3.1)

where D_e is the equivalent core diameter, defined as the core diameter D, for diametral tests, and as $4A/\pi$ for axial, block and lump tests. A is the minimum cross sectional area of a plane through the specimen and the platen contact points.

Brady and Brown (2005) also indicated that the index, I_s, varies with D_e and so size correction must be applied in order to obtain a unique point load strength Index for a particular rock sample for use for strength classification, preferably 50-55 mm diameter specimens for diametral tests. Likewise, Bieniawski (1974) earlier suggested that core samples with different diameters such as *BX* (42 mm) or *EX* (21.5 mm) have size effect correction. The size-corrected point load strength index, $I_{s(50)}$, is defined as the value of I_s that would have been measured in a diametral test with diameter 50 mm (Anon, 1985). Bieniawski (1974) rather used *NX* core (55 mm in diameter) for size correction in diametral test. Broch and Franklin (1972) showed that the value of I_s determined in a test of equivalent diameter D_e may be converted to $I_{s(50)}$ value by the relation given in the Equation 3.2.

$$I_{s(50)} = I_s \times \left(\frac{D_e}{50}\right)^{0.45} \tag{3.2}$$

Also, Broch and Franklin (1972) and other later researchers developed the correlation of the point load Index with the uniaxial compressive strength, UCS, as presented in the Equation 3.3.

$$UCS \approx (22 - 24)I_{s(50)} \tag{3.3}$$

Bieniawski (1974) later gave an empirical relation between the point load index and the unconfined compressive strength as given in Equation 3.4.

$$UCS = (24)I_s \tag{3.4}$$

Brady and Brown (2005) concluded that in the point load test, fracture is caused by induced tension, and it is essential that a consistent mode of failure should be produced for results of different specimens. However, very soft rocks and highly anisotropic rocks or rocks containing marked planes of weakness such as bedding planes are likely to give spurious results. Also, according to them, for anisotropic rocks, it is usual to determine a strength anisotropy index, $I_{a(50)}$, defined as the ratio of mean $I_{s(50)}$ values measured perpendicular and parallel to the planes of weakness.

In comparison, the direct method for UCS measurement is time-consuming and expensive that requires significant specimen preparation and the results may not be available for a long time after the samples are collected. Anon (2007) therefore suggested that when extensive testing and/or timely information is required for preliminary and reconnaissance information, the point load test could be used to reduce the time and cost of compressive strength tests, when used in the field. Such data could be used to make timely and more informed decisions during the exploration phases. Furthermore efficient and cost effective selection of samples for more precise and expensive laboratory tests could be done. Also, according to Anon (2007), the point load strength test is used as an index test for strength classification of rock materials, so the test results should not be used for design or analytical purposes.

According to Bieniawski (1974), with the point load test, a portable machine is used and smaller forces are needed. In his view, specimens in the form of cores are used and require no machining. Also more tests could be made with the same cost and fragile or broken specimens could be tested; results show less scatter than the direct method and measurement of strength anisotropy could be simplified. However, with the direct method, the testing procedure is better known and evaluated; results are available for a wide variety of rock types, together with experience on the linking of these results to field performance (Bieniawski, 1974). With these comparisons, the point load test is therefore recommended as a simple and convenient method for determining the unconfined compressive strength of rocks for practical engineering purposes limited to exploration purposes but for design and analytical purposes, the direct method is highly recommended which also have a lot of pitfalls mentioned above.

3.2 Petrophysical Properties of Rocks

A petrophysical property of rock is the rock capability to accumulate and transport reservoir fluid. These properties are porosity, permeability, capillarity, and fluid saturation in which pore-size distribution is the common link between them (Lucia, 2000, 2007). These are physical properties of rocks in relation to fluid flow in which porosity is the most common.

Porosity is a measure of the potential storage volume for fluids and is defined as pore volume divided by bulk volume. In examining the factors affecting porosity, Chatterjee *et al*. (2013) indicated that major microstructural parameters affect porosity at the pre-diagenesis stage which Al-Homadhi and Hamada (2001) earlier associated with depositional conditions. These parameters are grain size, grain packing, particle shape, and distribution of grain sizes. Al-Homadhi and Hamada (2001) also indicated that porosity depends essentially on rock texture, which is the geometric aspect of rock constituents such as grains and pore patterns. The grain characteristics that affect porosity are: size, sorting, shape, appearance and diagenetic changes, and the pore pattern features are pore size, shape, nature and distribution of pores.
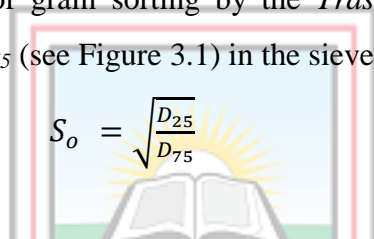
However, according to Glover (2017) pre-diagenesis porosity is rarely found in real rocks, as these have subsequently been affected by secondary controls. Porosity controlled by secondary processes usually result in compaction and dilatation. Glover (2017) categorized the secondary processes as mechanical processes, such as stress compaction, plastic deformation, brittle deformation and fracture evolution and geochemical processes, such as dissolution and precipitation. Rashid *et al*. (2015, 2017) however specified dissolution and cementation as major diagenetic processes affecting porosity especially carbonate rocks.

Rutter *et al.* (2017) further indicated that fine-scale layering of mineral components arising from sedimentation and compaction could results in microstructural anisotropy in sedimentary rocks. Schieber *et al.* (2013) earlier indicated that flocculation of clay minerals could lead to primary depositional porosities greater than that expected of equigranular particles of quartz, feldspar and carbonate minerals. Dewhurst *et al.* (1999), and Yang and Aplin (2007) in their view stated that mechanical compaction and collapsing of platy minerals towards a common bedding could rapidly reduce porosity.

With regards to the methods of determining porosity, Rutter *et al.* (2017) indicated that porosity determination may not be straightforward. Busch *et al.* (2017) therefore suggested multiple means of determining porosity. Different methods may result in different apparent porosities as suggested by Rutter *et al.* (2017) and prefers the gas adsorption method which allows access to pore sizes smaller than 10 nm. Seemann *et al.* (2017) used water vapor in the gas adsorption in their work due to its advantages. Glover (2017) in his

work suggested the saturation method, direct method, Boyle's law and mercury injection methods for determining porosity and particle density of rocks. These methods however measure the connected porosity of rocks except the direct method. The direct method however imposes measurement errors due to instrument and human.

With regards to grain size distribution in rocks, Glover (2017) stated that grain size distribution could be inferred from mercury porisimetry measurements or by direct sieving of disaggregated samples. The grain size distribution determines the particle density of the rock which is a function of the modal composition of the rock. According to researchers, increasing grain sorting in rocks increases its particle density. The particle density which is linked with the sorting of the grains could be quantitatively determined by specific gravity method. Meanwhile, according to Glover (2017), a sieve curve could give an indication of the degree of grain sorting by the *Trask coefficient,* S_o , which could be evaluated using D_{25} and D_{75} (see Figure 3.1) in the sieve curve using Equation 3.5.

$$S_o = \sqrt{\frac{D_{25}}{D_{75}}} \tag{3.5}$$
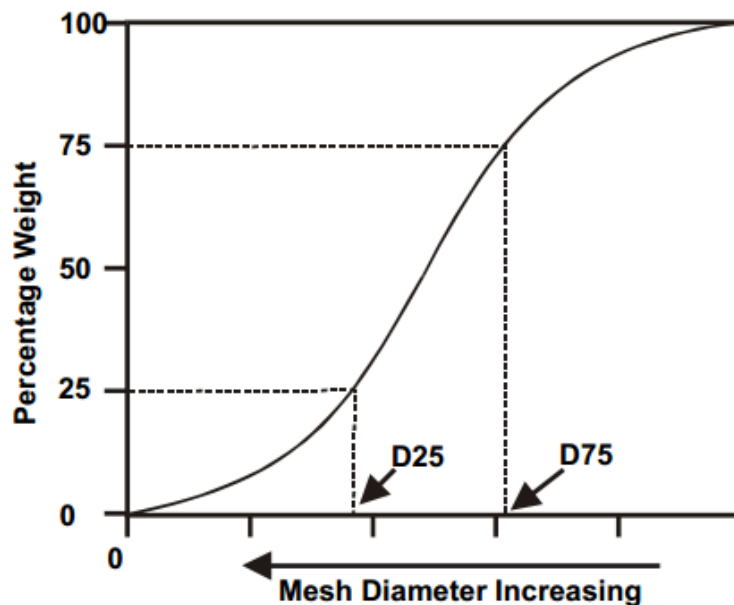
Figure 3.1: Cumulative Grain Size Distribution by Sieved Weight (After Glover, 2017)

The degree of grain sorting according to Glover (2017) could be classified based on the *Trask coefficient* as indicated in Table 3.1 which is essential in rock classification. Other researchers however estimate porosity from correlation analysis of geomechanical properties.

Table 3.1: The Trask Sorting Classification (After Glover, 2017)

Sorting Classification	Trask Coefficient
	1.00
Extremely well	
	1.10
Very well	
	1.20
Well	
	1.40
Moderately	
	2.00
Poorly	
	2.70
Very poorly	
	5.70

3.3 Correlation Analysis

A quantitative measure of the relationship between variables is called the sample correlation coefficient (Ross, 2009). According to Ross (2009) if s_x and s_y denote, respectively, the sample standard deviations of the x values and the y values, the sample correlation coefficient r of the data pairs (x_i, y_i), $i = 1, \ldots\ldots, n$ is defined in Equation 3.6 below.

$$r = \frac{\sum (x_i - \overline{x})(y_i - \overline{y})}{(n-1)s_x s_y} \tag{3.6}$$

Likewise, Walpole *et al.* (2012) indicated that the sample correlation coefficient, r, or Pearson product-moment correlation coefficient is an estimator of the population correlation coefficient, ρ, and also defined it as in Equation 3.7 below.

$$r = \frac{S_{xy}}{\sqrt{S_{xx} S_{yy}}} \tag{3.7}$$

$$S_{xx} = \sum_{i=1}^{n}(x_i - \bar{x})^2 \ , \ S_{yy} = \sum_{i=1}^{n}(y_i - \bar{y})^2 \ \text{and} \ Sxy = (x_i - \bar{x})(y_i - \bar{y}) \ .$$

When $r > 0$, the sample data pairs are positively correlated, and when $r < 0$ the sample data pairs are negatively correlated. Also, the population correlation coefficient which is estimated by the sample correlation coefficient should be tested.

To test the null hypothesis $H_o : \rho = 0$

that is there is no correlation between the response and the input variable in the population as against the alternative,

$$H_1 : \rho \neq 0 \ ,$$

Ross (2009) and Walpole *et al.* (2012) indicated that

$$\text{Reject } H_o : \rho = 0 \text{ if } t = \frac{r\sqrt{n-2}}{\sqrt{1-r^2}} > t_{\alpha/2, n-2} \tag{3.8}$$

Accept $H_1 : \rho \neq 0$ otherwise. The *p*-value is $2P(T_{n-2} \geq v)$

Ross (2009) and Walpole *et al.* (2012) however preferably use r^2 rather than r in order to avoid the ambiguities of the interpretations of r. r^2 which is referred to as the sample coefficient of determination and represents the proportion of the variation of s_{yy} explained by the regression of Y on x, namely SSR. That is, r^2 expresses the proportion of the total variation in the values of the variable Y that could be accounted for or explained by a linear relationship with the values of the random variable X.

However, the coefficient of determination has a number of drawbacks. The most important being that, due to the way it is defined, the larger the independent variables the larger the coefficient of determination whether the extra variables provide any important information about the response variable or not (Larsen, 2008). On this note, Larsen (2008) prefers the adjusted coefficient of determination since it does not include outliers and its value does not dependent on the number of independent variables. Briševac *et al.* (2016) clearly indicated in their review that the coefficient of correlation and determination could be misleading as more rigorous estimation methods such as the adjusted R square, root mean square error (RMSE), Akaike information criterion, or cross-validation, would give better results.

Many researchers examples Chatterjee and Mukhopadhyay (2002), Azizi and Memarian (2006) and Chatterjee *et al*. (2013) correlated geomechanical and petrophysical properties based on coefficient of determination. With regards to the nature of rocks as dry or saturated, Rajabzadeh *et al*. (2012) obtained a strong correlation between dry UCS and porosity but weak correlation between saturated UCS and porosity for carbonate rocks. Likewise, Hsu and Nelson (1993); Lashkaripour and Passaris (1993) obtained negative correlation between UCS and water content for shales.

3.4   Regression Analysis

Many engineering problems are concerned with determining a relationship between a set of variables (Ross, 2009; Walpole *et al.,* 2012). Knowledge of such a relationship would enable the researcher or professional to predict the output for various values of inputs. According to Ross (2009) and Walpole *et al.* (2012), many situations require a single response variable, also called the dependent variable, which depends on the value of a set of input, also called independent variables. Many of these relations are discussed in the various regression models in the various Sections below.

3.4.1 Linear Regression Model

Consider a dependent variable, Y, and a set of input variables, $x_i,...x_r$, for some constants, $\beta_o, \beta_1,...\beta_r$, the simplest linear relationship that would exist between the dependent variable and the independent variable is given in Equation 3.9 below.

$$Y = \beta_o + \beta_1 x_1 + ... + \beta_r x_r + e \qquad (3.9)$$

where *e* is a random error with mean of zero (Ross (2009) and Walpole *et al.* (2012)). The quantities, $\beta_o, \beta_1,...\beta_r$, are the regression coefficients which are estimated from a set of data. A regression equation containing a single independent variable that is $r = 1$ is called a simple linear regression model as shown in Figure 3.2 which could be expressed as in Equation 3.10.

$$Y = \alpha + \beta x + e \qquad (3.10)$$
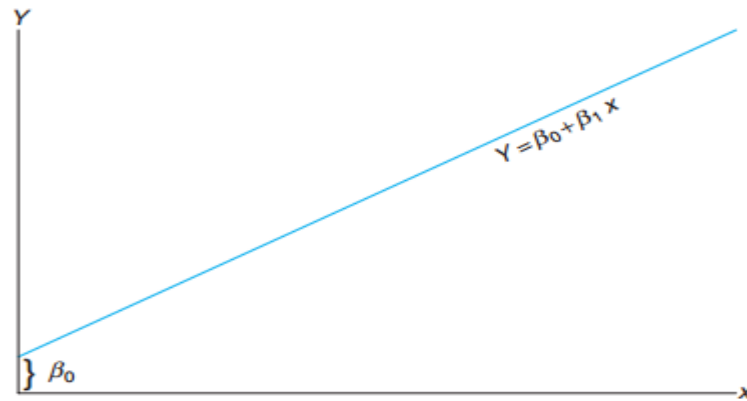
Figure 3.2: A Linear Model Showing Intercept β_o and Slope β_1 (After Walpole *et al.*, 2012)

The regression coefficients are estimated by the least square method. According to Ross (2009) the least square method minimizes the random error, e, as shown in Figure 3.3. Likewise, Walpole *et al.* (2012) indicated that the least square procedure produces a line that minimizes the sum of squares of vertical deviations from the points to the line (see Figure 3.3). The least square criterion is designed to provide a fitted line that result in "closeness" between the line and the plotted points.
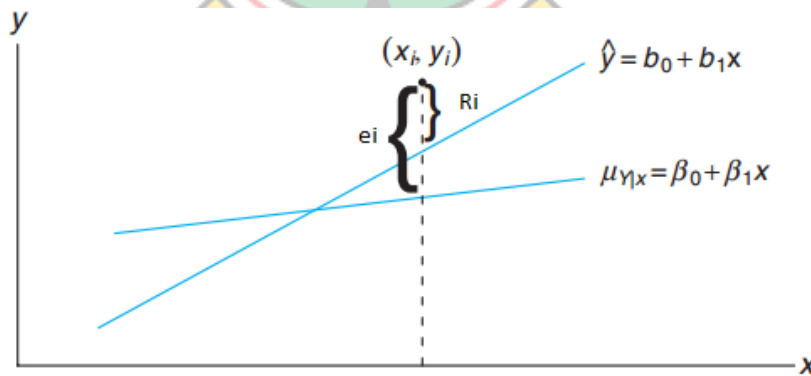
Figure 3.3: Ideal Model and Fitted Model Showing the Random Error e_i with the Residual R_i (after Walpole *et al.*, 2012)

3.4.2 Polynomial Regression Model

According to Ross (2009) and Walpole *et al.* (2012), when the functional relationship between the response, Y, and the independent variable, x, could not be adequately

29

approximated by a linear relationship, it is possible to obtain a reasonable fit by considering a polynomial relationship. That is, the data set is fit to a functional relationship of the form given in Equation 3.11 below.

$$Y = \beta_o + \beta_1 x + \beta_2 x^2 + ... + \beta_r x^r + e \qquad (3.11)$$

$\beta_o, \beta_1, ... \beta_r$ are regression coefficients to be estimated from data sets and e is a random error. According to Ross (2009), in fitting a polynomial to a set of data pairs, the degree of the polynomial should be determined by a study of the scatter diagram. The lowest possible degree that appears to adequately describe the data should be used.

3.4.3 Multiple Linear Regression Model

A regression Equation containing more than one independent variable is a multiple regression Equation. According to Ross (2009) and Walpole *et al.* (2012), a multiple regression model is of the form given in Equation 3.12 below.

$$Y = \beta_o + \beta_1 x_{1i} + \beta_2 x_{2i} + ... + \beta_r x_{ri} + e \qquad (3.12)$$

Where $x_{1i}, x_{2i}, ... x_{ri}$ are the independent variables.

3.4.4 Transformed Models

A transformed model is used when it is apparent that a transformation will provide an improvement in the model. According to Walpole *et al.* (2012), the measures of comparison are r^2 and the residual mean square, s^2. The models form before and after the transformation of the data should be written in the transformed model.

The Exponential Model

Walpole *et al.* (2012) represents the exponential model in its natural untransformed form given in Equation 3.13 while the transformed one in Equation 3.14 below.

$$y_i = \beta_o e^{\beta_1 x_i} .e \qquad (3.13)$$

$$\ln y_i = \ln \beta_o + \beta_1 x_i + \ln e \qquad (3.14)$$

The Power Model

Walpole *et al.* (2012) also represents the power model in its natural untransformed form given in Equation 3.15 and the transformed one in Equation 3.16 below.

$$y_i = \beta_o x_i^{\beta_1} . e \tag{3.15}$$

$$\log y_i = \log \beta_o + \beta_1 \log x_i + \log e \tag{3.16}$$

The Reciprocal Model

Walpole *et al.* (2012) further represents the reciprocal model in its natural untransformed form given in Equation 3.17 while the transformed model is given in Equation 3.18 below.

$$y_i = \beta_o + \beta_1 \left(\frac{1}{x_i}\right) \tag{3.17}$$

$$y_i = \beta_o + (x_i^*) \tag{3.18}$$

Where $x_i^* = \dfrac{1}{x_i}$

Many researchers have investigated possible relations between UCS and porosity, and UCS and density and obtained various models. Xu *et al.* (2016) obtained an inverse logarithmic and linear relations for UCS and porosity, and UCS and density respectively for sandstones whereas Rajabzadeh *et al.* (2012) and Chatterjee *et al.* (2013) obtained an inverse linear relation for cretaceous and carbonate sedimentary rocks respectively for UCS and porosity. Palchik (1999) and Tugrul (2004) however obtained inverse exponential relations for UCS and porosity for sandstones. Lashkaripour (2002) also obtained inverse exponential relations for UCS and porosity for shale, claystone and siltstone.

3.4.5 Hypotheses Testing and Level of Significance

A hypothesis is tested by measuring and examining a random sample of a population being analyzed. Random population samples are used to analyze two hypotheses thus the null and alternative hypotheses. The null hypothesis is the one believes to be true with the alternative being untrue. The comparison of the null and the alternative hypotheses is statistically significant according to the threshold probability thus the level of significance.

The level of significance is the probability of rejecting the null hypothesis when it is true which are run with alpha level of 5% in mining industry (Alhassan, 2017).

The common statistics used in testing hypothesis is the *z*-, *t*-, χ-square and *F*-statistics. According to Ross (2009) and Alhassan (2017), the *z*-statistic is used where the population means are known and normally distributed with large sample sizes (n>=30). The *t*-statistic is however used when the population variances or standard deviations are unknown and normally distributed or near normal distribution with small sample sizes (n<30) (Ross, 2009; Walpole, 2012; Alhassan, 2017). It is used for inferences about a population mean and for comparison of two sample means. Alhassan (2017) also indicated that the χ-square is used for "goodness-of-fit test" in which the distribution of a sample is being compared to a hypothetical distribution.

According to Al-hassan (2017), the *F*-statistic is used to test two (2) or more sample variances. Ross (2009) and Walpole (2012) also indicated that the *F*-statistic could be used to determine whether the means of three (3) or more samples are different or not and thus form the basis of analysis of variance, ANOVA. According to Ross (2009) and Walpole (2012), one way ANOVA tests the equality of three or more population means simultaneously using variances and compares three (3) or more levels of one factor or independent variable with the *F*-distribution. However, the two-way ANOVA is based on two factors and compares several levels of two independent variables. In regression testing, the *t*-statistic tests the significance of individual regression coefficients whereas the *F*-test tests the overall significance of a model (Ross, 2009; Walpole, 2012).

To test the regression coefficient, β_1, the test statistic is given in Equation 3.19 below.

$$T_o = (\hat{\beta_1} - \beta_{1,0}) / se(\hat{\beta_1}) \tag{3.19}$$

Where $\hat{\beta_1}$ is the least square estimate of β_1, $se(\hat{\beta_1})$ is its standard error and $\beta_{1,0}$ is some constant. The test statistic T_0 follows a distribution with (*n-2*) degrees of freedom where *n* is the total number of observations (Anon, 2015).

To test the significance of the regression model, the test statistic is given in equation 3.20 below.

$$F_0 = MS_R / MS_E = SS_R \setminus 1 / SS_E \setminus (n-2) \tag{3.20}$$

Where MS_R is the regression mean square and MS_E is the error mean square. Likewise, SS_R is the regression sum of squares with one degree of freedom and SS_E is the error sum of squares with (*n-2*) degrees of freedom (Anon, 2015).

3.5 Algorisms of Minitab 16 Programmable Language

According to Anon (2017), the methods and formulas that Minitab 16 uses in computations of statistics are shown in the various Equations below.

The commonly used measure of central tendency of observations called the mean is computed using Equation 3.19 below.

$$\bar{x} = \frac{\sum x_i}{N} \tag{3.19}$$

where:

x_i is the ith observation and

N is the number of nonmissing observations

The sample standard deviation which provides a measure of the spread of the data is computed using Equation 3.20 below.

$$s = \sqrt{\frac{\sum (x_i - \bar{x})^2}{N-1}} \tag{3.20}$$

where:

x_i is the ith observation;

$\bar{x}$ is mean of the observations and

N is the number of nonmissing observations

The variance which is a measure of how far the data are spread about the mean is computed by Minitab 16 by squaring the sample standard deviation as indicated in Equation 3.21.

$$s^2 = \frac{\sum (x_i - \bar{x})^2}{N-1} \tag{3.21}$$

where the symbols have their usual meanings.

Likewise, Minitab computes the standard error of mean using Equation 3.22 below.

$$SEmean = \frac{s}{\sqrt{N}}$$

(3.22)
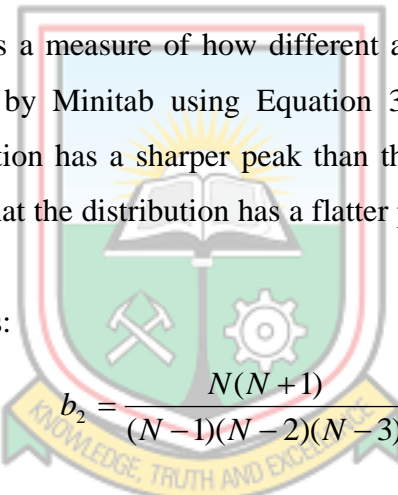
The skewness which is a measure of asymmetry is computed by Minitab using Equation 3.23 below. A negative value indicates skewness to the left, and a positive value indicates skewness to the right. However, a zero value does not necessarily indicate symmetry.

$$b_1 = \frac{N}{(N-1)(N-2)} \sum [(x_i - \bar{x})/s]^3$$

(3.23)

where the symbols have their usual meanings.

Also the kurtosis which is a measure of how different a distribution is from the normal distribution is computed by Minitab using Equation 3.24. A positive value typically indicates that the distribution has a sharper peak than the normal distribution whereas a negative value indicates that the distribution has a flatter peak than the normal distribution (Anon, 2017).

The formula for kurtosis is:

$$b_2 = \frac{N(N+1)}{(N-1)(N-2)(N-3)} \sum [(x_i - \bar{x})/s]^4 - \frac{3(N-1)^2}{(N-2)(N-3)}$$

(3.24)

Minitab 16 also does normality test by computing Anderson-Darling statistic which measures the area between the fitted line and the nonparametric step function. The statistic is a squared distance that is weighted more heavily in the tails of the distribution. A smaller Anderson-Darling value indicates that the distribution fits the data better (Anon, 2017).

The Anderson-Darling normality test is defined as:

H_o : The data follow a normal distribution;

H_A : The data do not follow a normal distribution.

The Anderson-Darling test statistic is defined in Equation 3.25 as

$$A^2 = -N - (1/N)\sum(2i-1)(\ln F(Y_i) + \ln(1 - F_{N-1-I}))) \quad (3.25)$$

where:

$F(Y_i) = \phi((Y_i - \bar{x})/s)$ is the cumulative distribution function of the standard normal distribution and Y_i are the ordered data.

Furthermore, the *p*-value of the normality test is a quantitative measure for reporting the result of the Anderson-Darling normality test. According to the test, a small *p*-value is an indication that the null hypothesis is false (Anon, 2017). Minitab calculates the *p*-value using A^2 as follows.

$$\text{Let } A^{\cdot^2} = A^2 * (1 + \frac{0.75}{N} + \frac{2.25}{N^2})$$

Depending on $A^{\cdot^2}$ the p-value is computed using the following Equations below.

$3 > A^{\cdot^2} > 0.600;$ $\qquad P = \exp(1.2937 - 5.709 * A^{\cdot^2} + 0.0186(A^{\cdot^2})^2)$ $\qquad$ (3.26)

$0.600 > A^{\cdot^2} > 0.340;$ $\qquad P = \exp(0.9177 - 4.279 * A^{\cdot^2} - 1.38(A^{\cdot^2})^2)$ $\qquad$ (3.27)

$0.340 > A^{\cdot^2} > 0.200;$ $\qquad P = \exp(-8.318 + 42796 * A^{\cdot^2} - 59.938(A^{\cdot^2})^2)$ $\qquad$ (3.28)

$A^{\cdot^2} < 0.200;$ $\qquad P = \exp(-13.436 + 101.14 * A^{\cdot^2} - 223.73(A^{\cdot^2})^2)$ $\qquad$ (3.29)

Minitab computes the true mean using the algorism as indicated in Equation 3.30 below.

$$\bar{x} - t_{N-1,\alpha/2}\frac{s}{N} < \mu < \bar{x} + t_{N-1,\alpha/2} \quad (3.30)$$

where $t_{N-1,\alpha}$ is the $(1-\alpha)$ 100th percentile of the t-distribution with (N-1) degrees of freedom.

For one sample *T* test, Minitab does the following hypotheses:

Null hypothesis, $H_0 : \mu = \mu_0$

Alternative hypothesis, $H_1 : \mu > \mu_0$ or $H_1 : \mu < \mu_0$ for one tail test and

$H_1 : \mu \neq \mu_0$ for two tail test.

Where μ is the population mean and μ_0 is the hypothesized mean.

The test statistic that Minitab 16 uses for the one sample T test is given in Equation 3.31 below.

$$t = (\bar{x} - \mu_o)/(s/\sqrt{n}) \tag{3.31}$$

However, for two samples T-test, Minitab uses the following hypotheses:

$H_0 : \mu_1 - \mu_2 = \delta_0$

$H_1 : \mu_1 - \mu_2 > \delta_0$ or $H_1 : \mu_1 - \mu_2 < \delta_0$ for one tail test and

$H_1 : \mu_1 - \mu_2 \neq \delta_0$ for two tail test. μ_1 is the mean for the first population and μ_2 is the mean for the second population. δ_0 however, is the hypothesized difference in means of the two populations.

The test statistic for the two sample T test is given by Minitab 16 in Equation 3.32 below.

$$t = ((\bar{x}_1 - \bar{x}_2) - \delta_o)/s \tag{3.32}$$

Where:

$s = \sqrt{\dfrac{s_1^2}{n_1} + \dfrac{s_2^2}{n_2}}$ and $\dfrac{(VAR_1 + VAR_2)^2}{[(VAR_1)^2/(n_1 - 1)] + [(VAR_2)^2/(n_2 - 1)]}$ is the degree of freedom for

unequal variances. For equal variances,

$s = s_p \sqrt{\dfrac{1}{n_1} + \dfrac{1}{n_2}}$ where $s_p^2 = \dfrac{(n_1 - 1)s_1^2 + (n_2 - 1)s_2^2}{n_1 + n_2 - 2}$ having $n_1 + n_2 - 2$ degree of

freedom.
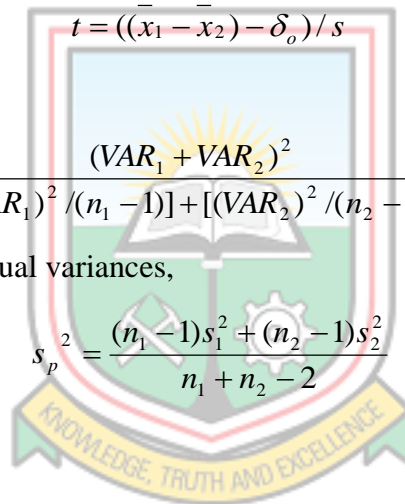
The 95% confidence interval for the difference in means is given in Equation 3.33 below.

$$(\bar{x}_1 - \bar{x}_2) - t_{\alpha/2}s < \mu_1 - \mu_2 < (\bar{x}_1 - \bar{x}_2) + t_{\alpha/2}s \tag{3.33}$$

Additionally, Minitab 16 computes the Pearson's correlation coefficient which measures the degree of linear relationship between two variables. The correlation coefficient assumes a value between -1 and +1. If one variable tends to increase as the other decreases, the correlation coefficient is negative. Conversely, if the two variables tend to increase together the correlation coefficient is positive. For the two variables x and y, the Pearson's correlation coefficient is given by Equation 3.34 below (Anon, 2017).

$$\rho = \frac{\sum\limits_{i=i}^{n}(x_i - \bar{x})(y_i - \bar{y})}{(n-1)s_x s_y}$$

(3.34)

Where s_x and s_y are the standard deviations for the first and second variables respectively.

Also, Minitab computes the p-value which is another quantitative measure for reporting the correlation between two variables and is used in hypothesis tests, where one either rejects or fails to reject a null hypothesis. The smaller the *p*-value, the smaller is the probability that you would be making a mistake by rejecting the null hypothesis.

For Pearson's correlation coefficient, the hypothesis; $H_o : \rho = 0$ versus $H_1 : \rho \neq 0$ is tested by Minitab 16. A small p-value is an indication that the null hypothesis is false. One can conclude that the correlation coefficient is different from zero and that a linear relationship exists. Minitab therefore rejects the null hypothesis if the *p*-value is smaller than 0.05 (Anon, 2017).

According to Anon (2017), Minitab 16 computes the relationship between variables by regression models. For a model with multiple predictors, the model is given in Equation 3.35.

$$Y = \beta_o + \beta_1 x_1 + ... + \beta_r x_r + e$$

(3.35)

The fitted model is given in Equation 3.36 below.

$$\bar{Y} = b_o + b_1 x_1 + ... + b_r x_r$$

(3.36)

Minitab fits data with the following models:

Linear: $Y = \beta_o + \beta_1 x_1 + e$

(3.37)

Quadratic: $Y = \beta_o + \beta_1 x_1 + \beta_2 x_1^2 + e$

(3.38)

Cubic: $Y = \beta_o + \beta_1 x_1 + \beta_2 x_1^2 + \beta_3 x_1^3 + e$

(3.39)

The regression coefficients in simple linear regression are computed using the following Equations presented in Equations 3.40 and 3.41 below.

$$b_1 = \frac{\sum(x_i - \bar{x})(y_i - \bar{y})}{(x_i - \bar{x})}$$

(3.40)

$$b_o = \overline{y} - b_1 \overline{x} \qquad\qquad (3.41)$$

Minitab 16 however uses Box-Cox transformation for non-normal data which selects lambda (λ) values that minimizes the residual sum of squares. The resulting transformation is Y^λ when $\lambda \neq 0$ and lnY when $\lambda = 0$. In General Regression, the Box-Cox transformation searches for an optimal value between -2 and 2. Values that fall outside of this interval may not result in a better fit (Anon, 2017). Some common transformations where Y' is the transformation of the data Y are:

$$Y' = Y^2 \text{ when } \lambda = 2$$

$$Y' = \sqrt{2} \text{ when } \lambda = 0.5$$

$$Y' = \ln Y \text{ when } \lambda = 0$$

$$Y' = 1/\sqrt{Y} \text{ when } \lambda = -0.5$$

$$Y' = 1/Y \text{ when } \lambda = -1$$
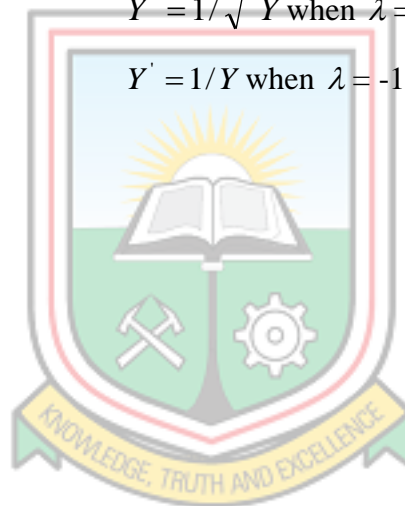
CHAPTER 4

METHODS USED

4.1 Materials

The tools and materials used for the fieldwork include: the geological hammer, geological compass, GPS, a scoop, chisel, lens, marker pen and a field note book. The purpose of the GPS was to record the elevation and location of each sample point. Likewise, the geological compass measured the dip amount and strike of each sample bed. The lens was used to determined the observable features of the intact rocks. Meanwhile, the geological hammer together with the chisel helped to obtain intact sample from a fresh bed. Lastly, the scoop helped to take soil samples from the study area whilst the marking pen was used to label the samples accordingly. All recordings were however done in the field note book.

4.1.1 Data Used

The data used in this research were obtained through laboratory investigations from the field samples. Sampling was done by simple random sampling technique. Simple random sampling was done on each lithological unit assuming homogeneity by assigning random numbers to fresh samples and randomly selecting thirty six (36) samples.

One hundred and eight (108) rock samples, but representatives of the three lithological units consisting of thirty six (36) samples, also representative of each lithological unit were collected from the study area in Efia Nkwanta beds in Essipon, Elmina sandstone in Aboadze and Takoradi sandstone in Monkey hill. The sampling was done by simple random sampling technique as discussed above since fresh samples were required. As stated, the purpose of the sampling was to obtain fresh samples for subsequent laboratory investigations and statistical analysis. The location coordinates and elevation of each sample point was measured and recorded in the field note book. The sampling locations are summarized in Figure 4.1. The results of the laboratory investigations of the rock samples with 95% confidence interval have been presented in Chapter 5.
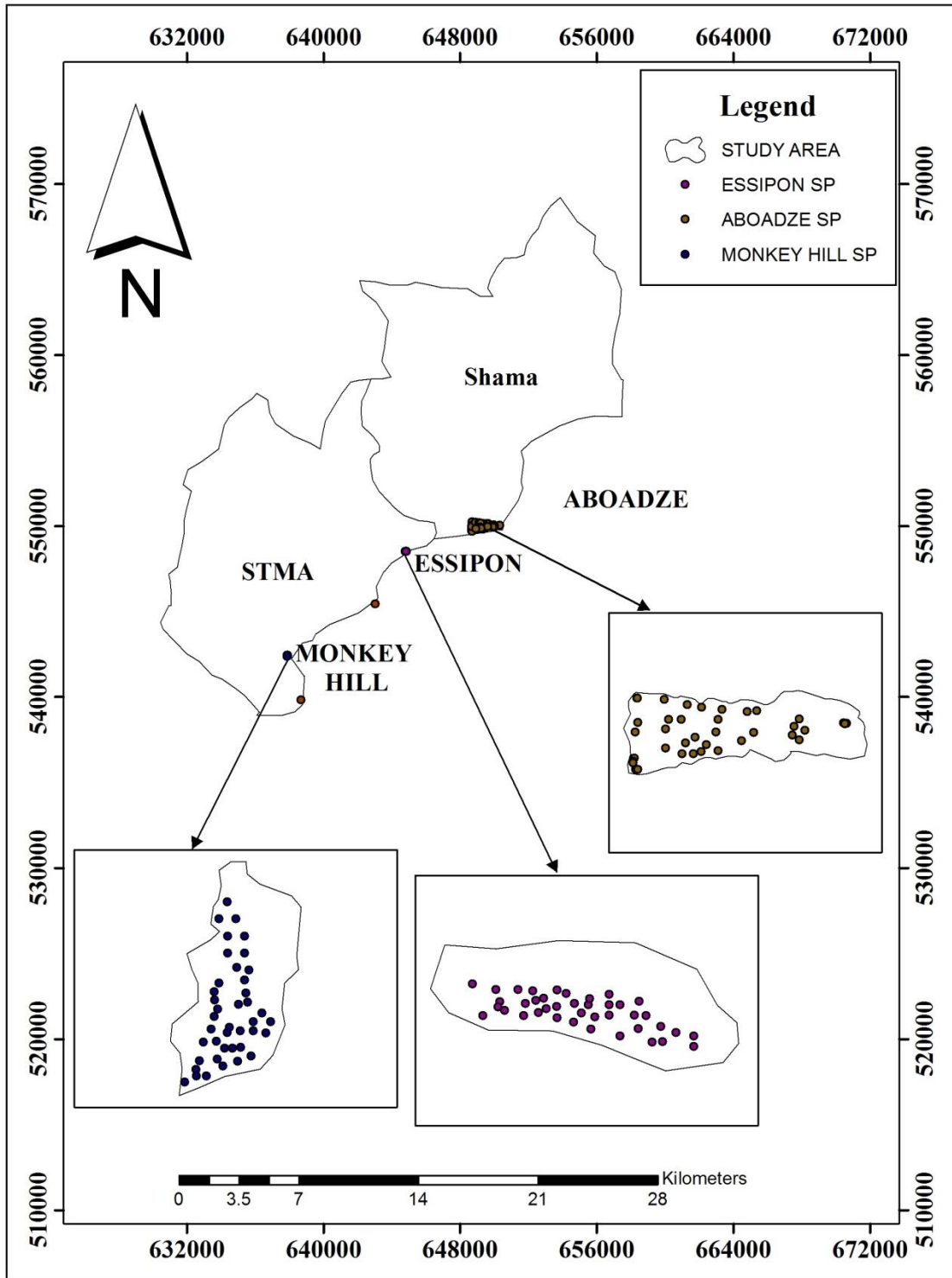
Figure 4.1: Sampling Location Map Showing Essipon, Aboadze and Monkey Hill in Sekondi-Takoradi Metropolitan Assembly and Shama

4.1.2 Equipment

The equiment used for the laboratory investigations were: specific gravity bottle, electronic balance, vernier caliper, rock cutter, UCS set-up, laboratory crusher, hammer mill and an electron microscope.

Laboratory Crusher

The laboratory crusher was used to crush samples when disaggregation of was needed for sieve analysis and particle density test. As shown in Figure 4.2, the crusher is housed in a protection case conforming to requirement and has a jaw opening (gape) of about 100x60 mm, jaw crushing adjustment of 2 to 18 mm and can produce from 100 to 400 kg of material per hour. This apparatus was required to obtain aggregates of about 5 mm which was further reduced using the hammer mill as shown in Figure 4.3 below.

Figure 4.2 Laboratory Crusher

The Hammer Mill

The hammer mill was used to reduce the sample size, previously crushed to 5 mm size with the laboratory crusher, in order to perform the various tests of the aggregates. As

shown in Figure 4.3, the machine consists of a grinding chamber, interchangeable fixed hammers, hopper and screens with desired opening sizes. The grinding operation is obtained by the combination of three efforts: impact, shear and rebound. After entering the grinding chamber through the hopper, the material reaches the required fineness and then pass through the filtering hoses to the collector.

Figure 4.3 The Hammer Mill

The Electron Microscope

The electron microscope was used for petrography analysis of samples obtained from the three lithological units. It consists principally of condensers, magnetic lenses, electron gun and recorder as indicated in Figure 4.4. It works with thin pieces of samples. The electron gun is a heated tungsten filament, which generates electrons when a high voltage is applied. The condenser focuses the electron beam onto a specimen. The travelling electrons are focused into a thin beam by another condenser which is accelerated by a high voltage applied between the tungsten filament and the anode. This focused high speed electrons illuminate the specimen. The beam is scattered depending upon the thickness or refractive index of the specimen. The magnetic lenses magnify the image for examination. The recorder records the results of the samples.
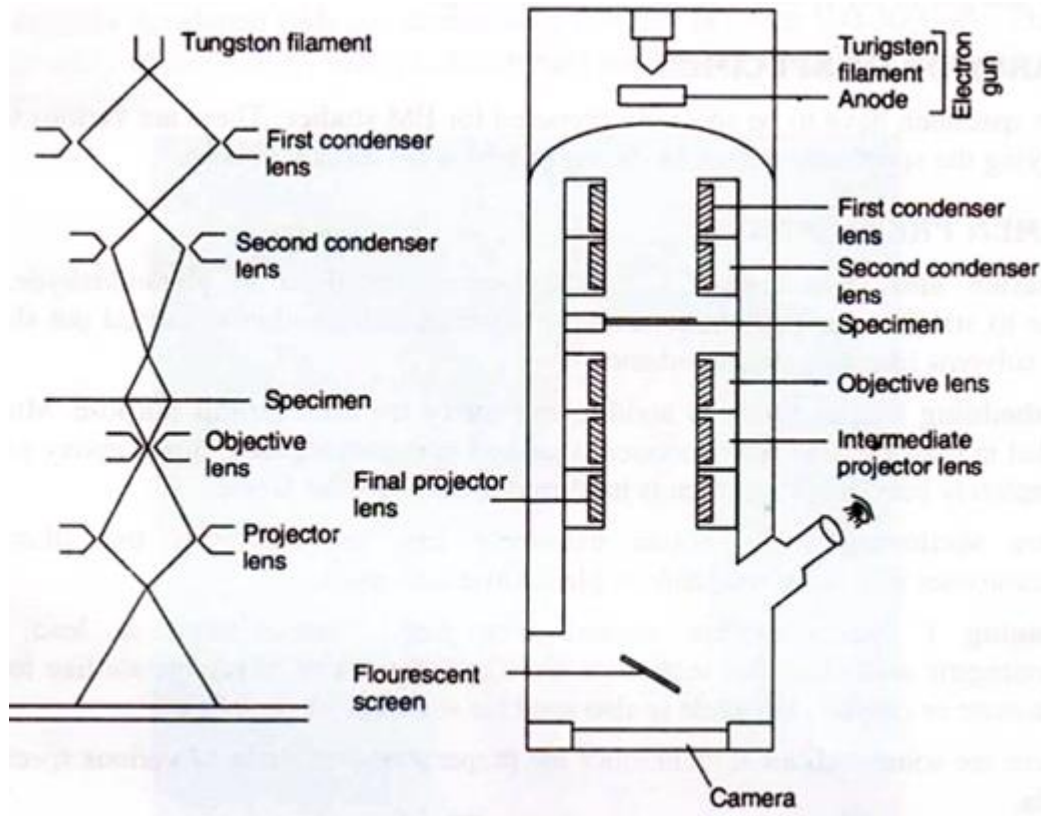
Figure 4.4: The Electron Microscope (Anon, 2017)

Rock Cutter

This equipment was used to cut fresh samples to required sizes during UCS sample preparations. It consists of a handle, blade, sample frame, equipment frame and a clamp to allow irregular specimen to be held firmly in place during the cutting operation as indicated in Figure 4.5. The equipment is electrically operated but mechanically controlled. The handle of the equipment controls the release and contact of the blade on the sample whilst the lever controls the speed of the blade. Accordingly, the blade cuts the sample to shape according to a standard specified by the operator. Meanwhile water is used to cool the blade during cutting operation.

Figure 4.5 Rock Cutting Equipment Used for Laboratory Sample Preparation
(Anon, 2017)

The UCS Sep-Up

The UCS machine was used to test the samples for unconfined compressive strength. The equipment (Figure 4.6) consists of servo-hydraulic control console for controlling load application, high stiffness testing frame for mounting the specimen, servo-hydraulic control console for lateral pressure control, and a gauge for load measurement. It is driven by a sophisticated micro-processed servo-control device at a very stable rate of stress and displacement or strain. It also provides an automatic control and management of cell pressure within the limits prescribed by the standards.

Figure: 4.6 The UCS Test Set-Up

4.2 Methods Used

The methods used to achieve the objectives of the research are discussed in the various Sections below.

4.2.1 Particle Size Analysis of Rock Samples

The samples obtained from the lithological units contain different particle sizes and therefore sieve analysis was conducted by the author based on the BS adopted method in UMaT geotechnical laboratory, Tarkwa. The purpose was to determine the particle size distribution for onward texture characterization and classification of the rocks.

According to the BS adopted procedure, about 500 g disaggregated samples were sieved through the standard sieve sizes (25 mm, 22.5 mm, 19 mm, 16 mm, 13.5 mm, 12.5 mm,

11.2 mm, 9.5 mm, 8 mm, 5.6 mm, 4 mm, 2.8mm, 2 mm, 1.18 mm, 600 μm, 425 μm, 300 μm, 212 μm, 150 μm, 75 μm and 63 μm) as indicated in Figure 4.7. The mass of the particles retained in the individual sieves was used to determine the percentage retained and the percentage passing of the individual particles through the sieves. The results are however presented in Chapter 5.

Figure 4.7 Sieving of Rock Aggregates

4.2.2 Petrographic Analysis

Petrography studies were performed on the samples by the author based on the BS adopted method in UMaT petrology laboratory, Tarkwa. The purpose was to determine the

mineralogy and particle characteristics of samples. Thin sections were performed and studied with the electron microscope to determine the mineralogy and grain characteristics of samples for subsequent lithological characterization. To perform the petrographic analysis, the author performed thin sections of about 20 μm-30 μm on a slide as indicated in Figure 4.8. After a voltage is applied, the electron gun releases electrons which were focused by a condenser onto the sample on the slides. The light beam was scattered depending upon the properties of the sample. These scatterings were studied and recorded. The results are presented in Chapter 5.
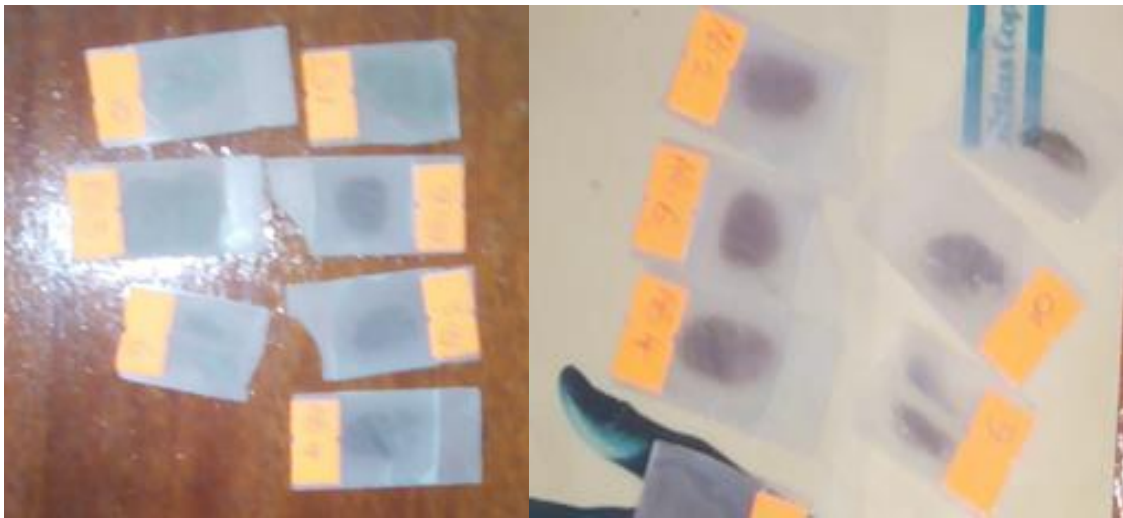
Figure 4.8 Thin Sections of Samples

4.2.3 UCS Test

The methods and procedures used to determine UCS in this research are discussed in the next two Sections.

Sample Preparation

The samples were prepared based on the ISRM adopted standard in UMaT geotechnical laboratory procedure. 50 mm x 50 mm x 50 mm cubic samples (see Figure 4.9) were prepared by applying a mechanically controlled pressure from a blade which is electrically operated on the sample. The blade accordingly cut the samples according to sizes. During the cutting, water was continuously supplied onto the sample, to prevent it and the blade from overheating. The handle of the equipment controls the release and contact of the blade on the sample whilst the lever controls the speed of the blade. During the sample

preparations, vernier caliper was used to measure sample dimensions. Also, perpendicularity and smoothness of surfaces were ensured.

Figure 4.9 UCS Samples Used for the Research

UCS Test Procedure

The unconfined compressive strength of samples was determined by the author based on the adopted UMaT geotechnical laboratory test procedure. The purpose was to determine UCS of the rock samples as input parameters for onward correlation and regression analyses.

50 mm x 50 mm x 50 mm cubic samples were loaded axially, in compression, to failure. During the compression test, a compression load was applied continuously on the rock specimen without shock, in such a manner that produced a strain rate as constant as possible, and caused failure within 5-10 min of loading or at a constant rate of stress, within the limits of 0.5-1.0 MPa/sec. The maximum failure loads were recorded and the unconfined compression strength was computed using Equation 4.1. The mean values were recorded and tabulated which are presented in Chapter 5 and Appendix A3.

$$UCS = \frac{P}{A} \tag{4.1}$$

where P is the failure load and A, the cross sectional area of the sample.

4.2.4 Porosity Test

Porosity measurements were performed by the author using the BS standard in UMaT geotechnical laboratory, Tarkwa. The purpose was to determine porosity of the rock samples as input parameters for onward statistical analysis.

The porosity was determined by measuring the mass of the rock samples, mass of saturated samples after saturating in distilled water for 24 hours and its dry mass after oven drying the rock samples to about 200˚C for 24 hours and subsequently determining the volume of void (V_V) as the difference of the saturated and dry samples. Also, the bulk volume (V_b) of the rock samples were determined by measuring the volume of water displaced in a measuring cylinder. Thus, the porosity was computed using Equation 4.3 below. Meanwhile, the mean porosity was recorded and tabulated and presented in Chapter 5 and Appendix A1.

$$e = (V_V / V_b) \times 100 \tag{4.2}$$

e is the porosity of rock sample, V_v is volume of void and V_b is the bulk volume of the rock sample.

4.2.5 Density Test

Particle density measurements were performed by the author in UMaT geotechnical laboratory using the BS adopted procedure. The purpose was to determine the particle density of disaggregated rock samples as input parameters for onward correlation and regression analyses.

The particle density was determined by measuring the mass of empty density bottle (m_1 g), the mass of the bottle with 10 g of grains of the rock samples (m_2 g), mass of bottle plus grains of rocks plus water (m_3 g) and mass of bottle with water only (m_4 g). The mass of water used (m_3-m_2) g, mass of grains used (m_2-m_1) g and volume of grains of rocks ((m_4-m_1)-(m_3-m_2)) cm^3 were subsequently determined. The grain density was computed using Equation 4.4. Meanwhile the average grain densities were recorded and presented in Chapter 5 and Appendix A2.

$$\rho = \frac{m_2 - m_1}{(m_4 - m_1) - (m_3 - m_2)} \qquad (4.3)$$

4.2.6 Statistical Analysis

Basic Statistical Analysis

Basic statistical analyses were performed on each data set obtained from the laboratory investigations of the lithological units using Minitab programming language. The normality, mean, mode, median as well as the confidence limits of mean, mode and median were determined. Also, standard deviation, variance, skewness and kurtosis were all determined. The normality tests were based on Anderson-Darling test using the *p*-value. The purpose was to determine the normality of the data to help direct the analysis. Also, the mean and the confidence intervals were important in detailed modeling presented in Chapter 5. Likewise, the standard deviation and the variance were equally important in the modeling. To perform the basic statistics, the author used "Stat > Basic statistics" dialogue box. These calculations are based on the theoretical background discussed in Chapter 3.

Two-Tailed t-Test

To investigate the population mean of each variable in a lithological unit, the author performed one sample *t-* test for each data set using Minitab programming language. This was done by testing the hypothesis of the population mean as zero versus the population mean not being zero. To perform the *t-* test, the author uses the "Stat > Basic Statistics > 1-Sample *T*". The results of these tests are presented in Chapter 5. Also, the *t-* test is based on the theoretical background discussed in Chapter 3 with 95% confidence interval. Its purpose was to establish the likelihood that UCS, porosity and particle density could be significant variables in the lithological units.

One-Way Analysis of Variance (ANOVA)

To determine whether a real difference exists in each variable in the three lithological units in the Sekondian Group, the author performed one-way analysis of variance (ANOVA) for each variable in the lithological units in the Sekondian Group. Subsequently, the hypotheses that the means of the respective variables in the lithological

units in the Sekondian Group are equal were therefore tested as against not being equal. The results are presented in Chapter 5. To perform the one-way ANOVA, the author used "Stat > ANOVA" with its command "One Way unstacked". Also, the one-way ANOVA test is based on the theoretical background discussed in Chapter 3 with 95% confidence interval.

Correlation Analysis

To determine a measure of the relationship between two variables in the lithological units in the Group the correlation analysis was performed using Minitab programmable language. The correlation coefficients were determined. Correlation analysis was performed using "Stat > Basic Statistics > Correlation" dialog window as discussed in Chapter 3. Subsequently, hypotheses were tested on the correlation coefficients using the same dialog box to determine whether correlation existed in the lithological units. The hypotheses that the population correlation coefficients were zero versus not zero were tested. The results are however presented in Chapter 5. These tests are based on the theoretical hypotheses tests discussed and presented in Chapter 3.

Regression Analysis

Regression analyses were performed on the variables in the lithological units using Minitab programmable language. The purpose was to determine the relationship between geomechanical and petrophysical properties of samples in the lithological units. Simple and multiple regressions were performed in each lithological unit. Whereas the simple regression was performed to determine the relation between UCS and each petrophysical property, the multiple regression was performed to relate the predictor variables (porosity and particle density) with the response variable (UCS). The purpose of the simple regression was to determine the significant relations for onward multiple regression modeling. The regression modeling was however performed on each lithological unit. The modeling was done using "Calc > regression" dialog box in the Minitab programmable language as discussed in Chapter 3.

The input parameters used for the modeling were: the UCS obtained from the unconfined compression tests, porosity obtained from the saturation tests and the particle density obtained from the specific gravity tests. Also, the regression models are based on the theoretical discussions presented in Chapter 3. The aim was not only to avoid the

expensive and time consuming laboratory measurements of geomechanical properties but to determine a model for future stability analysis of the study area. Also, the study aimed at obtaining a model for easy determination of essential petrophysical properties for reservoir characterization and other related industries. The study focuses on the interdependence of geomechanical and petrophysical properties by analyzing UCS as against porosity and particle density of the rocks.

Test of Models

The correlation coefficients and regression models were tested based on hypotheses. Both null and alternative hypotheses were formulated for the correlation coefficients and regression relations and tested with the *t*- and *F*-statistics using the *p*-values. The null hypothesis was tested as the correlation coefficient not being zero as against the alternative hypothesis as being zero with the *t*-statistic. That is the correlation coefficient is significant as against it being insignificant in the lithological unit. Likewise, for the regression relations, the null hypothesis was formulated as the relation being significant as against the alternative hypothesis as insignificant with the *F*-statistic. The null hypothesis was accepted when the *p*-value is less than the level of significance and rejected if otherwise. These tests were based on the Minitab 16 programmable language as discussed and presented in Section 3.5 in Chapter 3 above.
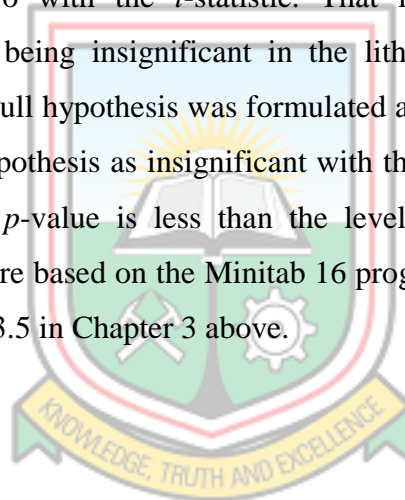
CHAPTER 5

RESULTS AND DISCUSSIONS

5.1 Results

The results obtained from the laboratory investigations of sandstones in the Sekondian Group are presented in the Sections below.

5.1.1 Sieve Analysis

The results obtained from the sieve analyses of samples in the Sekondian Group are presented in Figure 5.1. In Figure 5.1, the *Trask coefficient* was evaluated for each lithological unit. The purpose was to determine the degree of sorting of particles in the lithological units.

In Figure 5.1, the Takoradi sandstone has an estimated percentage fine gravel of 6.3%, coarse sand of 25.8%, medium sand of 20.7%, and fine sand of 47.2% and therefore consists of fine to medium to coarse sand grains. Based on Equation 3.5, the Takoradi sandstone has an estimated *Trask coefficient* of 0.371 (D_{25} = 0.11 mm, D_{75} = 0.8 mm, see Figure 5.1). Based on the *Trask* sorting classification (see Table 3.1, Section 3.2), the *Trask coefficient* indicates that the particle sizes in Takoradi sandstone are poorly sorted.

In Figure 5.1, the Elmina sandstone has an estimated percentage fine gravel of 4.4%, coarse sand of 27.8%, medium sand of 37.6%, and fine sand of 30.3% and also consists of all aggregates. Based on Equation 3.5 in Chapter 3, the Elmina sandstone has an estimated *Trask coefficient* of 0.4 (D_{25} = 0.2 mm, D_{75} = 0.9 mm, see Figure 5.1). Based on the *Trask* sorting classification (see Table 3.1, Section 3.2), the *Trask coefficient* indicates that the particle sizes in Elmina sandstone are also poorly to moderately sorted.
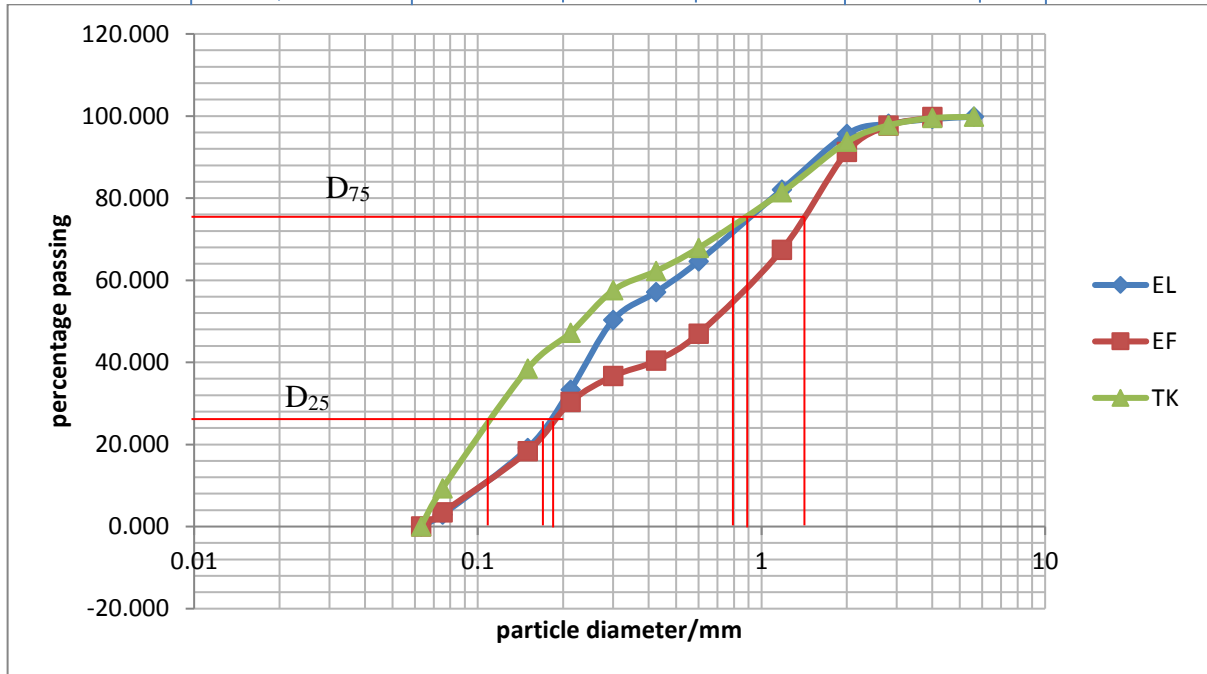
Figure 5.1: Results of Sieve Analysis for Elmina Sandstone (EL), Efia Nkwanta Beds (EF) and Takoradi Sandstone (TK) (Key: F: fine, M: medium, C: coarse)

In Figure 5.1, the Efia Nkwanta sandstone has an estimated fine gravel of 8.8%, coarse sand of 44.3%, medium sand of 16.7% and fine sand of 30.3% and therefore consists of all aggregates. The Efia Nkwanta sandstone has an estimated *Trask coefficient* of 0.9 (D_{25} = 1.2 mm, D_{75} = 1.5 mm, see Figure 5.1). The *Trask coefficient* indicates that the particle sizes in Efia Nkwanta beds are moderately well sorted.

Furthermore, the total sand percentage in Takoradi sandstone is about 93.7% and that of Elmina sandstone is about 95.7% whilst Efia Nkwanta beds has the minimum of about 91.3%. This suggests that the rocks in the lithological units are entirely sandstones.

5.1.2 Petrographic Analysis

The petrography obtained from the laboratory investigations of the samples in the lithological units are presented in Figure 5.2.

54

As indicated in Figure 5.2a, the sandstones in Efia Nkwanta beds are generally fine grained and well sorted consisting of quartz and chlorite minerals and therefore classify as quartz sandstone. Figure 5.2b indicates that the Elmina sandstone is medium to coarse grained and moderately sorted with sub angular to angular shape. The minerals are predominately biotite, quartz and plagioclase feldspar and classify as arkose. The Takoradi sandstone are fine to medium to coarse grained and poorly sorted with sub angular to angular shape as indicated in Figure 5.2c. It is predominately quartz and classify as quartz graywackes.

a
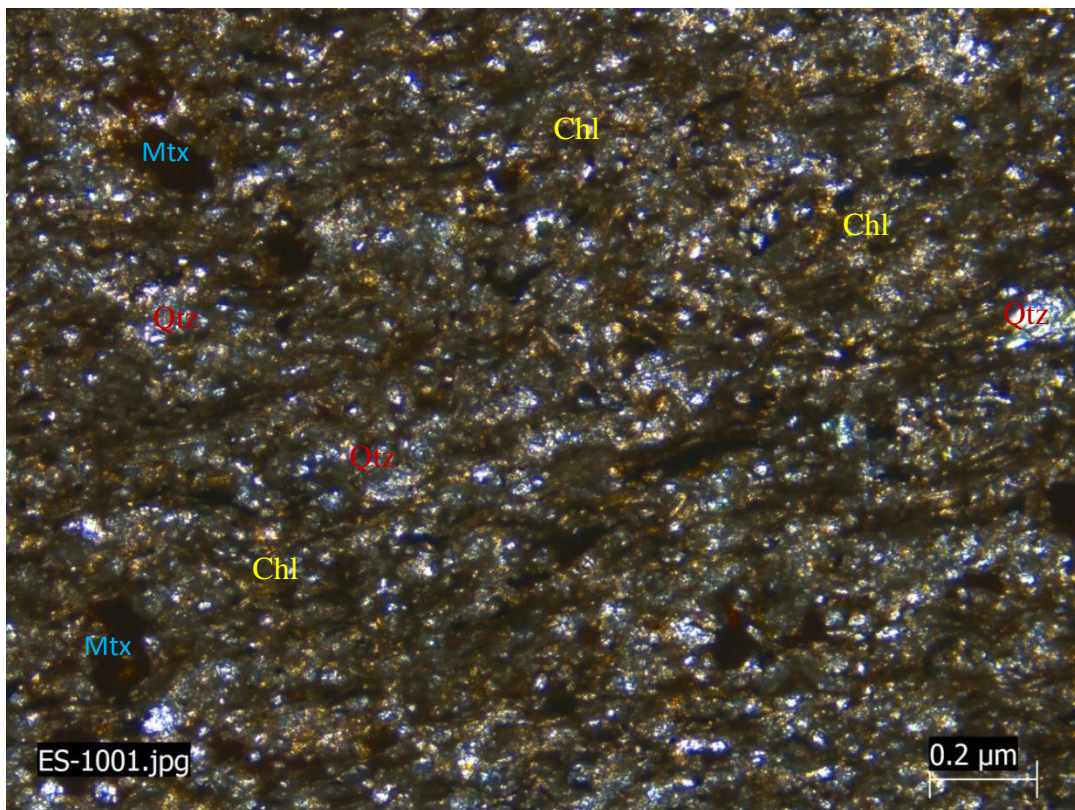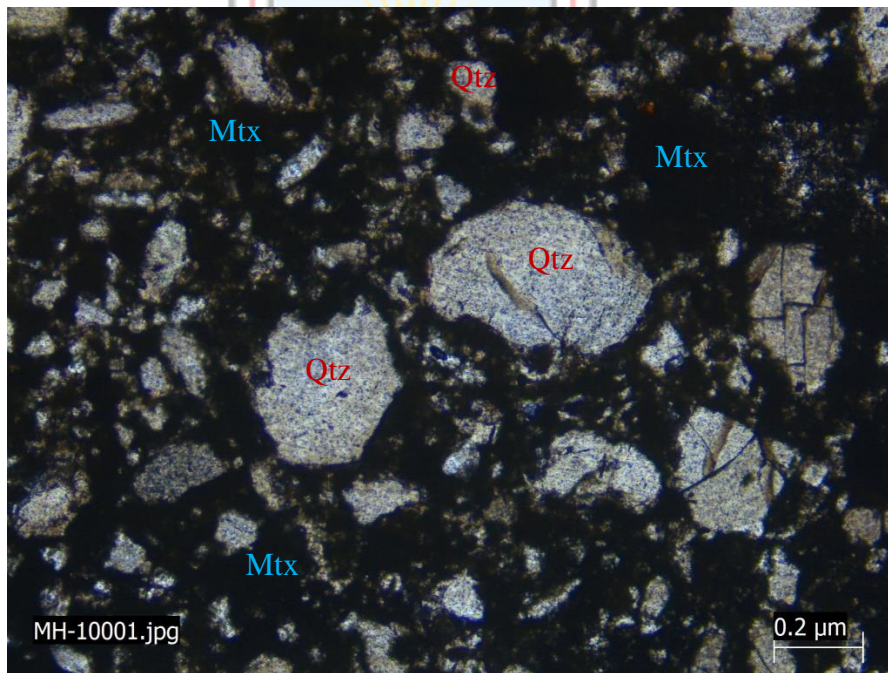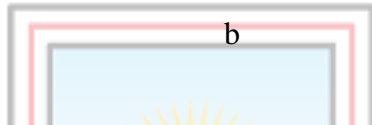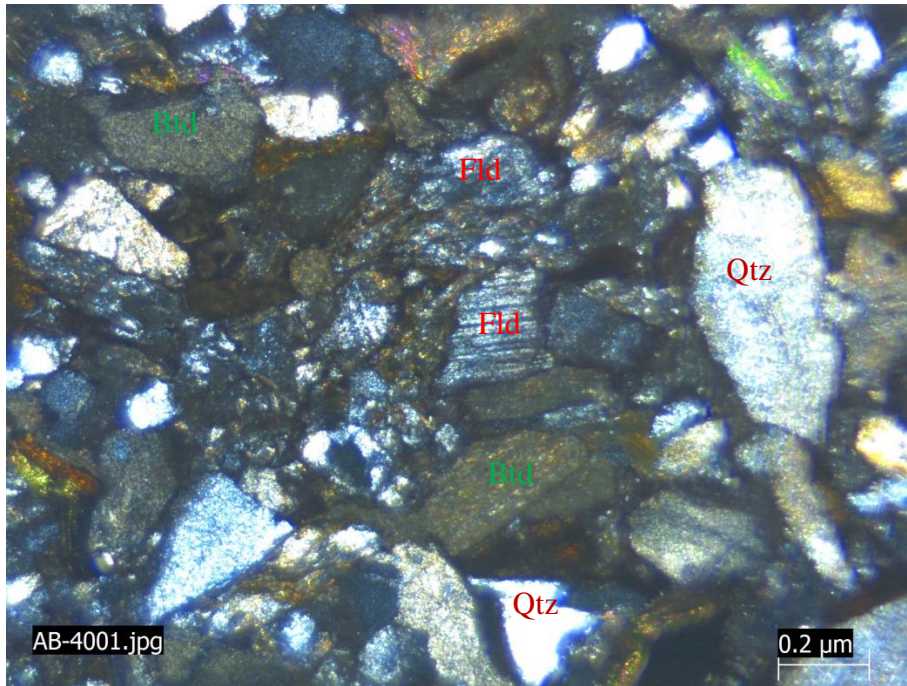
Figure 5.2: Photomicrographs of Samples in (a) Efia Nkwanta Beds (b) Elmina Sandstone and (c) Takoradi Sandstone Under Plane Polarized Light (Key: Btd: Biotite, Fld: Plagiosclase Feldspar, Mtx: Matrix, Qtz: Quartz)

5.1.3 Porosity Test

The statistical summary of the results of porosity of the samples obtained from the laboratory investigations are presented in Figures 5.3-5. The results of porosity measurements are indicated in Appendix A1.

Figure 5.3 indicates that the mean porosity of Efia Nkwanta sandstone is 14.0% having a standard deviation of 5.1 and a variance of 25.6. The 95% confidence limit for the mean is 12.3 - 15.7%. The *p*-value for the Anderson-Darling normality test indicates that the porosity in the lithological unit follows normal distribution since the *p*-value is greater than the 0.05 α-level of significance. Though the porosity in the lithological unit is normally distributed, the degree of normality is however not strong. This may be due to microstructural anisotropy in the lithological unit or errors with sampling or laboratory analysis.

Figure 5.3: The Statistical Summary of Porosity in Efia Nkwanta Beds

Figure 5.4: The Statistical Summary of Porosity in Elmina Sandstone

Figure 5.5: The Statistical Summary of Porosity in Takoradi Sandstone

Figure 5.4 indicates that the mean porosity of Elmina sandstone is 8.3% having a standard deviation of 1.8 and a variance of 3.3. The 95% confidence limit for the mean is 7.7 - 8.9%. The *p*-value for the Anderson-Darling normality test indicates that the porosity follows normal distribution since it is greater than the 0.05 α-level of significance. The *p*-value indicates a strong normal distribution in the lithological unit.

Figure 5.5 indicates that the mean porosity of Takoradi sandstone is 15.6% having a standard deviation of 3.7and a variance of 13.7. The 95% confidence interval for the mean is 14.4 and 16.9%. The Anderson-Darling normality test indicates that the porosity in the lithological unit follows normal distribution since the *p*-value for the normality test is greater than the 0.05 α-level of significance. The *p*-value indicates that the porosity is not strongly normally distributed in the lithological unit. This may be due to microstructural anisotropy in the lithological unit as observed in Figure 5.2c, Section 5.1.2 or errors with sampling or laboratory analysis.

5.1.4 Density Test

The statistical summary of the results of particle density of the rock samples obtained from the laboratory investigations are presented in Figure 5.6, Figure 5.7 and Figure 5.8. The results of particle density measurements are indicated in Appendix A2.

Figure 5.6 indicates that the mean density of sandstones in Efia Nkwanta beds is 2.7gcm^{-3}, having a standard deviation of 0.2 and a variance of 0.04. The 95% confidence limit for the mean particle density in the lithological unit is 2.7 - 2.8 gcm^{-3}. The Anderson-Darling normality test indicates that the density follows normal distribution in the lithological unit since the *p*-value is greater than the 0.05 level of significance.

Also, Figure 5.7 indicates that the mean density of Elmina sandstone is 2.5035 gcm^{-3}, having a standard deviation of 0.2 and a variance of 0.04. The 95% confidence limit for the mean is 2.4and 2.6 gcm^{-3}. Furthermore, the particle density follows normal distribution in the lithological unit since the *p*-value for the normality test is greater than the 0.05 level of significance.
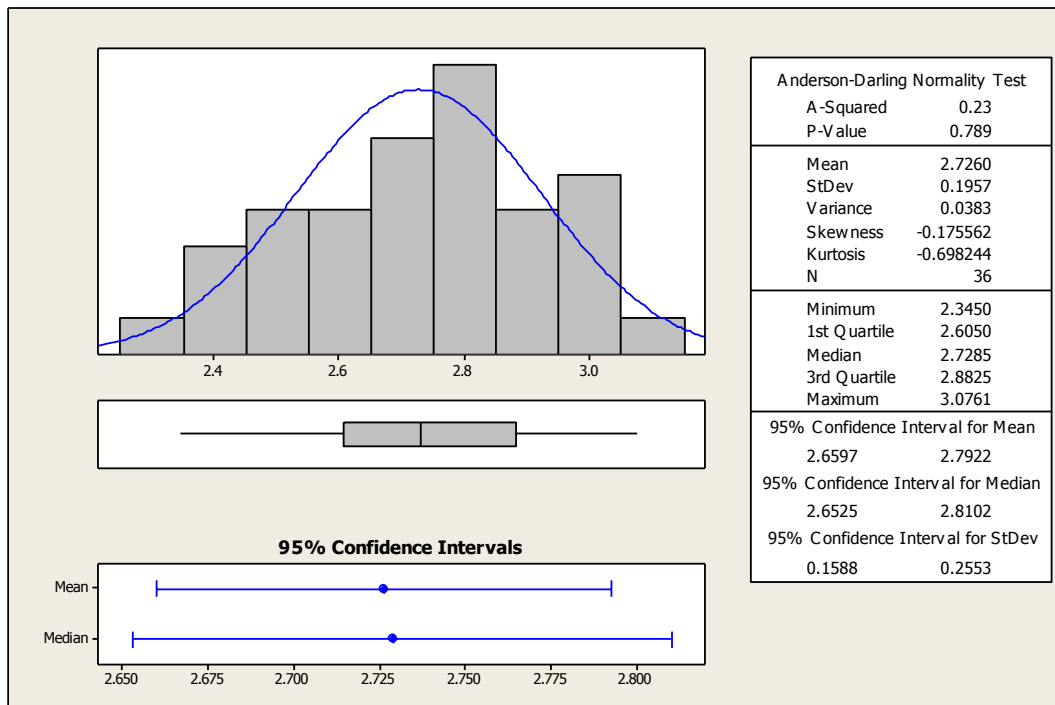
Figure 5.6: The Statistical Summary of Particle Density in Efia Nkwanta Beds
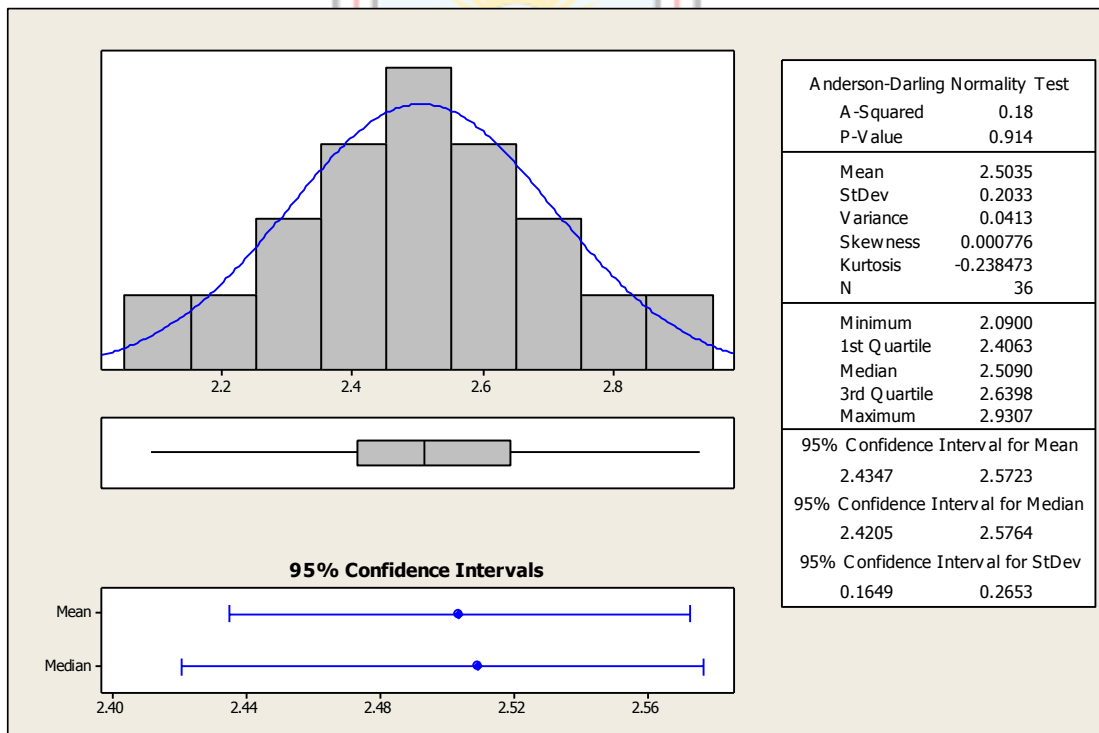
Figure 5.7: The Statistical Summary of Particle Density in Elmina Sandstone
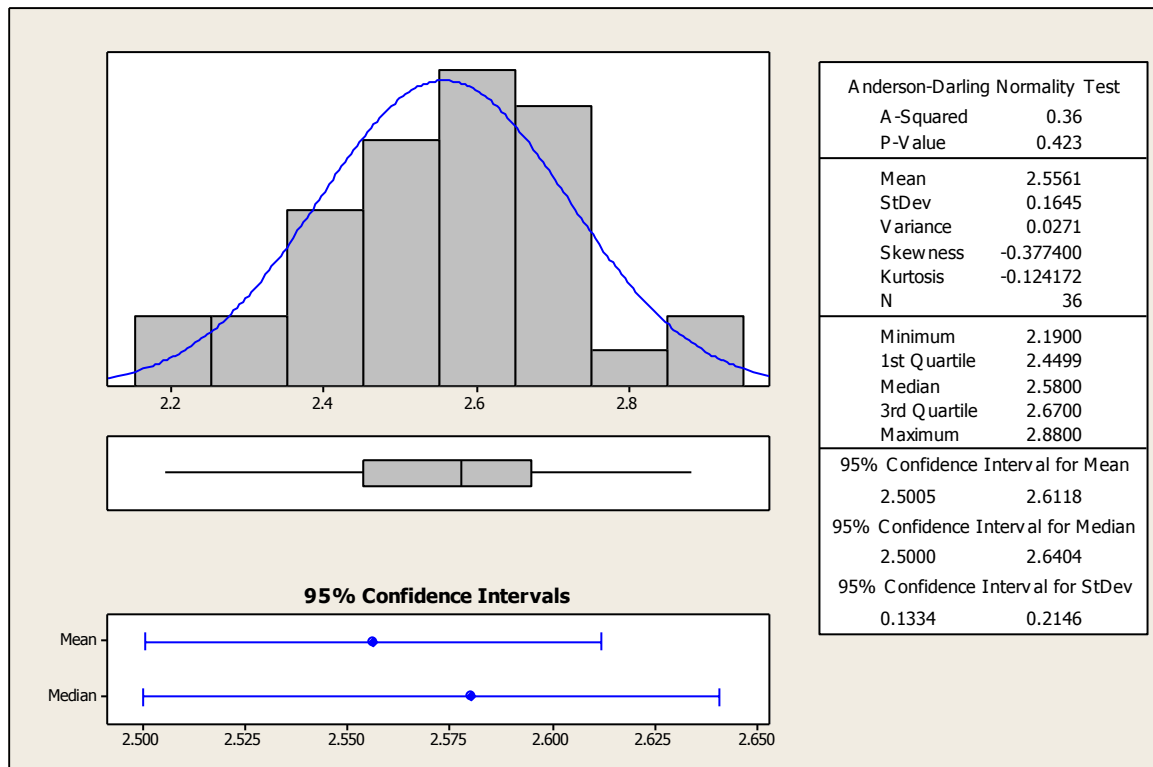
Figure 5.8: The Statistical Summary of Particle Density in Takoradi Sandstone

Likewise, in Figure 5.8, the mean density of Takoradi sandstone is 2.6 gcm^{-3}, having a standard deviation of 0.1645 and a variance of 0.03. The 95% confidence limit for the mean is 2.5 - 2.6 gcm^{-3}. Furthermore, from the Anderson-Darling normality test, the results indicate that density is normally distributed in the lithological unit since the *p*-value for the normality test is greater than the 0.05 level of significance. However, the degree of normality is not strong in the lithological unit. This may be due to errors associated with sampling and or laboratory analysis.

5.1.5 UCS Test

The results of UCS of the rock samples obtained from the laboratory analysis are presented in Figure 5.9, Figure 5.10 and Figure 5.11. The results of UCS measurements are presented in Appendix A1.

Figure 5.9 indicates that the mean UCS of the sandstone in Efia Nkwanta beds is 46.6MPa having a standard deviation of 19.4 and a variance of 378.3. The 95% confidence limit for the mean is 40.0 - 53.2 MPa. From the Anderson-Darling normality test, the UCS in the

lithological unit does not follow normal distribution since the *p*-value of the test is less than the 0.05 level of significance. This is possibly due to microstructural anisotropy of the sandstones in the lithological unit or errors during sampling and or laboratory analysis.
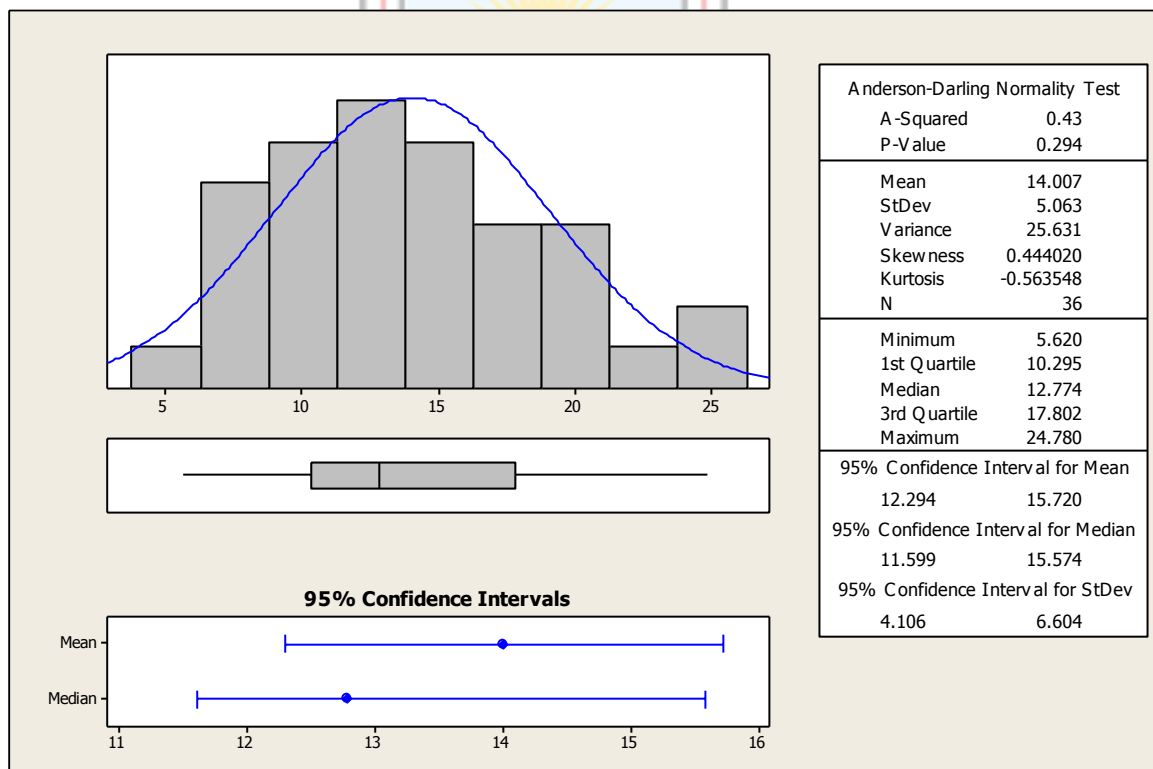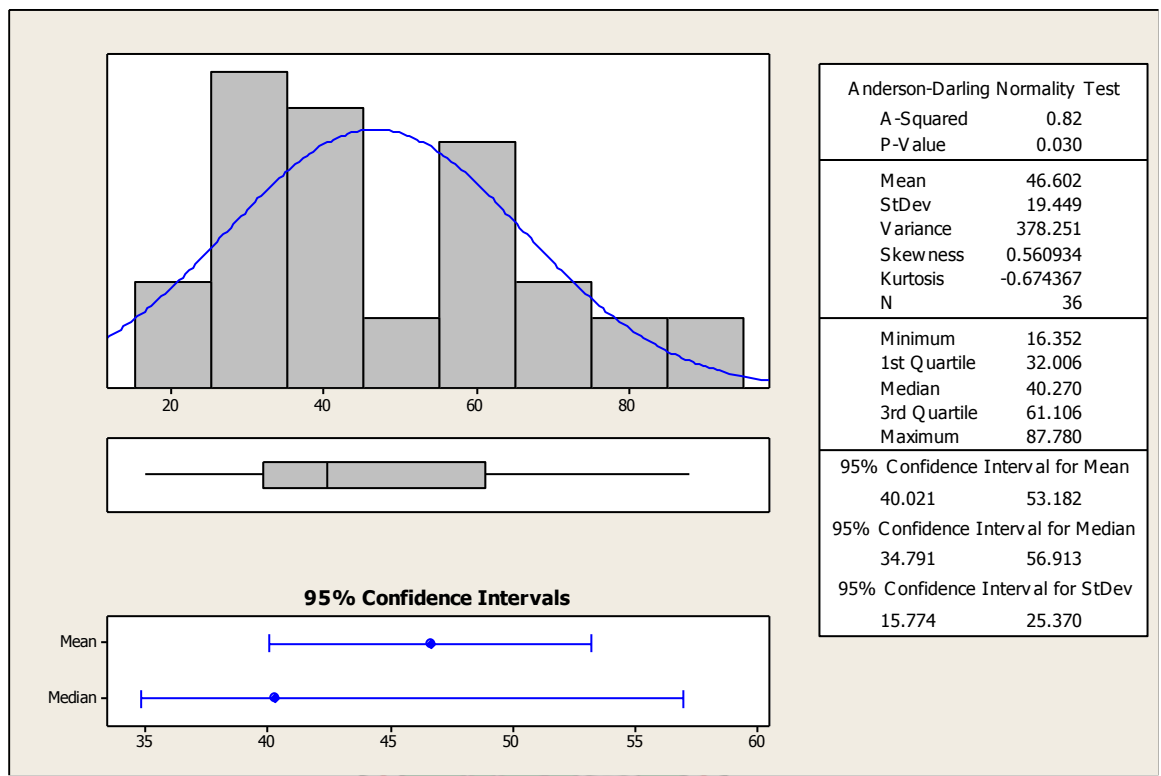

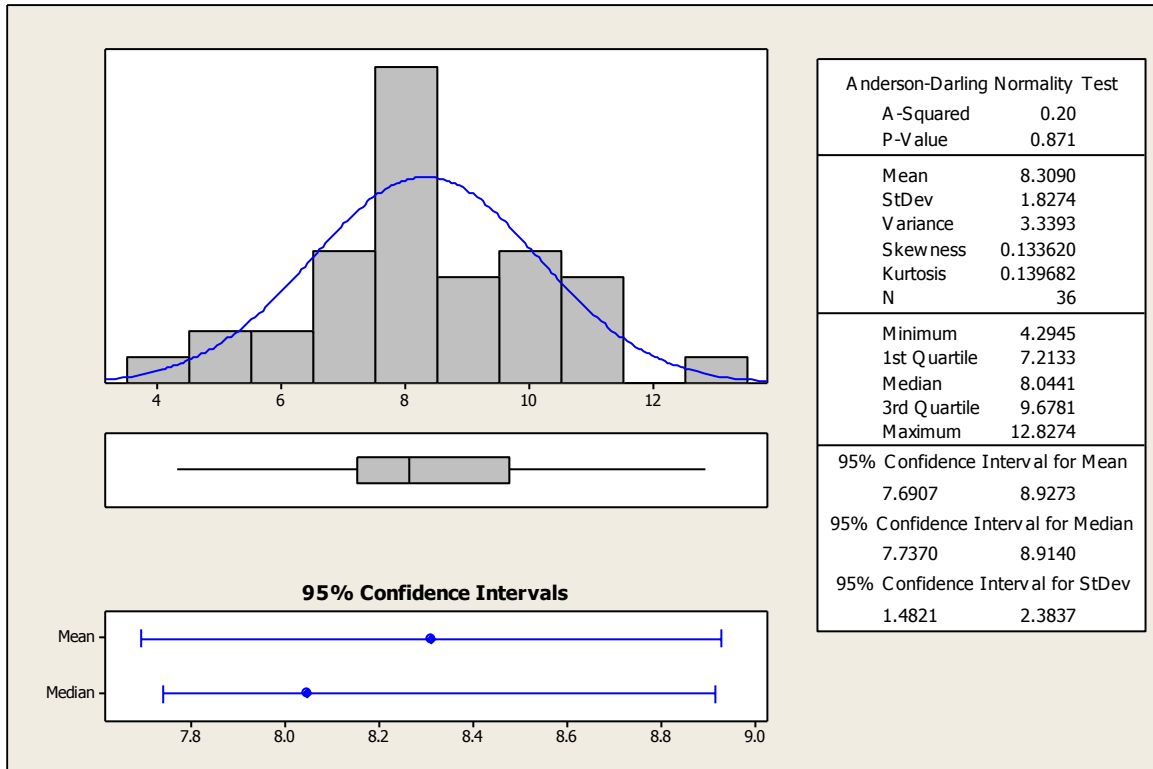**Figure 5.9: The Statistical Summary of UCS in Efia Nkwanta Beds**

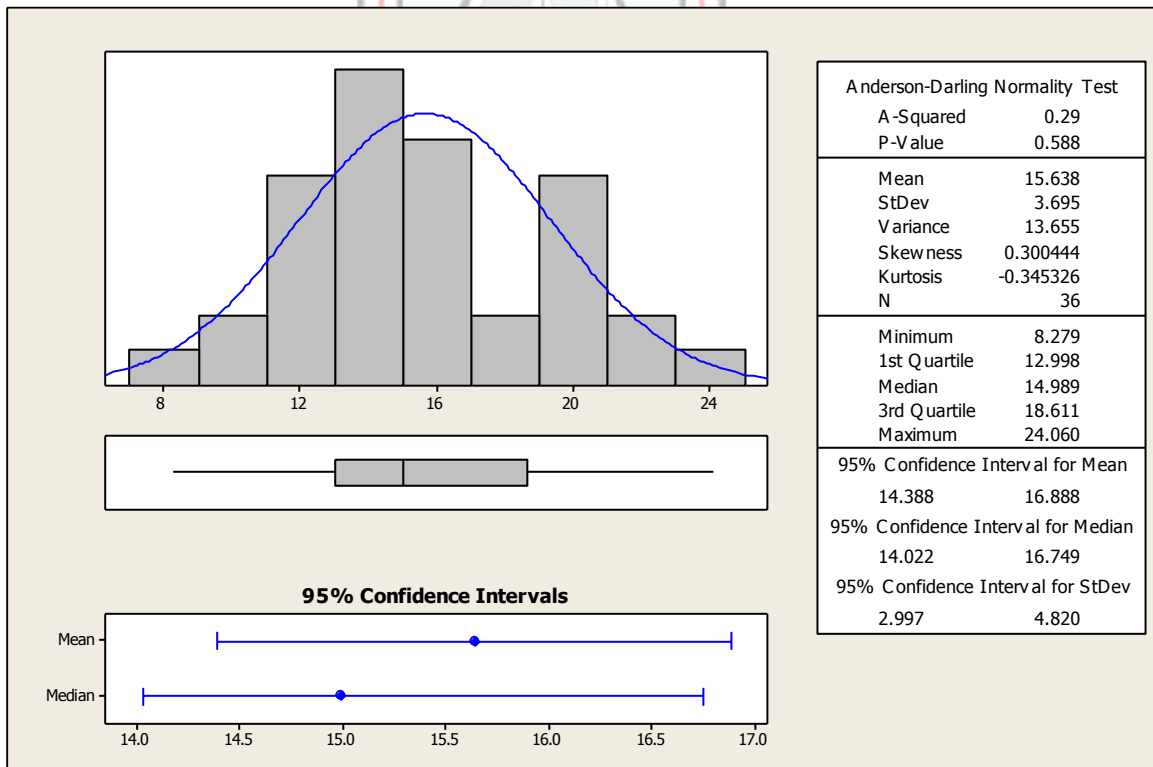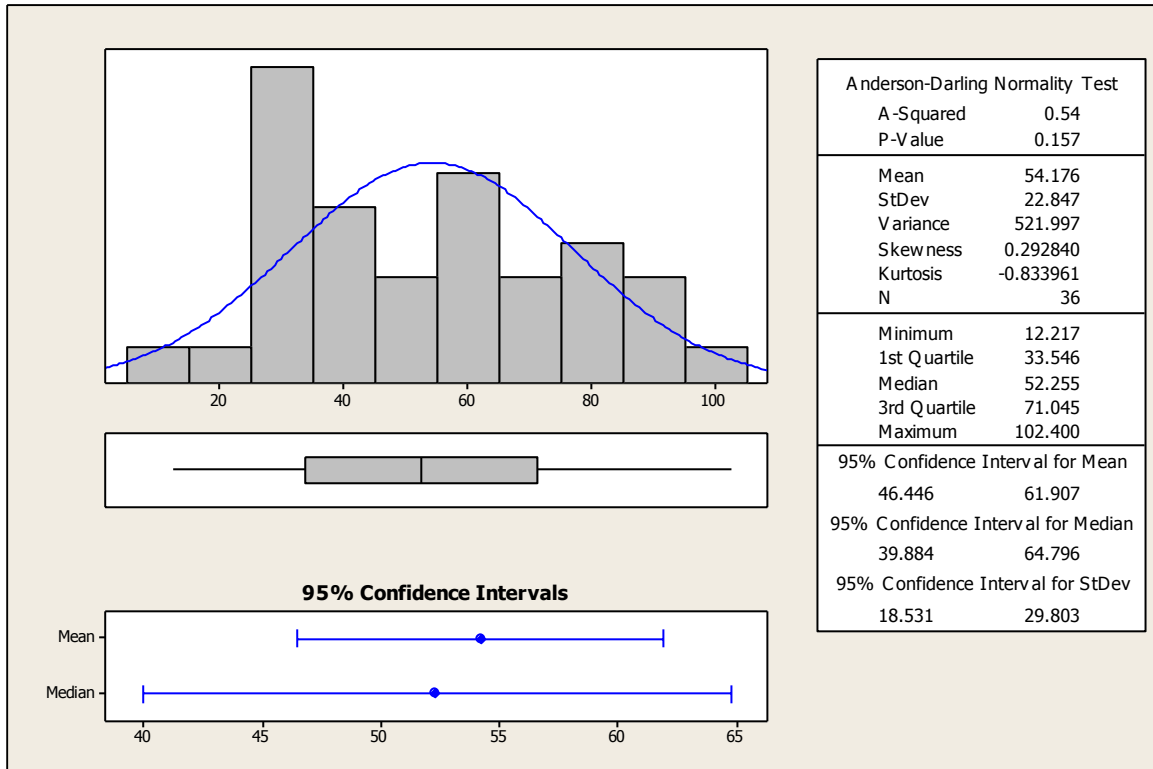**Figure 5.10: The Statistical Summary of UCS in Elmina Sandstone**
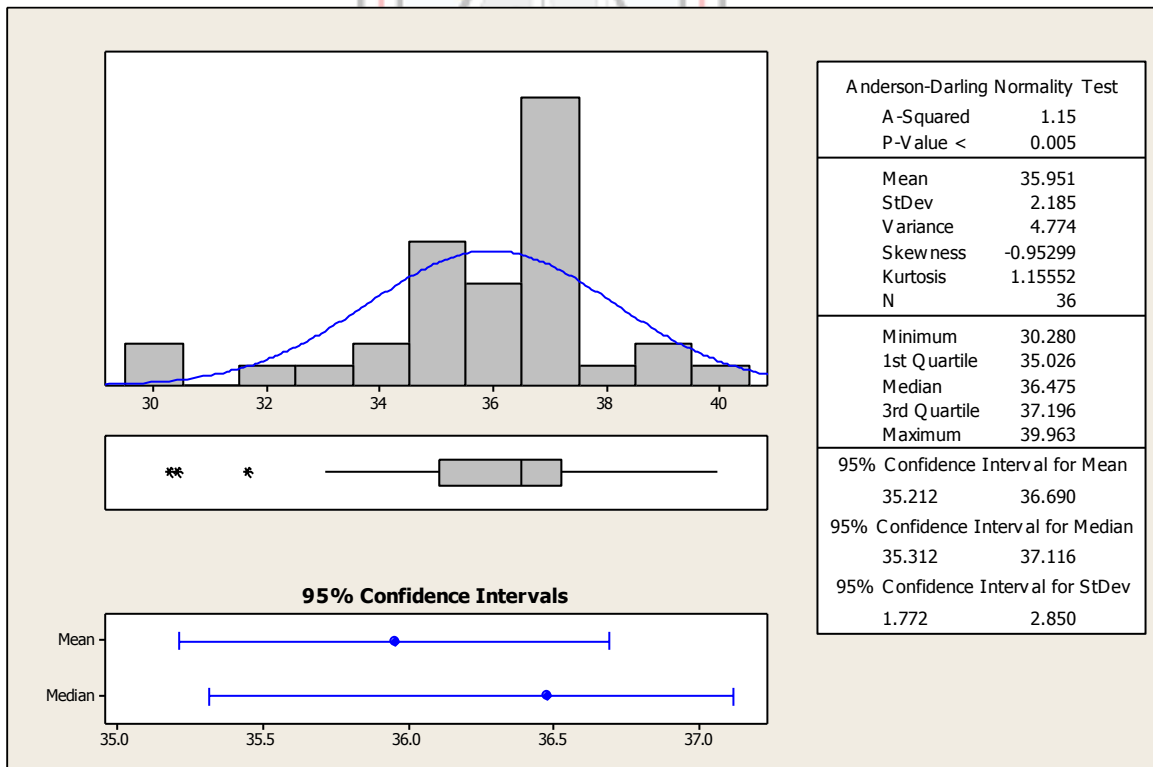
Figure 5.11: The Statistical Summary of UCS in Takoradi Sandstone

Figure 5.10 indicates that the mean UCS of Elmina sandstone is 54.2 MPa having a standard deviation of 22.8and a variance of 521.9. The 95% confidence limit for the mean in the lithological unit is 46.4 - 61.9 MPa. The UCS however follows normal distribution in the lithological unit since the *p*-value of the Anderson-Darling test is greater than the 0.05 level of significance. The degree of normality is however not strong. This is possibly due to microstructural anisotropy of the sandstones in the lithological unit or errors during sampling and or laboratory analysis.

Furthermore, Figure 5.11 indicates that the mean UCS of Takoradi sandstone is 35.9 MPa having a standard deviation of 2.2 and a variance of 4.8. The 95% confidence limit for the mean in the lithological unit is 35.2 and 36.7 MPa. The UCS in the unit does not follow normal distribution since the *p*-value of the Anderson-Darling normality test is less than the 0.05 level of significance. This is possibly due to microstructural anisotropy of the sandstones in the lithological unit or errors during sampling and or laboratory analysis.

5.1.6 Two Tailed One-Sample *t*-Test

To investigate the population mean of porosity, particle density and UCS of sandstones in the lithological units, one sample *t*-test for porosity, density and UCS were performed using Minitab programming language. The hypothesis that each population mean of porosity, particle density and UCS of the sandstones in the lithological units is zero versus it is not zero was tested using two tailed *t*-test. The results for the tests are presented in Table 5.1.

Table 5.1: Results of One Sample Two Tailed *T*-Test

EFIA NKWANTA BEDS			
Parameter	**Mean**	**95% Confidence Interval**	***P*-Value**
Porosity (%)	14.0	12.3 - 15.7	0.0
Particle Density (gcm^{-3})	2.7	2.7- 2.8	0.0
UCS (MPa)	46.6	40.0 - 53.2	0.0
ELMINA SANDSTONE			

Porosity (%)	8.3	7.7 - 8.9	0.0
Particle Density (gcm^{-3})	2.5	2.4 - 2.8	0.0
UCS (MPa)	54.2	46.5 - 61.9	0.0
TAKORADI SANDSTONE			
Porosity (%)	15.6	14.4 - 16.9	0.0
Particle Density (gcm^{-3})	2.6	2.5 - 2.69	0.0
UCS (MPa)	35.9	35.2 - 36.7	0.0

The results in Table 5.1 indicate that the population means are not zero and therefore exist in the lithological units since the *p*-values are less than 0.05 α level of significance. From the results, one could therefore conclude that UCS, porosity and particle density are significant variables in the lithological units.

5.1.7 Analysis of Variance (ANOVA) for Porosity, Particle Density and UCS Results

The test results of the one-way ANOVA for porosity, particle density and UCS in the lithological units performed by the author using Minitab programmable language with input parameters obtained from the laboratory investigations are presented in Table 5.2.

Table 5.2: One-Way ANOVA Results for Porosity, Particle Density and UCS

Parameter (Mean)	Efia Nkwanta Beds	Elmina Sandstone	Takoradi Sandstone	*P*-Value	Pooled Standard Deviation
Porosity (%)	14.0	8.3	15.6	0.0	3.8
Particle Density (gcm^{-3})	2.7	2.5	2.6	0.0	0.2
UCS (MPa)	46.6	54.2	35.9	0.0	17.4

The *p*-values for porosity, particle density and UCS indicate that there are significant differences in porosity, particle density and UCS of sandstones in the lithological units since the *p*-values are less than the 0.05 α level of significance. However, the pooled standard deviation which is a measure of the common variance for sandstones in all the

65

lithological units thus Efia Nkwanta beds, Elmina sandstone and Takoradi sandstone is 3.925 for porosity, 0.1822 for particle density and 17.61 for UCS. This suggests that porosity could not be combined in the three lithological units likewise particle density and UCS. Each lithological unit should therefore be treated separately.

5.1.8 Geomechanical Modeling

The Series geomechanical models were evaluated by correlation and regression methods using Minitab statistical software package with input parameters obtained from the laboratory investigations. The basic principles of the computer software and the review of correlation and regression models are presented in Chapter 3.

Essential geomechanical and petrophysical properties of the lithological units indicated in Appendix A1, Appendix A2 and Appendix A3 were considered for the geomechanical modeling.

Selected Regression Models
The most common regression models used were linear, logarithmic and exponential models in simple and multiple regressions. As indicated in the previous Section, the simple regression was performed to identify the significant predictor variables for subsequent multiple regression modeling based on the *R*-square, *p*- values and residual standard deviation.

Model Assumptions
The assumptions of the models obtained from the geomechanical modeling are:
  i.   Each unit is homogeneous and isotropic.
  ii. The errors are normally distributed with mean zero.
  iii. The error variation does not change for different levels of a lithological unit.
  iv. Each error is independent of all other errors.

Selected Input Parameters

The UCS parameters obtained from the unconfined compression tests, porosity parameters obtained from the saturation tests and the particle density parameters obtained from the specific gravity tests were selected as input parameters for the modeling. The various reasons for the selection are presented in the various Sections in Chapter 4. The selected input parameters used for the modeling are however summarized in Appendix A1, Appendix A2 and Appendix A3.

5.1.9 Correlation Modeling

Fresh samples were investigated for UCS, porosity and particle density as presented in Chapter 4. Each lithological unit was sampled at thirty six (36) different locations which is a representative of the unit. Thirty six (36) samples for each variable were used for the correlation modeling. The correlation coefficients were modeled using Minitab statistical software as discussed in Chapter 3. Finally, the hypotheses of the correlation coefficients were tested as whether linear associations existed between the predictor variables and the response variable in the lithological units as against the alternative hypotheses with the *t*-statistic. The results of the correlation models are presented in Table 5.3 below.

Table 5.3: Results of Correlation Models

EFIA NKWANTA BEDS		
Correlation	Correlation Coefficient, *r*	*P*-Value
UCS versus Porosity	-0.351	0.036
UCS versus Particle Density	-0.194	0.258
ELMINA SANDSTONE		
UCS versus Porosity	-0.067	0.698
UCS versus Particle Density	0.305	0.070
TAKORADI SANDSTONE		
UCS versus Porosity	-0.054	0.753
UCS versus Particle Density	0.079	0.646

The correlation coefficients suggest that there is association between UCS and porosity, and UCS and particle density in all lithological units. The association however is moderate

between UCS and porosity in Efia Nkwanta beds though in the reverse direction but weaker between UCS and particle density. Also, the association between UCS and porosity in both Elmina sandstone and Takoradi sandstone are weaker. However, the association between UCS and particle density is weaker in both Elmina sandstone and Takoradi sandstone. The *p*-values further suggest that a linear association only exists between UCS and porosity in Efia Nkwanta beds since the *p*-value is less than the α-level of significance (0.05).

5.1.10 Regression Modeling

Simple and multiple regression modellings were performed in all lithological units using Minitab programmable language. The significance of the models was tested by testing the hypotheses of the regression coefficients and the regression relations using *t*- and *f*-statistics to ascertain the validity of the models.

The *t*-statistic was used to test the significance of the regression coefficients whereas the *F*-statistic (analysis of variance approach) was used to test the significance of the overall regression models using the *p*-values. This was done by formulating the null hypothesis as significant as against the alternative hypothesis as insignificant in accordance with Minitab 16 programmable language. The modeling was carried out using Minitab software programming language. Figure 5.12, Figure 5.13, Figure 5.14, Figure 5.15, Figure 5.16 and Figure 5.17 show the scatter plots for UCS versus petrophysical properties in the three lithological units using Microsoft excel. The purpose of the scatter plots was to ascertain the "first hand" relation that would exist between the response and the predictor variables.
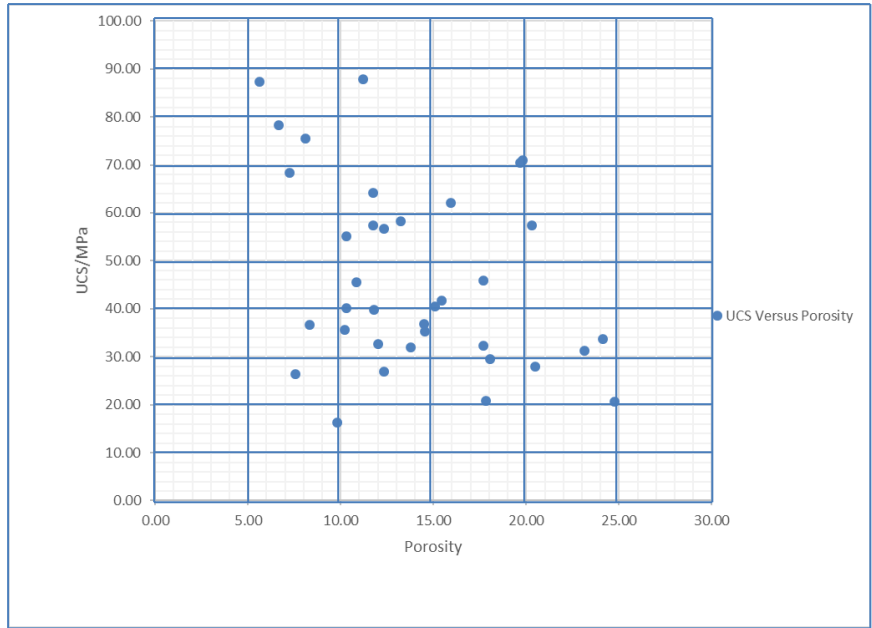
Figure 5.12: Scatter Plot for UCS Versus Porosity in Efia Nkwanta Beds
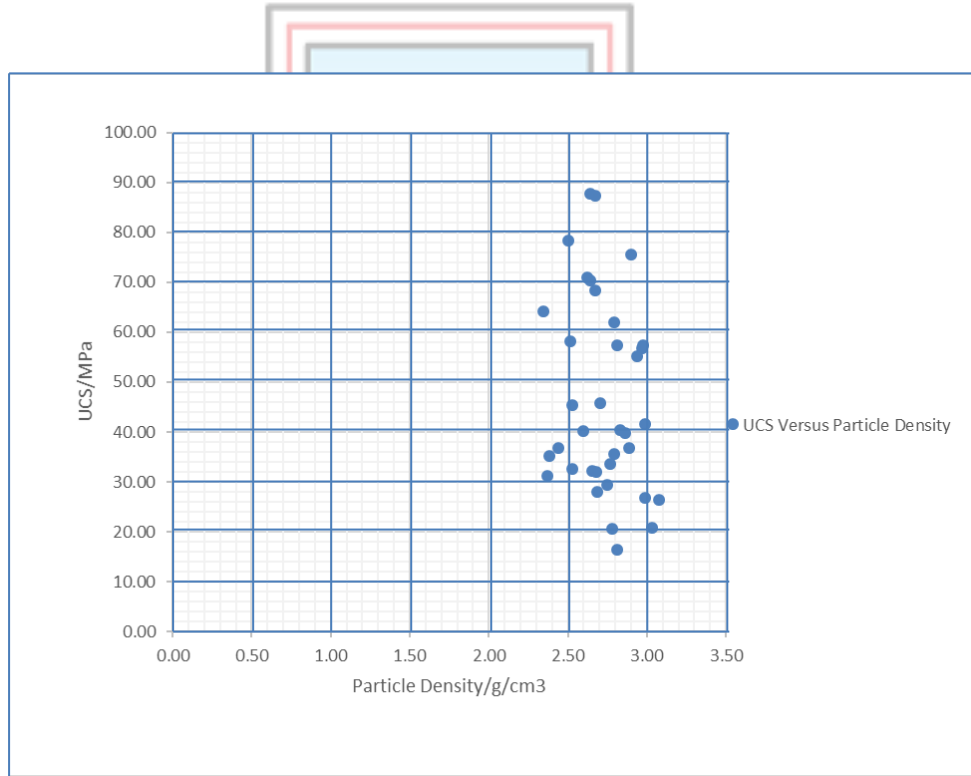
Figure 5.13: Scatter Plot for UCS Versus Particle Density in Efia Nkwanta Beds
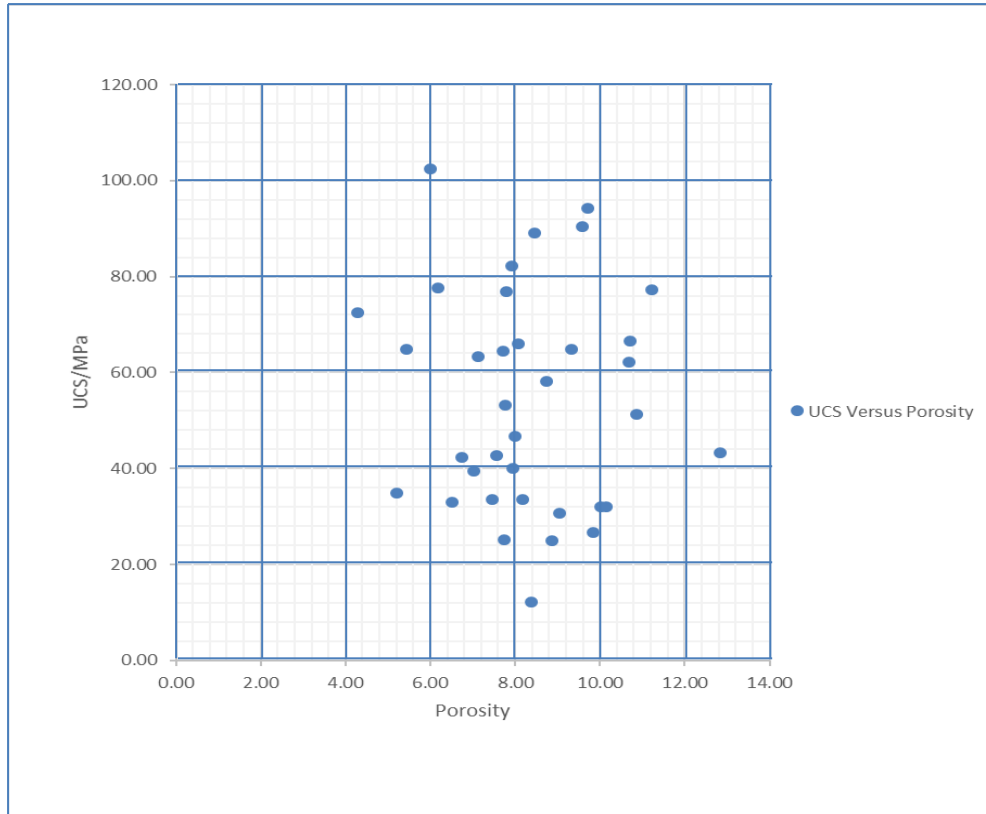
Figure 5.14: Scatter Plot for UCS Versus Porosity in Elmina Sandstone
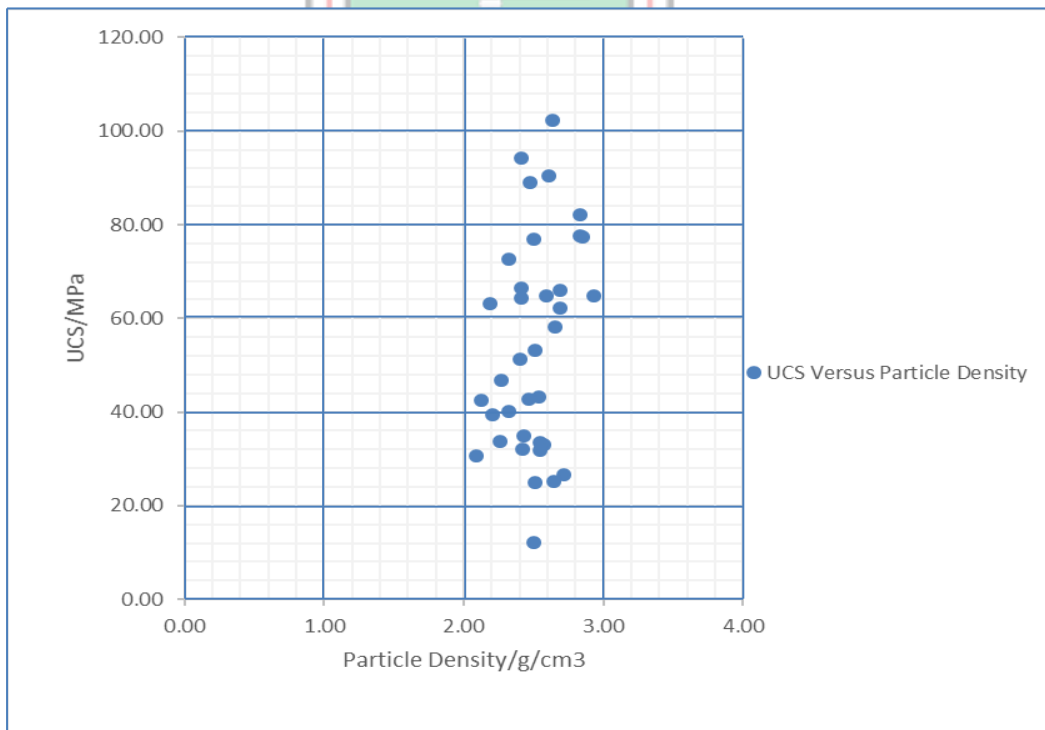
Figure 5.15: Scatter Plot for UCS Versus Particle Density in Elmina Sandstone
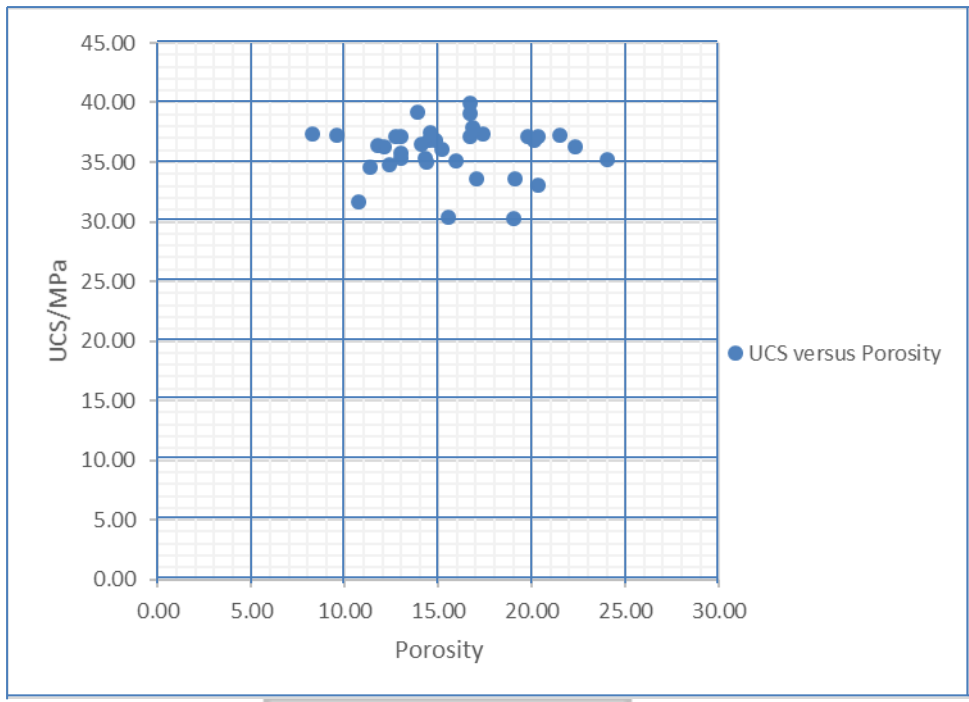
Figure 5.16: Scatter Plot for UCS Versus Porosity in Takoradi Sandstone
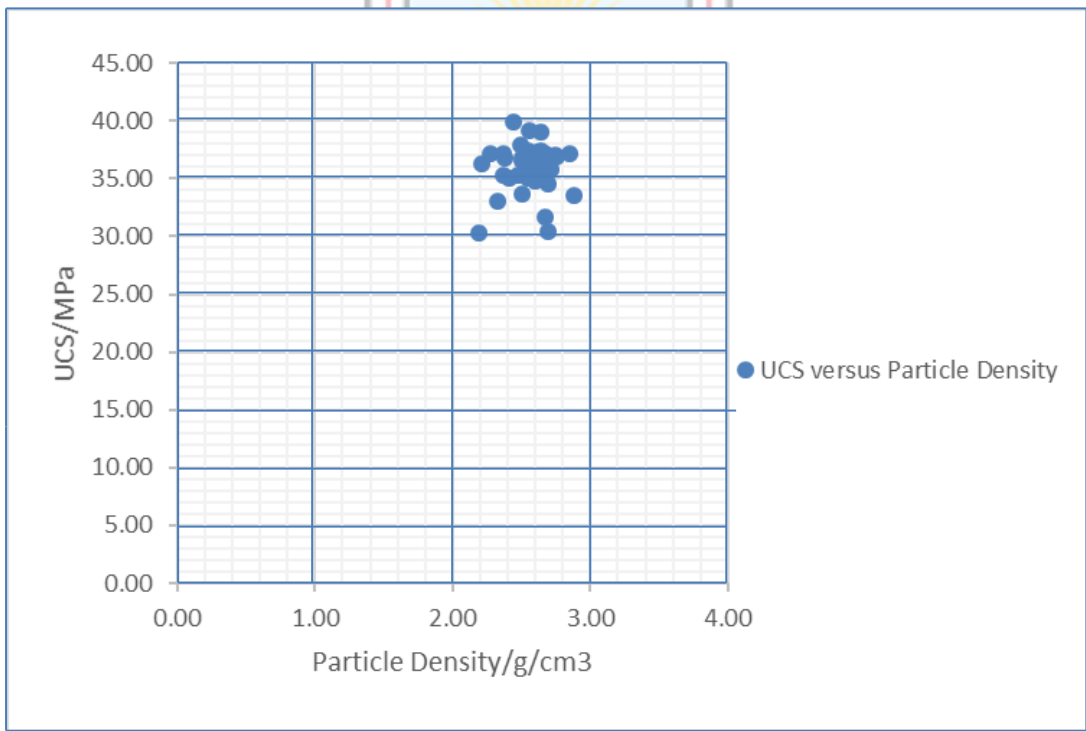
Figure 5.17: Scatter Plot for UCS Versus Particle Density in Takoradi Sandstone

The scatter plots above indicate that a significant relation only exists between UCS and porosity in the sandstones in Efia Nkwanta beds (see Figure 5.12).

Simple Regression Modeling

Simple regression modeling was used to obtain the relation between UCS and each petrophysical property in all the lithological units. This was performed using Minitab 16 programmable language. As stated in Section 5.1.9, 36 of the input parameters were used for the modeling for the response variable and each predictor variable in each lithological unit. This was performed to obtain significant relations for onward multiple regression modeling. The results of the simple regression modeling are present in the Sections below.

Simple Regression Modeling of Efia Nkwanta Beds

The results of the simple regression models obtained for the sandstones in Efia Nkwanta beds are presented in Figure 5.18 and Figure 5.19, and summarized in Table 5.4 and Table 5.5.

Figure 5.18: Simple Regression Fitted Model for UCS Versus Porosity in Efia Nkwanta Beds

Table 5.4 shows the selected simple regression model as indicated in Figure 5.18 above and the alternative model based on the *R*-square, *p*-value and simplicity.

Table 5.4: Selected and Alternative Simple Regression Models for UCS versus Porosity in Efia Nkwanta Beds

Model Characteristics	Selected Model	Alternative Model
Equation	UCS = 65.5 - 1.35 υ	ln(UCS) = 4.14077 - 0.0275485 υ
R-Square	12.3%	10.58%
P-Value	0.036	0.053
Residual Standard Deviation	18.475	0.4114

In Table 5.4, 12.3% of the variations of UCS could be accounted for by porosity in the selected model whilst 10.6% of the variation of UCS could be accounted for by porosity in the transformed alternative model. The selected and alternative models were tested using the *F*-statistic by formulating the null hypothesis as significant as against the alternative hypothesis as insignificant. The *p*-values for the tests indicate that the selected model is significant since the *p*-value is less than the α-level of significance. Furthermore, the difference between observed and predicted value is 18.5 for the selected model while that for the alternative model is 0.4.

The simple regression fitted model obtained for UCS versus particle density in Efia Nkwanta beds is presented in Figure 5.19 and summarized in Table 5.5.
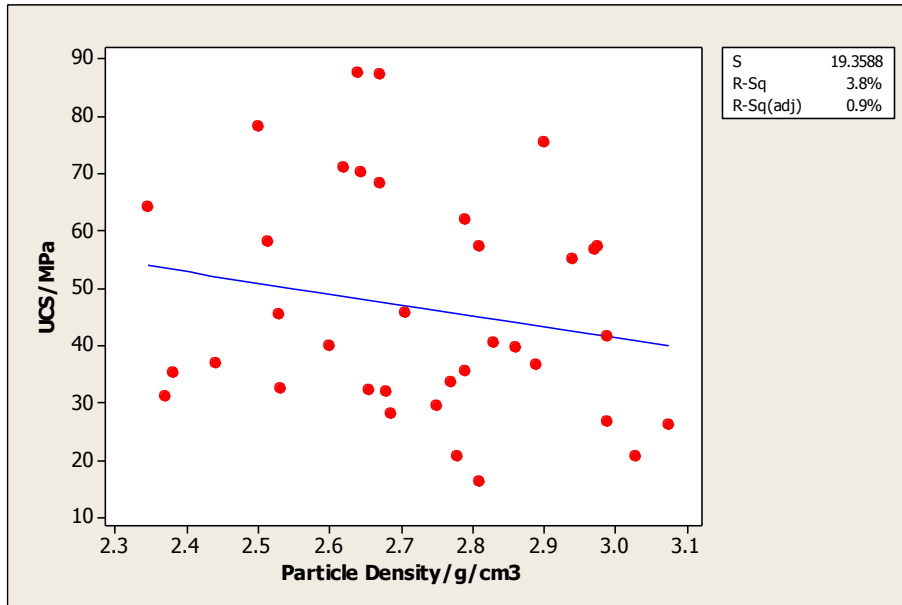
Figure 5.19: Simple Regression Fitted Model for UCS versus Particle Density in Efia Nkwanta Beds

Table 5.5 shows the selected simple regression model as indicated in Figure 5.19 and the alternative model based on the R-square, p-value and simplicity.

Table 5.5: Selected and Alternative Simple Regression Models for UCS versus Particle Density in Efia Nkwanta Beds

Model Characteristics	Selected Model	Alternative Model
Equation	UCS = 99.07 - 19.25 ρ	ln(UCS) = 5.02736 - 0.466791 ρ
R-Square	3.8%	4.5%
P-Value	0.3	0.2

In Table 5.5, 3.8% of the variations of UCS could be accounted for by particle density in the selected model whilst 4.5% of the variation of UCS could be accounted for by particle density in the transformed alternative model. The selected and alternative models were tested with the F-statistic by formulating the null hypothesis as significant as against the alternative hypothesis as insignificant. This was based on Minitab 16 programmable language. The p-values for the tests indicate that the selected and alternative models are insignificant since the p-values are greater than the α-level of significance (0.05). Though, the extent of significance of the selected linear model is less than that of the alternative logarithmic model, the simple linear model is selected due to its simplicity.

Simple Regression Modeling for Elmina Sandstone

The results of simple regression models obtained for UCS versus porosity, and UCS versus particle density in Elmina sandstone are presented in Figure 5.20 and Figure 5.21, and Summarized in Table 5.6 and Table 5.7.
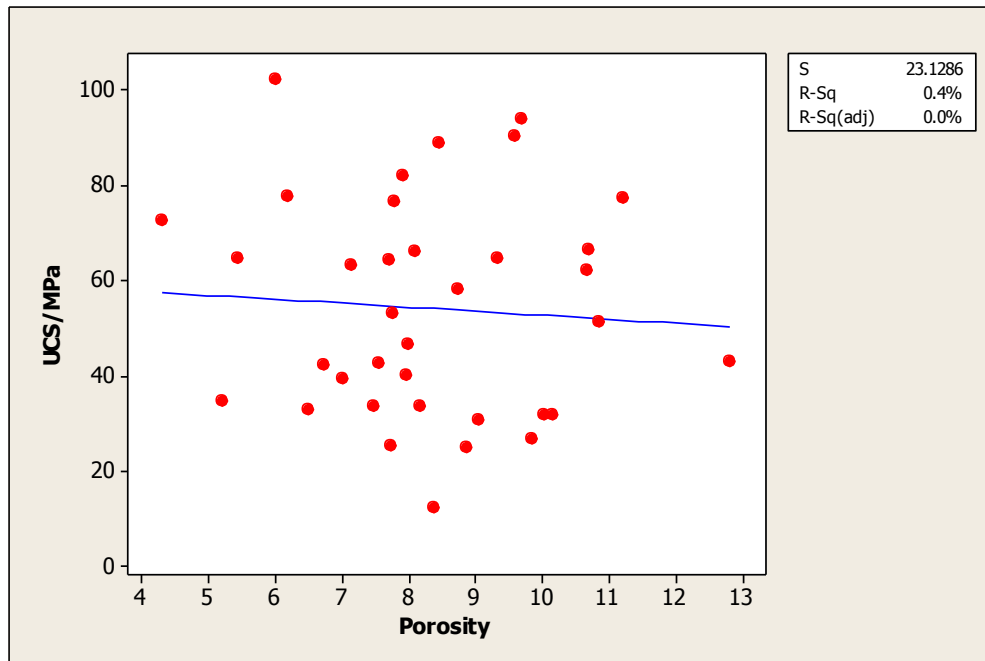
Figure 5.20: Simple Regression Fitted Model for UCS versus Porosity in Elmina Sandstone

Table 5.6 shows the selected simple regression model as indicated in Figure 5.20 above and the alternative model based on the *R*-square, *p*-value and simplicity.

Table 5.6: Selected and Alternative Simple Regression Models for UCS versus Porosity in Elmina Sandstone

Model Characteristics	Selected Model	Alternative Model
Equation	UCS = 61.14 - 0.838 υ	UCS^0.5 = 7.65428 - 0.0558036 υ
***R*-Square**	0.4%	0.4%
***P*-Value**	0.7	0.7

In Table 5.6, 0.4% of the variations of UCS could be accounted for by porosity in the selected model. Likewise, 0.4% of the variation of UCS could be accounted for by porosity in the transformed alternative model. The selected and alternative models were

75

tested with the *F*-statistic by formulating the null hypothesis as significant as against the alternative hypothesis as insignificant. This was based on Minitab 16 programmable language. The *p*-values for the tests indicate that the selected and alternative models are insignificant since the *p*-values are greater than the α-level of significance (0.05). The extent of significance of the selected linear model is greater than that of the alternative exponential model.

The simple regression fitted model obtained for UCS versus particle density in Elmina sandstone is presented in Figure 5.5.
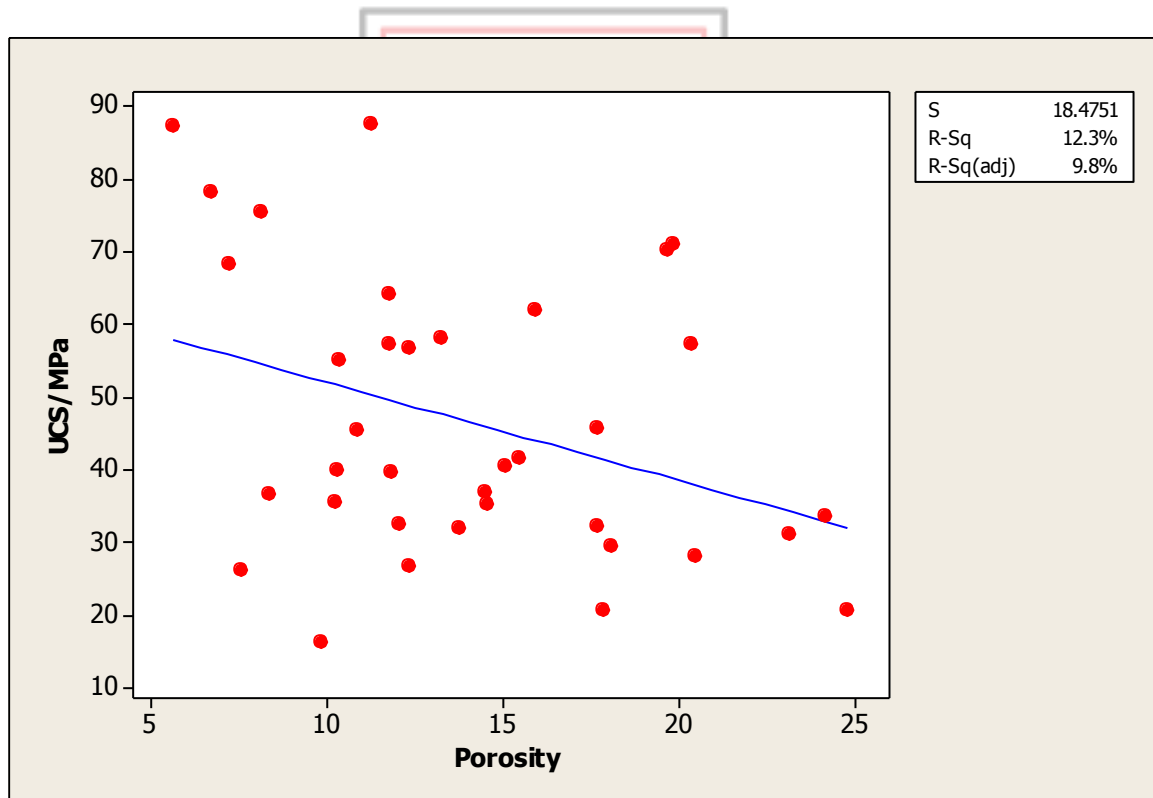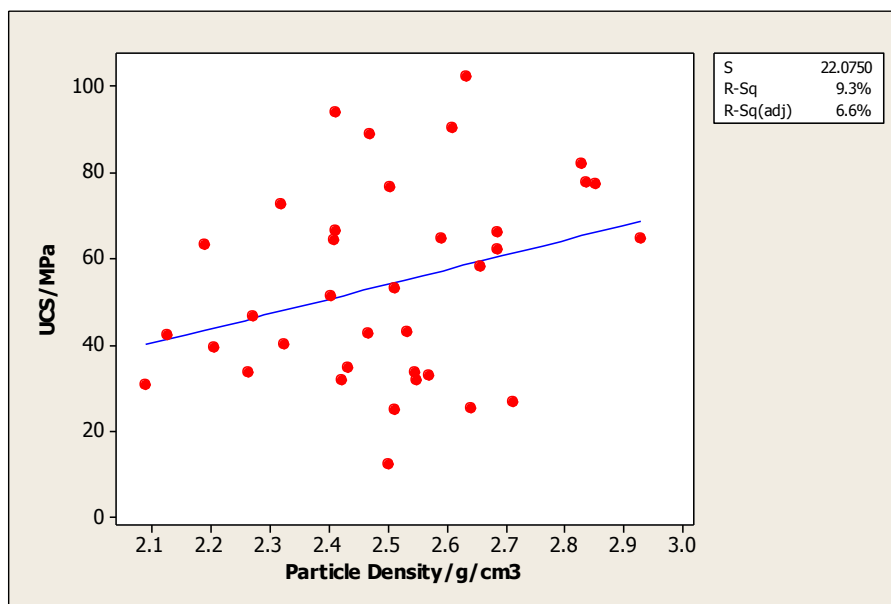

Figure 5.21: Simple Regression Fitted Model for UCS versus Particle Density in Elmina Sandstone

Table 5.7 shows the selected simple regression model as indicated in Figure 5.21 above and the alternative model based on the *R*-square, *p*-value and simplicity.

Table 5.7: Selected and Alternative Simple Regression Models for UCS versus Particle Density in Elmina Sandstone

Model Characteristics	Selected Model	Alternative Model
Equation	UCS = - 31.67 + 34.29 ρ	UCS^0.5 = 1.61 + 2.23 ρ
_R_-Square	9.3%	8.1%
_P_-Value	0.07	0.09

In Table 5.7, 9.3% of the variations of UCS could be accounted for by particle density in the selected model whilst 8.1% of the variation of UCS could be accounted for by particle density in the transformed alternative model. The selected and alternative models were tested with the *F*-statistic by formulating the null hypothesis as significant as against the alternative hypothesis as insignificant. This was based on Minitab 16 programmable language. The *p*-values for the tests indicate that the selected and alternative models are insignificant since the *p*-values are greater than the *α*-level of significance (0.05). However, the extent of significance of the linear model is greater than that of the exponential model.

Simple Regression Modeling of Takoradi Sandstone

The results of simple regression models obtained for UCS versus porosity, and UCS versus particle density for Takoradi sandstone are presented in Figure 5.22 and Figure 5.23 and Summarized in Table 5.8 and Table 5.9.

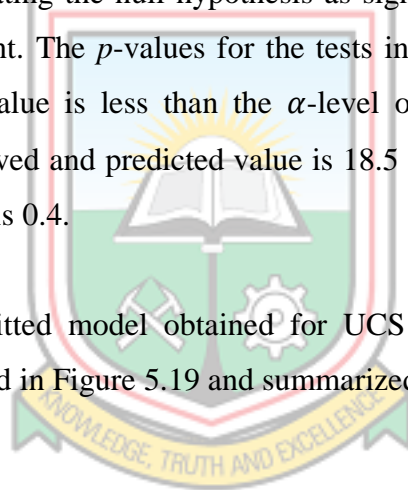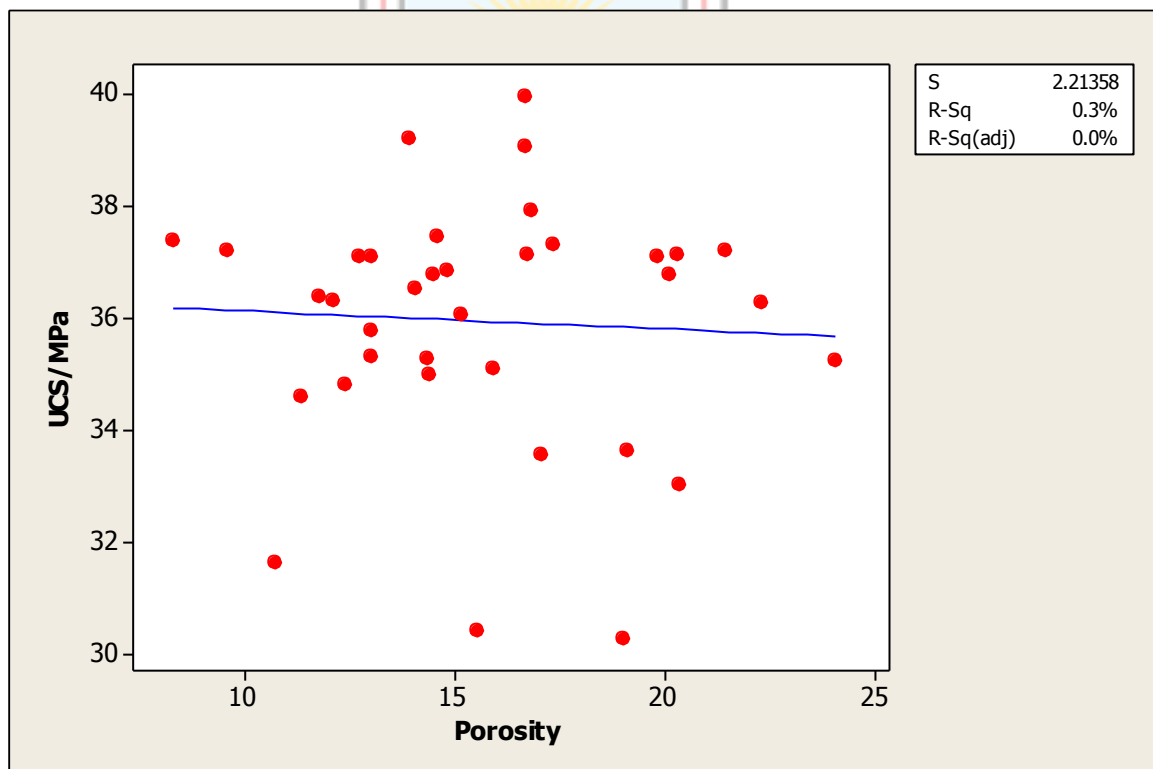**Figure 5.22: Simple Regression Fitted Model for UCS versus Porosity in Takoradi Sandstone**

Table 5.8: Selected and Alternative Simple Regression Models for UCS versus Porosity in Takoradi Sandstone

Model Characteristics	Selected Model	Alternative Model
Equation	UCS = 36.45 - 0.03 υ	(UCS^5)/(6*36^(5)) = 6.7 - 0.02 υ
R-Square	0.3%	0.2%
P-Value	0.8	0.8

In Table 5.8, 0.3% of the variations of UCS could be accounted for by porosity in the selected model whilst 0.2% of the variation of UCS could be accounted for by porosity in the transformed alternative model. The selected and alternative models were tested with the *F*-statistic by formulating the null hypothesis as significant as against the alternative hypothesis as insignificant. This was based on Minitab 16 programmable language. The *p*-values for the tests indicate that the selected and alternative models are insignificant since the *p*-values are greater than the α-level of significance. However, the extent of significance of the selected linear model is greater than that of the alternative exponential model. The simple linear model is therefore selected.
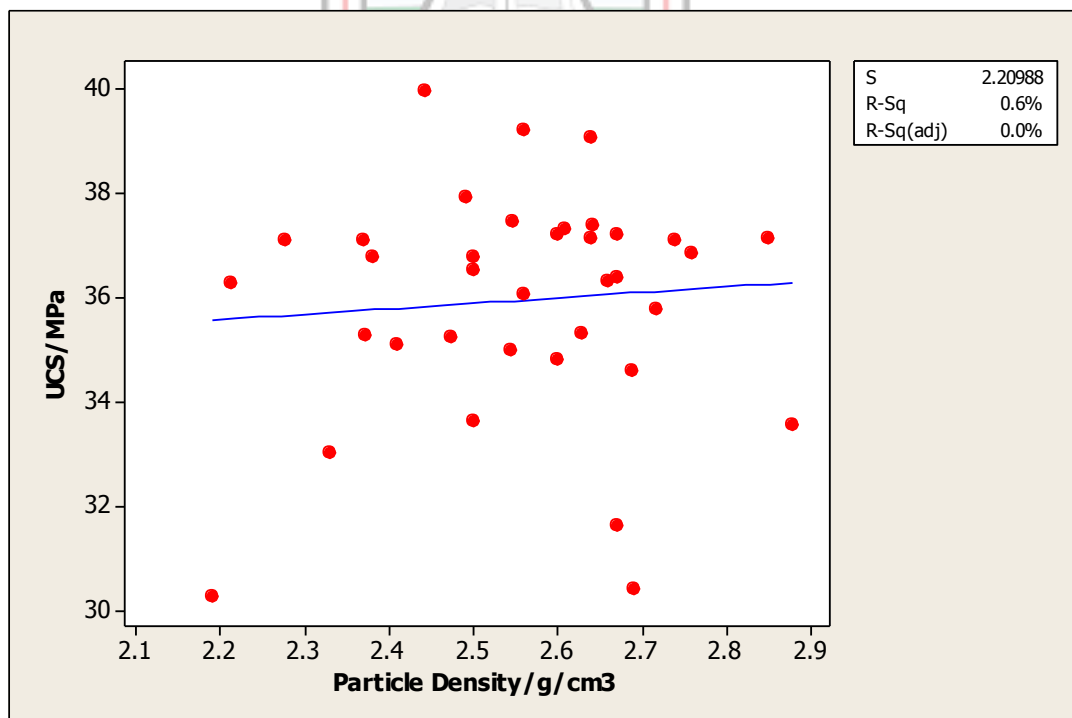
Figure 5.23: Simple Regression Fitted Model for UCS versus Particle Density in Takoradi Sandstone

Table 5.9: Selected and Alternative Simple Regression Models for UCS versus Particle density in Takoradi Sandstone

Model Characteristics	Selected Model	Alternative Model
Equation	UCS = 33.26 + 1.052 ρ	(UCS^5)/(6*36^(5)) = 4.66 + 0.66ρ
_R_-Square	0.6%	0.3%
_P_-Value	0.6	0.8

In Table 5.9, 0.6% of the variations of UCS could be accounted for by particle density in the selected model whilst 0.3% of the variation of UCS could be accounted for by particle density in the transformed alternative model. The selected and alternative models were tested with the _F_-statistic by formulating the null hypothesis as significant as against the alternative hypothesis as insignificant. This was based on Minitab 16 algorisms. The _p_-values for the tests indicate that the selected and alternative models are insignificant since the _p_-values are greater than the α-level of significance. However, the extent of significance of the selected linear model is greater than that of the alternative exponential model; the simple linear model is selected due to its simplicity.

Multiple Regression Modeling

Multiple regression modeling was used to obtain a relationship between UCS and the predictor variables in Efia Nkwanta lithological unit only. However, the multiple regression could not be used to fit UCS and the predictor variables (porosity and particle density) in Elmina sandstone and Takoradi sandstone since the simple regression presented in the previous Sections gave an indication that both porosity and particle density could not fit with UCS. Simple regression gave an indication that porosity is well fit with UCS in Efia Nkwanta beds (see Table 5.5). The multiple regression modeling was performed using Minitab programmable language. As stated in Section 5.1.9, 36 of the input parameters were used for the modeling.

The model obtained was tested using the _F_-statistics by formulating the null hypothesis as at least a relation exists between UCS, porosity and particle density as against the alternative hypothesis as no relation exists between them. Likewise, the _F_-statistic was used to test the relation between UCS and porosity, and UCS and particle density separately in the model. The hypothesis that a relation exists between them was

formulated as against the alternative. The results of the multiple regression model are summarized in Table 5.10. Residual versus fit analyses are presented in Figure 5.24.

Table 5.10: Fitted Multiple Regression Model in Efia Nkwanta Beds

Model Characteristics	Selected Model
Equation	UCS = 126 - 1.41 υ - 21.8 ρ
_R_-Square	17.1%
_P_-Value (model)	0.05
_p_-Value (Porosity term)	0.03
_p_-Value (Particle Density term)	0.2
Residual Standard Error	18.2

In Table 5.10, the selected model that describes the relationship between UCS, porosity and particle density in Efia Nkwanta beds is UCS = 126 - 1.41 υ - 21.8 ρ. In the model, only 17.1% of the variation of UCS could be accounted for by porosity and particle density. The relationship between UCS and porosity in the model was tested using the _F_-statistic to determine the significance by formulating the null hypothesis as significant as against the alternative hypothesis as insignificant. The test suggests that the relationship between UCS and porosity is significant since the _p_-value is less than the level of significance. This suggests that porosity is well fit in the model. Likewise, the relationship between UCS and particle density in the model was tested using the _F_-statistic to determine the significance by formulating the null hypothesis as significant as against the alternative hypothesis as insignificant. The test suggests that the relationship between UCS and particle density is insignificant since its _p_-value is greater than the level of significance. This suggests that particle density is not well fit in the model as indicated in the simple regression model in Table 5.5.

The relationship between UCS, porosity and particle density in the model was tested using the _F_-statistic to determine the significance of the model by formulating the null hypothesis as the model is significant as against the alternative hypothesis as insignificant. The _p_-value for the model suggests that the model is significant since the _p_-value is less than the level of significance. The _p_-value for the model also suggests that both porosity and particle density are well fit in the model.

Comparison of the Simple and Multiple Regression Models

The fitted simple regression model obtained in Efia Nkwanta beds is UCS = 65.5 - 1.35 υ with a tested *p*-value of 0.04 and a residual standard deviation of 18.5. However, the fitted multiple regression model obtained in Efia Nkwanta beds is UCS = 126 - 1.41 υ - 21.8 ρ with a tested *p*-value of 0.05 and a residual standard deviation of 18.2. Both models are well fit, however the *p*-values suggest that the simple regression model is better fit than the multiple regression model. The residual standard deviations indicate that the difference between observed and predicted observation for the simple model is 18.5 and 18.2 for the multiple regression model.

Furthermore, the normal probability plot in Figure 5.24 indicates that the residuals follow a straight line for the simple regression model. Hence, there is no evidence of nonnormality, skewness, outliers or unidentified variables. Also, for the residual order plot indicated in Figure 5.24, the residuals are randomly scattered about the zero line. Hence, there is no evidence that the errors are correlated with one another. However, the histogram of the residuals show in Figure 5.24 indicates a slight skewness. This is an indication that few outliers exists in the data.

In Figure 5.25, the normal probability plot indicates that the residuals also follow a straight line for the multiple regression model with few deviations. There is no evidence of nonnormality, skewness and outliers. Also, for the residual order plot indicated in Figure 5.25, the residuals are randomly scattered about the zero line. Hence, there is no evidence that the errors are correlated with one another. Likewise, the histogram of the residuals indicates a slight skewness. This is an indication that few outliers also exist in the data.

In a whole, the simple regression model is better fit than the multiple regression model in the Efia Nkwanta beds.
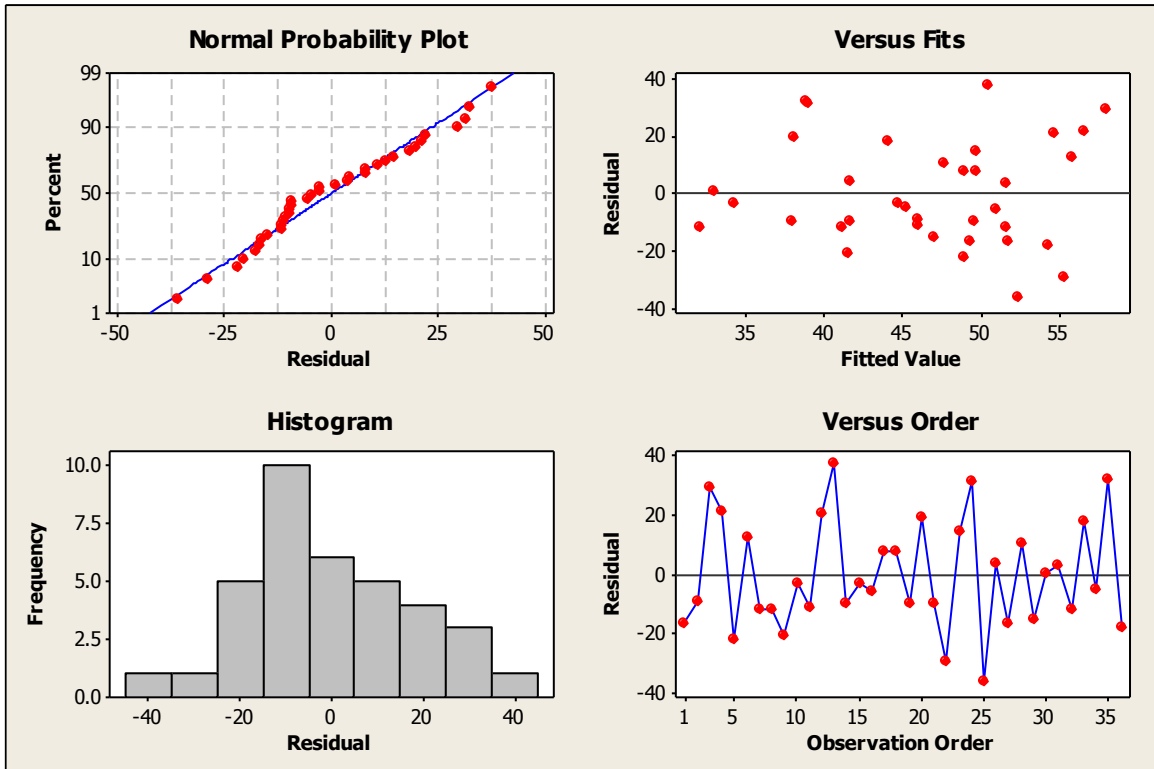
Figure 5.24: Residual Plots for the Simple Regression Model in Efia Nkwanta Beds
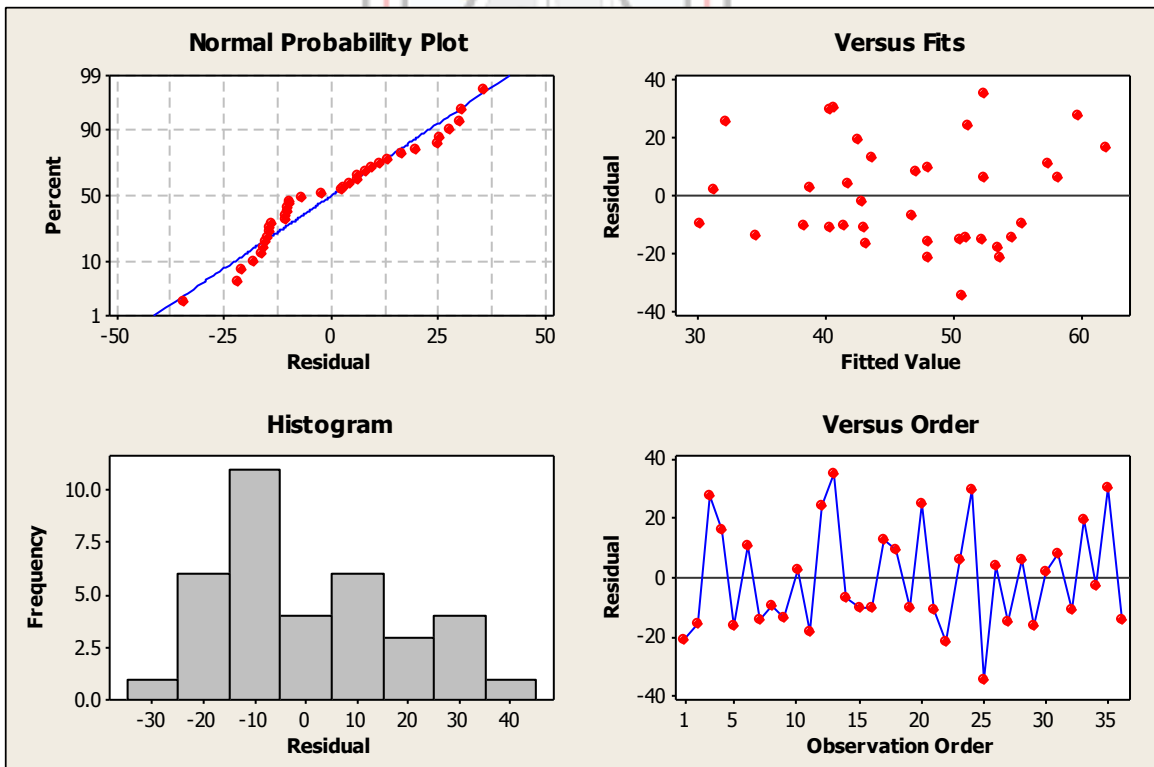
Figure 5.25: Residual Plots for the Multiple Regression Model in Efia Nkwanta Beds

5.2 Discussions

Three lithological units were selected for the study in the Sekondian Group: Efia Nkwanta sandstone, Elmina sandstone and Takoradi sandstone.

5.2.1 Porosity

The mean porosity for the sandstones in Efia Nkwanta beds is 14.0% having a 95% confidence interval of 12.3 - 15.7%. Also, the mean porosity for Elmina sandstone is 8.309% having a 95% confidence interval of 7.7 - 8.9%. Takoradi sandstone has a mean porosity of 15.6% having a 95% confidence interval of 14.4 - 16.9%.

From the ANOVA outcomes presented in Section 5.1.7, there are significant differences in porosity in the Series. The analysis indicates that Elmina sandstone has the lowest porosity whilst Takoradi sandstone has the highest porosity. These differences are due to differences in microstructural parameters (texture) in the lithological units in the Sekondian Group as described in the sieve and petrographic analyses in Section 5.1.1 and Section 5.1.2 respectively. The microstructural parameters such as grain size, grain packing and sorting, particle shape, and the distribution of grain sizes according to Chatterjee *et al*. (2013) and Glover (2017) affect porosity in which Al-Homadhi and Hamada (2001) associated it as depositional conditions. When the degree of sorting of grains increases, porosity also increases. However, connected porosity may not be due to particle shape. Particles with subangular to angular shape would decrease connected porosity due to interlocking as sorting increases.

From the petrographic and sieve analyses in addition to the theoretical background in Chapter 2 and 3, the textural characteristics of the sandstones in Efia Nkwanta beds are fine grained and well sorted but the Elmina sandstone are medium to coarse grained and poorly sorted with sub angular to angular shape. Likewise, the Takoradi sandstone is fine to medium to coarse grained and poorly sorted with sub angular to angular shape. Fine and well sorted grains have higher porosity than that of coarse and poorly sorted grains (Glover, 2017). Also, rounded grains have higher connected pores than sub angular to angular shape grains due to the interlocking of the grains. As discussed and presented in

Chapter 3, secondary porosity resulting from secondary processes is higher than primary porosity.

The petrographic analysis (see Figure 5.2c, Section 5.1.2) shows that the Takoradi sandstones have microcracks. This is due to diagenesis such as mechanical processes (e.g. stress compaction, brittle deformation and fracture evolution) and geochemical processes (e.g.dissolution, precipitation, and mineralogical changes) resulting in the highest porosity. These microcracks give the microstructural anisotropy of the Takoradi sandstones as also observed in the normality test in Figure 5.11. The sandstones in Efia Nkwanta beds are fine grained and well sorted. This therefore accounts for the higher porosity of the Efia Nkwanta lithological unit than the Elmina sandstone having moderately sorted grains with subangular to angular shape.

5.2.2 Particle Density

The mean particle density of the sandstones in Efia Nkwanta beds is 2.7 gcm^{-3} having a 95% confidence interval of 2.7 - 2.8 gcm^{-3}. Also, the mean particle density of Elmina sandstone is 2.5035 gcm^{-3} having a 95% confidence interval of 2.4 - 2.6 gcm^{-3}. Takoradi sandstone has a mean particle density of 2.6 gcm^{-3} having a 95% confidence interval of 2.5 - 2.6 gcm^{-3}.
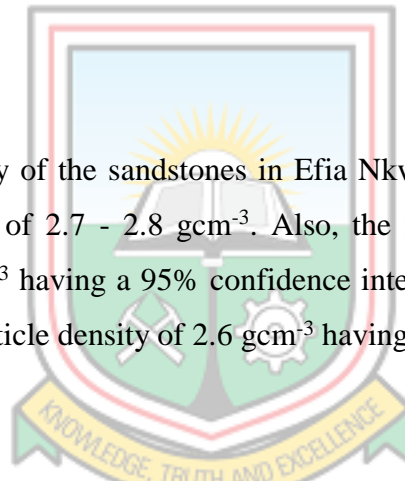
From the ANOVA outcomes presented in Section 5.1.7, there are significant differences in particle density in the lithological units. The analysis indicated that Efia Nkwanta beds have the highest particle density whilst Elmina sandstone has the lowest particle density.

Particle density is a measure of the modal composition of rocks that is the grain size distribution and sorting of grains in rocks. Efia Nkwanta sandstone, Elmina sandstone and Takoradi sandstone have different grain size distribution and sorting as observed in the sieve and petrographic analyses in Figure 5.1.1 and Figure 5.1.2 respectively. Whilst Efia Nkwanta beds are fine grained with a certain amount of medium and coarse grains and well sorted, Elmina sandstone is medium to coarse grained with fine grains and poorly sorted. Likewise, Takoradi sandstone is fine to medium to coarse grained and also poorly sorted.

As discussed and presented in the theoretical background in Chapter 3, particle density is determined by the degree of grain sorting in rocks. Well sorted grains have greater particle density than poorly sorted grains. The Efia Nkwanta beds are well sorted and therefore have the highest particle density than Elmina and Takoradi sandstones. The Takoradi sandstone however has a higher particle density than Elmina sandstone though it is more poorly sorted than Elmina sandstone. This is due to its greater percentage finer than that of Elmina sandstone (see Figure 5.1, Section 5.1.1). These microstructural variations in the sandstones accounted for the variations in the particle density.

5.2.3 UCS

The mean UCS of the sandstones in Efia Nkwanta beds is 46.6 MPa having a 95% confidence interval of 40.0 - 53.2 MPa. Also, the mean UCS of Elmina sandstone is 54.18 MPa having a 95% confidence interval of 46.5 - 61.9 MPa and Takoradi sandstone has a mean UCS of 35.9 MPa having a 95% confidence interval of 35.2 - 36.7 MPa. The normality tests indicated in Figure 5.9 and Figure 5.11 above however suggest that UCS in Efia Nkwanta beds and Takoradi sandstone do not follow normal distribution. This suggests that the sandstones in these lithological units are microstructurally anisotropic or errors associated during sampling and laboratory investigation.

From the ANOVA results presented in Section 5.1.7, there are significant differences in the UCS in the lithological units. Elmina sandstone has the highest UCS whilst Takoradi sandstone has the lowest UCS.

As stated in the theoretical background in Chapter 3, the strength of rocks depends on the rock anisotropy, influence of fluid pressure, and the influence of environment (temperature and moisture), time (weathering and time dependent mechanical behavior) and specimen size (Hoek, 1966). Likewise, Parterson (1978) included rock type and composition, grain size, density and porosity, rate of loading, confining stresses, geometry, shape of test specimen and testing apparatus (end effects, stiffness) as factors that affect rock strength. Bell *et al.* (1999) also stated mineral composition and constitution that is its structural and textural features affecting rock strength.

The differences in UCS in the lithological units are principally due to rock anisotropy and heterogeneity among the three units. This is due to differences in mineral and textural characteristics, density and porosity, weathering, moisture condition, fluid pressure and confining stresses. These differences are evidenced in the description of the geologic setting of the study area presented in Chapter 2 and the sieve and petrographic analyses in Section 5.1.1 and Section 5.1.2.

The results also indicated that Elmina sandstone has the highest UCS whilst Takoradi sandstone has the lowest UCS and Elmina sandstone has the lowest porosity and Takoradi sandstone has the highest porosity. This indicates that porosity and UCS may have linear association though in the reverse direction as evidenced in the correlation analysis. Microstructures (texture) and diagenesis processes may have significant effect on UCS but in the reverse direction. Decreasing grain sizes and increasing pore spaces may decrease UCS. Likewise, increasing diagenesis processes increases pore spaces which decrease UCS. Porosity which is a function of both microstructures (texture) and diagenesis affect UCS of rocks.

Likewise, particle density which is a function of the modal composition of rocks affects UCS. Rocks with greater particle density (well sorted) have greater UCS but when secondary activities occur, UCS may be affected. This is evidenced in the correlation and regression analyses presented above. This suggests that particle density has no linear association with UCS.

5.2.4 Correlation Analysis

The correlation coefficients and the hypotheses tests for the correlation coefficients were modeled using Minitab statistical software. The results of the correlation modeling are presented in Section 5.1.9. As discussed in the theoretical background in Chapter 3, the correlation coefficient is very important in engineering analyses. It gives an indication of the degree of grain sorting, pore connection and the state of the rock as dry, less saturated or saturated with fluid, and the type of fluid saturating the rock, likewise its strength implications.

Also, as presented in the theoretical background in Chapter 3, when fluid of higher dielectric constant saturates a rock, the dielectric property of the rock will increase. This decreases the elastic limit of the rock and therefore decreases the strength of the rock. Furthermore, fluids of higher dielectric constants use energy against the pore spaces and the crack surfaces of rocks resulting in a decrease in the maximum tangential stress or minimum energy density or surface energy of the pores and crack surfaces. This decreases the strength of the rock. However, when fluid of lower dielectric constant saturates a rock, the dielectric constant of the rock also decreases resulting in an increase of the surface energy in pores and crack borders and an increase in the strength of the rock. This scenario is similar to dry rocks as discussed and presented in Chapter 3. The degree of saturation, grain sorting and pore connection are however interrelated and could be hinted by the correlation coefficient.

The correlation coefficient obtained between UCS versus porosity in Efia Nkwanta beds suggests a moderate linear association between UCS and porosity in the lithological unit though in the reverse direction. The *p*-value concludes that the association between UCS and porosity in the population is linear since it is less than the α-level of significance. This further suggests that UCS is dependent on porosity in the lithological unit. As stated in the theoretical background in Chapter 3, porosity depends on both texture and secondary processes. There is therefore an influence of microstructural parameters (texture) and secondary processes (diagenesis) on UCS in Efia Nkwanta beds.

The microstructural characteristics of the Efia Nkwanta beds are their well sorted grains and well-connected pores as observed in the sieve and petrographic analyses in Section 5.1.1 and Section 5.1.2. The correlation coefficient suggests that the unconfined compressive strength in the lithological unit is dependent on the degree of grain sorting and connected pores. Thus, well connected pores have greater influence on UCS in the lithological unit. The negative coefficient however suggests that as the degree of grain sorting and pore connection increases, UCS rather decreases in the lithological unit.

The nature of pore connection in the lithological unit suggests that the sandstones are good geological targets for civil works with regards to foundations and underground excavations as saturation is less obvious but ground improvement is necessary to prevent seepage. However, in environmental mitigation such as underground waste disposal, the

transportation of hazardous chemicals or particles from waste site to neighborhoods is obvious due to the connected pores of the sandstones. These sandstones are therefore not good geological targets for underground waste disposal. Furthermore, the degree of pore connection of the lithological unit gives it demerit in dam foundation since saturation of rock is needed. Meanwhile, the lithological unit is also a good target for onshore petroleum exploration and reservoir development due to its connected porosity and enhanced mechanical stability from the petroleum products (lower dielectric constant).

The correlation coefficient obtained between UCS versus particle density in Efia Nkwanta beds rather suggests a weak linear association between UCS and particle density in the lithological unit though in the reverse direction. The *p*-value however suggests that the association between UCS and particle density in the lithological unit is not linear since it is greater than the level of significance. This further suggests that the dependence of UCS on particle density in the lithological unit is negligible. Particle density which is a measure of the modal composition of rock has little influence on UCS in the lithological unit.

The weak association between UCS and particle density in the Efia Nkwanta beds is an indication that UCS is less dependent on the degree of grain sorting in the lithological unit. Thus, the well sorted grains in the lithological unit as obtained in the *Trask coefficient* in the sieve analysis in Section 5.1.1 and petrographic analysis in Section 5.1.2 in has less influence on UCS. The negative coefficient suggests that particle density, which is a measure of the degree of grains sorting and the compressive strength are in the reverse direction. Increasing grain sorting increases particle density which increases porosity of the rocks. This result in a decrease in the compressive strength of the rocks as already discussed in the theoretical background in Chapter 3. The nature of the grains sorting in the lithological unit also suggests its suitability in foundations but not in underground waste disposal.

The correlation coefficient obtained between UCS versus porosity in Elmina sandstone suggests a weak linear association between UCS and porosity in the reverse direction. The *p*-value however suggests that there is no linear association between UCS and porosity in the lithological unit. This is an indication that the influence of porosity on UCS in the lithological unit is negligible. As stated in the theoretical background in Chapter 3, porosity depends on both texture and secondary processes.

The microstructural characteristics of the Elmina sandstones are their moderately sorted grains with subangular to angular shapes and poorly connected pores as observed in the sieve and petrographic analyses in Section 5.1.1 and Section 5.1.2. The correlation coefficient is an indication that UCS is less dependent on these microstructural characteristics of the lithological unit. Thus, poorly connected pores due to the sorting and angularity of grains have negligible influence on UCS in the lithological unit. The negative coefficient however suggests that the degree of pore connection and UCS are in the reverse direction in the lithological unit. Increasing pore connection as a result of microstructural and diagenetic changes decreases the compressive strength of the sandstones in the lithological unit.

The nature of pore connection due to sorting and angularity of grains in the lithological unit suggests that the Elmina sandstones are not good geological targets for civil works with regards to foundations and underground excavations as saturation would be eminent. However, in environmental mitigation such as underground waste disposal, the transportation of hazardous chemicals or particles from waste site to neighborhoods is less obvious. These sandstones are therefore good geological targets for underground waste disposal. Furthermore, the degree of pore connection as a result of sorting and angularity of grains of the lithological unit gives it merit in dam foundation since saturation of rock is needed but ground improvement is needed to prevent the effect of pore water pressure on the compressive strength.

The correlation coefficient obtained between UCS versus particle density in Elmina sandstone also suggests a weak linear association between UCS and particle density in the lithological unit though in the reverse direction. The *p*-value however concludes that there is no linear association between UCS and particle density in the lithological unit since it is greater than the level of significance. This further suggests that the dependence of UCS on particle density in the lithological unit is negligible. Particle density which is a measure of the modal composition of rock has little influence on UCS in the lithological unit.

The microstructural characteristics of Elmina sandstone are their moderately sorted grains with subangular to angular shape as obtained in the *Trask coefficient* in the sieve analysis in Section 5.1.1 and the petrographic analysis in Section 5.1.2. Thus, this microstructural characteristic has negligible influence on UCS in the lithological unit. The positive

coefficient suggests that the degree of sorting and the compressive strength of the lithological unit are in the same direction. There is interlocking of grains due to grain angularity and infilling of finer particles resulting in a decrease in porosity and an increase in compressive strength as sorting increases. The nature of the sorting of the lithological unit suggests its suitability in dam foundation and underground waste disposal but not in foundations.

The correlation coefficient obtained between UCS versus porosity in Takoradi sandstone indicates a very weak linear association between UCS and porosity though in the reverse direction. The *p*-value however concludes that no linear association exists between UCS and porosity in the lithological unit. This further suggests that porosity is less dependent on UCS in the lithological unit. As stated in the above discussions, porosity depends on both texture and secondary processes suggesting that there is negligible influence of microstructural parameters (texture) and secondary processes (diagenesis) on UCS in the Takoradi sandstone.

The Takoradi sandstone is poorly sorted with subangular to angular shape with poorly connected pores as observed in the sieve and petrographic analyses in Section 5.1.1 and Section 5.1.2. Thus, poorly connected pores have negligible influence on UCS in the lithological unit. The negative coefficient however suggests that the degree of pore connection and UCS are in the reverse direction in the lithological unit. Increasing pore connection as a result of microstructural and diagenetic changes decreases the compressive strength of the sandstones in the lithological unit.

The nature of pore connection in the lithological unit suggests that the sandstones are good geological targets for civil works with regards to foundations and underground excavations but for its microstructural anisotropy due to microcracks as observed in the petrographic analysis in Section 5.1.2c. Also, in environmental mitigation such as underground waste disposal, the transportation of hazardous chemicals or particles from waste site to neighborhoods is less obvious but for its microstructural anisotropy. These sandstones are therefore not good geological targets for underground waste disposal. Furthermore, the degree of pore connection in the lithological unit gives it merit in dam foundation since saturation of rock is needed but for its microstructural anisotropy. The

lithological unit is therefore not recommended for any engineering project; accept using any ground improvement methods such as grouting.

The correlation coefficient between UCS and particle density obtained in Takoradi sandstone suggests a weak linear association between UCS and particle density in the lithological unit. The *p*-value however concludes that no linear association exists between UCS and particle density in the lithological unit. The dependence of UCS on particle density in the unit is also negligible. Particle density which is a measure of modal composition of rocks has negligible influence on UCS in the lithological unit.

The weak association further suggests that the poorly sorted grains, as observed in the sieve and petrographic analyses in Section 5.1.1 and Section 5.1.2 respectively, have negligible influence on UCS. The positive coefficient rather suggests that increasing particle density (increasing sorting) increases the compressive strength of the sandstones in the lithological unit. However, increasing grain sorting increases porosity which decreases the compressive strength of sandstones. But due to the grain angularity and infilling of finer particles rather decreases porosity with sorting and increases compressive strength of the sandstones in the lithological unit.

5.2.5 Regression Analysis

Simple and multiple regression modeling were carried out using Minitab 16 programmable language. The significant relationships obtained in the simple regression models were however used in the multiple regression modeling. The purpose for the multiple regression modeling is presented in Chapter 4.

The fitted Equation that describes the relationship between UCS and porosity in the simple regression model in Efia Nkwanta beds is UCS = 65.5 - 1.35 υ with *R* square of 12.3% and a *p*-value of 0.04. 12.3% of the variation of UCS could be accounted for by porosity in the sandstones in Efia Nkwanta beds. The *p*-value however concludes that the relationship between UCS and porosity in the lithological unit is significant. Likewise, the fitted Equation that describes the relationship between UCS and particle density in the simple regression model in Efia Nkwanta beds is UCS = 99.1 - 19.3 ρ with *R* square of 3.8% and

a *p*-value of 0.3. 3.8% of the variation of UCS could be accounted for by particle density in Efia Nkwanta beds. The *p*-value however indicates that the relationship is insignificant in the lithological unit. Also, the *p*-value for the porosity term in the multiple regression model (UCS = 126 - 1.4 υ - 21.8 ρ) indicates a significant relation with UCS whereas the particle density term indicates an insignificant relation with UCS in the lithological unit (see Table 5.10, Section 5.1.10).

The models in the Efia Nkwanta lithological unit suggest that well connected pores, which are controlled by both texture and diagenesis has a significant effect on UCS. However, particle density which is controlled by the degree of grain sorting has an insignificant effect on UCS. This further indicates that UCS is predominantly dependent on the degree of pore connection but less dependent on the degree of grain sorting. This scenario is empirically observed in the multiple regression model where the *p*-value in the porosity term is less than the level of significance whereas that of the particle density term is greater than the level of significance. The relations therefore suggest that the effect of porosity on UCS is greater than that of particle density. When both mechanical and geochemical activities in the lithological unit are changed, the compressive strength of the rocks would be affected in a greater extent affecting it mechanical stability. Thus, increasing grain sorting and increasing pore connection decreases UCS in the lithological unit.

The fitted Equation that describes the relationship between UCS and porosity in the simple regression model in Elmina sandstone is UCS = 61.1 - 0.8 υ with *R* square of 0.4% and a *p*-value of 0.7. 0.4% of the variation of UCS could be accounted for by porosity in the lithological unit. The *p*-value however concludes that the relationship is insignificant in the unit. Likewise, the fitted Equation that describes the relationship between UCS and particle density in the simple regression model in Elmina sandstone is UCS = - 31.7 + 34.3 ρ with *R* square of 9.3% and a *p*-value of 0.07. 9.3% of the variation of UCS could be accounted for by particle density in the lithological unit. The *p*-value also concludes that the relationship is insignificant in the lithological unit.

The microstructural characteristics of the Elmina sandstones are their moderately sorted grains with subangular to angular shape and poorly connected pores as observed in the sieve and petrographic analyses in Sections 5.1.1 and 5.1.2 respectively. The models

suggest that microstructural characteristics of this nature have negligible influence on UCS. Thus, poorly connected pores and moderately sorted grains which are depend on both texture and diagenesis have negligible effect on UCS in the lithological unit. This indicates that UCS is dependent on the degree of pore connection. Though the grains in the lithology are moderately sorted, the subangular to angular particles decrease the connected pores. This decrease in the connected pores resulted in its insignificant effect on UCS in the lithology which is observed in the models. The models moreover suggest that increasing porosity decreases UCS however, increasing particle density increases UCS. Thus, for sandstones with subangular to angular grains, increasing grain sorting decreases porosity due to interlocking of grains. This phenomenon increases UCS as observed in the models.

The fitted Equation that describes the relationship between UCS and porosity in the simple regression model in Takoradi sandstone is UCS = 36.5 - 0.03 υ with R square of 0.3% and a p-value of 0.8. 0.3% of the variation of UCS could only be accounted for by porosity in the sandstones in the lithological unit. The p-value however concludes that the relationship is insignificant in the lithological unit. Likewise, the fitted Equation that describes the relationship between UCS and particle density in the simple regression model in Takoradi sandstone is UCS = 33.3 + 1.1 ρ with R square of 0.6% and a p-value of 0.6. 0.6% of the variation of UCS could only be accounted for by particle density in the lithological unit. The p-value however concludes that the relationship does not exist in the lithological unit.

The insignificant relationships obtained between UCS and porosity and that of particle density are due to the microstructural characteristics of the lithology. The microstructural characteristics of the Takoradi sandstones are its poorly sorted grains with subangular to angular shape and poorly connected pores as observed in the sieve and petrographic analyses in Sections 5.1.1 and 5.1.2 respectively. As presented in the previous discussions, UCS is highly dependent on connected porosity which is due to connected pores. The greater the connected pores, the greater its effect on UCS. The poorly sorted grains in the lithology with subangular to angular shape have poorly connected pores which have less influence on UCS. This influence resulted in the insignificant relations obtained in the models above. The models moreover suggest that increasing porosity decreases UCS however, increasing particle density increases UCS. Thus, for sandstones with subangular to angular grains, increasing grain sorting decreases porosity due to interlocking of grains

which increases UCS. Hence, particle shape has significant influence on UCS than grain sorting.

CHAPTER 6

CONCLUSSIONS AND RECCOMMENDATIONS

6.1 Conclusions

Three sandstone lithological units were selected for the study in the Sekondian Group: Efia Nkwanta beds, Elmina sandstone and Takoradi sandstone. Fresh samples were obtained for investigations of porosity, particle density and UCS in the lithological units. Correlation analyses were performed for porosity and particle density as against UCS. Also, regression analyses were performed for porosity and particle density as against UCS. The study therefore concludes that:

- Linear association only exists between UCS and porosity in sandstones with well sorted grains and connected pores. The association between UCS and particle density is nonlinear.
- UCS is predominantly dependent on the degree of pore connectivity.
- Increasing the degree of pore connectivity decreases UCS in sandstones.
- Particles shape has significant influence on UCS than particles sorting.
- A significant relationship only exists between UCS and porosity for sandstones with well-connected pores. However, an insignificant relationship exists between UCS and particle density.
- The prediction of geomechanical and petrophysical properties of the Sekondian Group is only possible for UCS and porosity for sandstones with well sorted grains and connected pores.

6.2 Recommendations

From the study, it is recommended that:

- Large sample size should be used to investigate the relationship between geomechanical and petrophysical properties of the Sekondian Group.
- Analytical tool should be used to investigate the relationship between geomechanical and petrophysical properties of the Sekondian Group.

REFERENCES

Al-hassan, S. (2017), "Unpublished MSc Lecture Notes: Statistical Models", *Testing of Hypothesis and Significance*, University of Mines and Technology, Tarkwa, Ghana, pp. 1-17.

Al-hassan, S. (2017), "Unpublished MSc Lecture Notes: Statistical Models", *Analysis of Variance (ANOVA)*, University of Mines and Technology, Tarkwa, Ghana, pp. 1-22.

Al-hassan, S. (2017), "Unpublished MSc Lecture Notes: Statistical Models", *Estimation Theory,* University of Mines and Technology, Tarkwa, Ghana, pp. 1-12.

Al-Homadhi, E.S. and Hamada, G.M. (2001), "Determination of Petrophysical and Mechanical Property Interrelationships for Simulated Sandstone Rocks", *Proceedings of the 6th Nordic Symposium on Petrophysics*, Trondheim, Norway, pp. 1-3.

Al-Maamori, H.M.S., El Naggar, M.H. and Micic, S. (2014), "A Compilation of the Geo-Mechanical Properties of Rocks in Southern Ontario and the Neighboring Regions", *Open Journal of Geology*, Scientific Research Publishing Inc., Canada, Vol. 4, pp. 210-227.

Anon (1979), "Suggested Methods for Determining the Uniaxial Compressive Strength and Deformability of Rock Materials", *Int. J. Rock Mech Min Sci Geomech*., www.methods-for-determining-unixial-compressive-strength, Vol. 16, No. 2, pp. 135-140. Accessed: June, 2017.

Anon (1985), "Suggested Method for Determining Point Load Strength", *Int. J. Rock Mech. Min. Sci. and Geomech*, www.methods-for-determining-point-load-strength, Vol. 22, No. 2, pp. 51–60. Accessed: June, 2017.

Anon (1999), "Draft ISRM Suggested Method for the Complete Stress-Strain Curve for Intact Rock in Uniaxial Compression", *Int J Rock Mech Min Sci*., www.methods-for-stress-strain-curve, Vol. 36, No. 3, pp. 279-289. Accessed: July, 2017.

Anon (2007), "Standard Test Method for Determination of the Point Load Strength Index of Rock and Application to Rock Strength Classifications", *ASTM International,* United State, www.point-load-standard-test.com, pp. 1-10. Accessed: August, 2017.

Anon (2010), "2010 Population and Housing Census District Analytical Report", *Secondi-Takoradi Metropolitan*, Ghana Statistical Service, www.statsghana.gov.gh, pp. 1-3. Accessed: July 16, 2017.

Anon (2015), "Experimental Design and Analysis" *Chapter 3: Simple Linear Regression Analysis*, ReliaSoft Corporation, http://Reliawiki.org/index/phd/simplelinear, pp. 23-48.

Anon (2017),"Laboratory Cutting Saws and Coring Machines", http://www.controls-group.com/eng/aggregates-testing-equipment/laboratory-crusher.php, pp.169. Accessed: November, 2017.

Anon (2017),"Minitab 16", www.minitab.com, pp. 1-5. Accessed: July 4, 2017.

Anon (2017),"Working Principle of an Electron Microscope with a Diagram", www.yourarticlelibrary.com/microeconomics/working-principle-of-a-electron-microscopes-with-diagram, pp. 1-2. Accessed: June 28, 2017.

Aryal, K.P. (2006), *Slope Stability Evaluations by Limit Equilibrium and Finite Element Method*, Doctoral Thesis at NTNU 2006: 66, Norwegian University of Science and Technology, Trondheim, Norway, 1 p.

Asef, M. R. and Farrokhrouz, M. (2010), "Governing Parameters for Approximation of Carbonates UCS", *Electronic Journal of Geotechnical Engineering*, Vol. 15, Bund. N. pp. 1581-1592.

Asiedu, D.K., Atta-Peters, D., Hegner, E., Rocholl, A. and Shibata, T. (2010), "Palaeoclimatic Control on the Composition of Palaeozoic Shales from Southern Ghana, West Africa", *Ghana Mining Journal*, Vol. 12, pp. 7-16.

Asiedu, D.K., Hegner, E., Rocholl, A., and Atta Peters, D. (2005), "Provenance of Late Ordovician to Early Cretaceous sedimentary rocks from southern Ghana, as inferred from Nd isotopes and trace elements", *Journal African Earth Science*, Vol. 41, pp. 316–328.

Atubrah P. (2017), *Unpublished Geologic Report on the Sekondian Series at Sekondi-Takoradi in the Western Region*. Atta-Peters, D., Asiedu, D.K. and Sakyi, P.A. (eds.), Department of Earth Science, University of Ghana, 32 pp.

Azizi, V. and Memarian, H. (2006), "Estimation of Geomechanical Parameters of Reservoir Rocks Using Conventional Porosity Log", *Conference Paper*, School of Mining Engineering, University of Tehran, Iran, pp. 1-6.

Backers, T. (2013), "Borehole Geomechanics", *IGA Academy Report* 103, Potsdam, Germany, pp 1-5.

Ballivy, G. and Colin, J.C. (1999), "Stockage Souterrain: Influence de la Nature du Fluide Sur les Propriétés Mécaniques de la Roche en Paroi", *9th Int. Cong. On Rock Mech. Paris*, Vol. 2, pp. 563-567.

Benz, T. and Schwab, R. (2008), "A Quantitative Comparison of Six Rock Failure Criteria", *International Journal of Rock Mechanics and Mining Sciences*, Vol. 45 No. 7, pp. 1176-1186.

Bieniawski, Z.T. (1974), "Estimating the Strength of Rock Materials", *A Journal of the South African Institute of Mining and Metallurgy*, Vol. 74, pp. 312-319.

Brady, B.H.G. and Brown, E.T. (2005), *Rock Mechanics for Underground Mining*, Kluwer Academic Publishers, New York, 3rd ed., pp. 85-161.

Briševac, Z., Hrženjak, P. and Buljan, R. (2016), *Models for Estimating Uniaxial Compressive Strength and Elastic Modulus*, Građevinar, Vol. 1, pp. 1-22.

Broch, E. and Franklin, J.A. (1972), "The Point Load Strength Test", *Int. J. Rock Mech. Min. Sci.*, Vol. 9 No. 6, pp. 669–97.

Busch, A., Schweinar, K., Kampman, N., Coorn, A., Pipich, V., Feoktystov, A., Leu, L., Amann-Hildenbrand, A., and Bertier, P. (2017). "Determining the Porosity of Mudrocks Using Methodological Pluralism". *Geological Society of London,* Rutter, E.H., Mecklenburgh, J. and Taylor, K.G. (eds.), Vol. 454. pp. 15-38.

Camp, H., Irvine, M., De Jong, A., Armah, A. and Andorful, A. (2012), "Scoping Report and Terms of Reference", *Tweneboa, Enyenra, Ntomme (T.E.N) Development*, Tullow Ghana Limited, pp. 2-24.

Chatterjee, R. and Mukhopadhyay, M. (2002), "Petrophysical and Geomechanical Properties of Rocks from the Oil Fields of Krishna-Godavari and Cauvery Basins", *Bulletins of Engineering Geology and Environment*, Vol. 61, pp. 169-178.

Chatterjee, R., Manoharan, K. and Mukhopadhyay, M. (2013), "Petrophysical and Mechanical Properties of Cretaceous Sedimentary Rocks of Cauvery Basin, Eastern Continental Margin of India", *Journal of India Geophysics Union,* Vol. 17 No. 4, pp. 349-359.

Cook, J. (2015), "Geomechanics", *Oil Field Review*, Schlumberger, 2 pp.

Daneshy, A. (2017), "Mechanics of Rock Failure" *unpublished Oil and Gas Operations and Formation Failure*, Daneshy Consultants International, 13 pp.

Dewhurst, D.N., Aplin, A.C. and Sarda, J.P. (1999), "Influence of Clay Fraction on Pore-Scale Properties and Hydraulic Conductivity of Experimentally Compacted Mudstones", *Journal of Geophysical Research,* Vol. 104, pp. 29 261–29 274.

Esmailzadeh, A., Behnam, S., Mikaeil, R, Naghadehi, M.Z. and Saei, S (2017), "Relationship between Texture and Uniaxial Compressive Strength of Rocks", *Civil Engineering Journal*, Vol. 3, No. 7, p. 480.

Glover, P.W.J. (2017), *Petrophysics MSC Course Notes*, School of Earth and Environment, University of Leeds, UK, Unpublished, 20 pp.

Griffith, A.A. (1921), "The Phenomena of Rupture and Flow in Solids", *Phil. Trans Roy. Soc.*, Vol. A221, pp. 163–97.

Hawkes, I. and Mellor, M. (1970), "Uniaxial Testing in Rock Mechanics Laboratories", *Engineering Geol*ogy, Vol. 4, No. 3, pp. 177–285.

Hoek, E. (1966), "Rock Mechanics - An Introduction for the Practical Engineer Part I", *Mining Magazine*, Imperial College of Science and Technology, London, pp. 1-13.

Hoek, E. and Brown, E.T. (1988), "The Hoek-Brown Criterion – A 1988 Update", *Proc. 15th Can. Rock Mech. Symp.*, University of Toronto, pp. 31–38.

Hsu, S.C. and Nelson, P. (1993), "Characterization of Cretaceous Clay-Shales in North America", *Geotechnical Engineering of Hard Soils and Soft Rocks*, Balkema, pp 139-146.

Kesse, G.O., (1985), "The Mineral and Rock Resources of Ghana", *the Coastal Sedimentary Basins,* A.A. Balkema, Rotterdam/Boston, pp. 50-62.

Larsen, P.V. (2008) "Master of Applied Statistics", *ST111: Unpublished Regression and Analysis of Variance,* 13 pp.

Lashkaripour, G.R. (2016), "Predicting Mechanical Properties of Mudrock from Index Parameters", *Bulletin of Engineering Geology and the Environment*. Briševac, Z., Hrženjak, P., Buljan, R. (eds.), Vol. 1, p. 21.

Liang, W., Yang, C., Zhao, Y., Dusseault, M.B. and Liu, J. (2007), "Experimental Investigation of Mechanical Properties of Bedded Salt Rock", *International Journal of Rock Mechanics and Mining Sciences*, Vol. 44, No. 3, pp. 400-411.

Lucia, F.J. (2007), "Chapter 1, Petrophysical Rock Properties", *Carbonate Reservoir Characterization, an Integrated Approach*, Springer Publications, 26 pp.

Palchik, V. (2016), "Influence of Porosity and Elastic Modulus on Uniaxial Compressive Strength in Soft Brittle Porous Sandstones", *Rock Mechanics and Rock Engineering*. Briševac, Z., Hrženjak, P. and Buljan, R. (eds.), Vol. 1, p 21.

Paterson, M.S. (1978), *Experimental Rock Deformation,* the Brittle Field, Springer Verlag.

Rajabzadeh, M.A., Moosavinasab, Z. and Rakhshandehroo, G. (2012) "Effects of Rock Classes and Porosity on the Relation between Uniaxial Compressive Strength and Some Rock Properties for Carbonate Rocks", *Article in Rock Mechanics and Rock Engineering,* Vol. 45, pp. 113–122.

Rashid, F, Glover, P.W.J., Lorinczi, P, Collier, R., Lawrence, J. (2015),"Porosity and Permeability of Tight Carbonate Reservoir Rocks in the North of Iraq", *Journal of Petroleum Science and Engineering*, Vol. 133, pp. 147 - 161.

Rashid, F., Glover, P.W.J., Lorinczi, P., Hussein, D., Lawrence, J.A. (2017), "Microstructural Controls on Reservoir Quality in Tight Oil Carbonate Reservoir Rocks", *Journal of Petroleum Science and Engineering,* Vol. 156, pp. 814-826.

Romana, M. and Vásárhelyi, B. (2007), "Discussion on the Decrease of Unconfined Compressive Strength between Saturated and Dry Rock Samples", *Proceedings of 11th congress of the International Society of Rock Mechanics,* Vol. 1, pp. 139-142.

Ross, S.M. (2009), *Introduction to Probability and Statistics for Engineers and Scientists*, Elsevier publishers, California, Berkeley, 4th edition, 647 pp.

Ruther, E., Mecklenburgh, J. and Taylor, K. (2017), "Geomechanical and Petrophysical Properties of Mudstone, Introduction", *Geological Society of London*, Vol. 454, pp. 1-13.

Rybacki, E., Meier, T. and Dresen, G. (2016), "What Controls the Mechanical Properties of Shale Rocks? – Part II: Brittleness", *Journal of Petroleum Science and Engineering*, Vol. 144, pp. 39–58.

Rybacki, E.*,* Reinicke, A.*,* Meier, T.*,* Makasi, M. *and* Dresen, G. *(*2015*), "*What Controls the Mechanical Properties of Shale Rocks? – Part I: Strength and Young's Modulus", *Journal of Petroleum Science and Engineering, Vol.* 135*, pp.* 702–722.

Schieber, J.*,* Southard, J.B.*,* Kissling, P.*,* Rossman, B. *and* Ginsburg, R. *(*2013*), "*Experimental Deposition of Carbonate Mud from Moving Suspensions: Importance of Flocculation and Implications for Modern and Ancient Carbonate Mud Deposition", *Journal of Sedimentary Research, Vol.* 83*, pp.* 1026–1032.

Schon, J. H. (2011), *Hand Book of Petroleum Exploration and Production*, Elsevier Publication, Vol. 8, pp. 245-271.

Seemann, T.*,* Bertier, P.*,* Krooss, B.M. *and* Stanjek, H. (2017), "Water Vapour Adsorption on Mudrocks", *Geological Society of London.* Rutter, E.H.*,* Mecklenburgh, J. and Taylor, K.G. (eds.)*.* Vol. 454, pp. 1-13.

Sun, W., Wang, L. and Wang, Y. (2017), "Mechanical Properties of Rock materials with Related to Mineralogical Characteristics and Grain Size through Experimental Investigation: a Comprehensive Review", Higher Education Press and Springer-Verlag Berlin Heidelberg, *Front. Struct. Civ. Eng,* Vol. 11, No. 3, pp 322–328.

Tugrul, A. (2016), "The Effect of Weathering on Pore Geometry and Compressive Strength of Selected Rock Types from Turkey", *Engineering Geology*. Briševac, Z., Hrženjak, P. and Buljan, R. (eds.), Građevinar Vol. 1, p. 21.

Vásárhely, B. and Bobet, A. (2000), "Modeling of crack initiation, propagation and coalescence in unconfined compression", *Rock Mech. Rock Eng*, Vol. 33, No. 2, pp. 119-139.

Vásárhely, B. and Ledniczky, K. (1999), "Influence of Water Saturation and Weathering on Mechanical Properties of Sivac Marble", *9th Int. Cong. On Rock Mech. Paris*. Vol. 2, pp. 691-693.

Vutukuri, V.S. (1974), "The Effects of Liquids on the Tensile Strength of Limestone" *International Journal of Rock Mechanics and Mining Science*, Vol. 11, pp. 27-29.

Walpole, R.E, Myers, R.H., Myers, S. L.and Ye, K. (2012), *Probability and Statistics for Engineers and Scientists*, Pearson Education Inc., Boston , 9th Edition, 785 pp.

Wawersik, W.R. and Fairhurst, C. (1970), "A Study of Brittle Rock Fracture in Laboratory Compression Experiments", *Int. J. Rock Mech. Min. Sci.*, Vol. 7, No. 5, pp. 561–750.

Wilson, M .J., Wilson, L. and Shaldybin, M. V. (2017), "The Importance of Illitic Minerals in Shale Instability and in Unconventional Hydrocarbon Reservoir", *Geological Society of London*. Rutter, E. H., Mecklenburgh, J. and Taylor, K.G. (eds.), Vol. 454, pp. 1-13.

Xu, H., Zhou, W., Xie, R., Da, L., Xiao, C., Shan, Y. and Zhang, H. (2016), "Characterization of Rock Mechanical Properties Using Lab Tests and Numerical Interpretation Model of Well Logs", *Mathematical Problems in Engineering*, Hindawi Publishing Corporation, Vol. 2016, No. 5967159, 12 pp.

Yang, Y. and Aplin, A.C. (2007), "Permeability and Petrophysical Properties of 30 Natural Mudstones", *Journal of Geophysical Research*, Vol. 112, No. B03206, pp. 1-13.

Yendaw, J.A. (2012), *Unpublished Lecture Notes: Geology of Ghana*, University of Mines and Technology, Tarkwa, Ghana, pp. 10-13.

APPENDICES

APPENDIX A

APPENDIX A1: Porosity Measurements in Efia Nkwanta Beds, Elmina Sandstone and Takoradi Sandstone

ESSIPON		ABOADZE		MONKEYHILL	
Sample ID	Porosity %	Sample ID	Porosity %	Sample ID	Porosity %
ES1	12.03	AB1	8.87	MH1	21.46
ES2	14.50	AB2	7.96	MH2	13.91
ES3	5.62	AB3	8.19	MH3	11.75
ES4	6.67	AB4	10.15	MH4	15.17
ES5	12.31	AB5	12.83	MH5	14.47
ES6	7.23	AB6	6.00	MH6	12.38
ES7	10.29	AB7	10.87	MH7	14.06
ES8	24.78	AB8	10.68	MH8	13.01
ES9	17.84	AB9	7.78	MH9	20.35
ES10	15.45	AB10	6.18	MH10	19.13
ES11	14.53	AB11	11.23	MH11	16.68
ES12	8.11	AB12	8.73	MH12	13.01
ES13	11.22	AB13	6.50	MH13	9.57
ES14	11.80	AB14	7.76	MH14	15.91
ES15	23.15	AB15	5.21	MH15	20.13
ES16	10.82	AB16	10.71	MH16	11.35
ES17	12.31	AB17	9.71	MH17	10.70
ES18	11.76	AB18	7.46	MH18	22.32
ES19	20.47	AB19	8.08	MH19	24.06
ES20	20.32	AB20	9.58	MH20	14.60
ES21	17.69	AB21	8.00	MH21	14.37
ES22	7.56	AB22	7.55	MH22	16.82
ES23	11.73	AB23	6.73	MH23	13.00
ES24	19.68	AB24	7.02	MH24	16.72
ES25	9.80	AB25	4.29	MH25	14.32
ES26	17.68	AB26	8.37	MH26	12.74
ES27	10.23	AB27	9.32	MH27	8.28
ES28	13.23	AB28	9.85	MH28	17.35
ES29	13.78	AB29	5.43	MH29	20.30
ES30	24.15	AB30	7.75	MH30	16.70
ES31	10.31	AB31	10.03	MH31	15.56
ES32	18.06	AB32	7.71	MH32	17.05

ES33	15.92	AB33	7.92	MH33	19.81
ES34	15.07	AB34	9.05	MH34	19.03
ES35	19.82	AB35	7.13	MH35	14.81
ES36	8.33	AB36	8.47	MH36	12.09

APPENDIX A2: Particle Density Measurements in Efia Nkwanta Sandstones, Elmina Sandstones and Takoradi Sandstone

EFIA NKWANTA BEDS		ELMINA SANDSTONE		TAKORADI SANDSTONE	
Sample ID	**Particle Density g/cm^3**	**Sample ID**	**Particle Density g/cm^3**	**Sample ID**	**Particle Density g/cm^3**
ES1	2.53	AB1	2.51	MH1	2.67
ES2	2.44	AB2	2.32	MH2	2.56
ES3	2.67	AB3	2.26	MH3	2.67
ES4	2.50	AB4	2.42	MH4	2.56
ES5	2.99	AB5	2.53	MH5	2.50
ES6	2.67	AB6	2.63	MH6	2.60
ES7	2.60	AB7	2.41	MH7	2.50
ES8	2.78	AB8	2.69	MH8	2.63
ES9	3.03	AB9	2.51	MH9	2.33
ES10	2.99	AB10	2.84	MH10	2.50
ES11	2.38	AB11	2.85	MH11	2.64
ES12	2.90	AB12	2.66	MH12	2.74
ES13	2.64	AB13	2.57	MH13	2.60
ES14	2.86	AB14	2.51	MH14	2.41
ES15	2.37	AB15	2.43	MH15	2.38
ES16	2.53	AB16	2.41	MH16	2.69
ES17	2.97	AB17	2.41	MH17	2.67
ES18	2.81	AB18	2.55	MH18	2.21
ES19	2.69	AB19	2.69	MH19	2.47
ES20	2.98	AB20	2.61	MH20	2.55
ES21	2.66	AB21	2.27	MH21	2.54
ES22	3.08	AB22	2.47	MH22	2.49
ES23	2.35	AB23	2.13	MH23	2.72
ES24	2.64	AB24	2.21	MH24	2.64
ES25	2.81	AB25	2.32	MH25	2.37
ES26	2.71	AB26	2.50	MH26	2.28
ES27	2.79	AB27	2.59	MH27	2.64
ES28	2.51	AB28	2.71	MH28	2.61
ES29	2.68	AB29	2.93	MH29	2.85
ES30	2.77	AB30	2.64	MH30	2.44
ES31	2.94	AB31	2.55	MH31	2.69
ES32	2.75	AB32	2.41	MH32	2.88

ES33	2.79	AB33	2.83	MH33	2.37
ES34	2.83	AB34	2.09	MH34	2.19
ES35	2.62	AB35	2.19	MH35	2.76
ES36	2.89	AB36	2.47	MH36	2.66

APPENDIX A3: UCS Measurements in Efia Nkwanta Sandstones, Elmina Sandstones and Takoradi Sandstone

EFIA NKWANTA BEDS		ELMINA SANDSTONE		TAKORADI SANDSTONE	
Sample ID	UCS/MPa	Sample ID	UCS/MPa	Sample ID	UCS/MPa
ES1	32.58	AB1	24.88	MH1	37.23
ES2	36.83	AB2	40.02	MH2	39.21
ES3	87.27	AB3	33.62	MH3	36.41
ES4	78.34	AB4	32.01	MH4	36.06
ES5	26.82	AB5	43.22	MH5	36.78
ES6	68.40	AB6	102.40	MH6	34.82
ES7	40.10	AB7	51.27	MH7	36.54
ES8	20.68	AB8	62.13	MH8	35.32
ES9	20.78	AB9	76.80	MH9	33.02
ES10	41.66	AB10	77.65	MH10	33.64
ES11	35.19	AB11	77.29	MH11	39.09
ES12	75.56	AB12	58.21	MH12	37.10
ES13	87.78	AB13	33.00	MH13	37.21
ES14	39.82	AB14	53.24	MH14	35.11
ES15	31.24	AB15	34.86	MH15	36.80
ES16	45.47	AB16	66.53	MH16	34.59
ES17	56.74	AB17	94.18	MH17	31.64
ES18	57.40	AB18	33.52	MH18	36.30
ES19	28.03	AB19	66.05	MH19	35.25
ES20	57.43	AB20	90.45	MH20	37.47
ES21	32.24	AB21	46.71	MH21	35.00
ES22	26.33	AB22	42.64	MH22	37.93
ES23	64.17	AB23	42.39	MH23	35.79
ES24	70.36	AB24	39.51	MH24	37.14
ES25	16.35	AB25	72.55	MH25	35.29
ES26	45.85	AB26	12.22	MH26	37.11
ES27	35.54	AB27	64.91	MH27	37.38
ES28	58.27	AB28	26.61	MH28	37.31
ES29	31.93	AB29	64.76	MH29	37.15
ES30	33.68	AB30	25.17	MH30	39.96
ES31	55.12	AB31	31.92	MH31	30.41
ES32	29.45	AB32	64.45	MH32	33.56
ES33	62.05	AB33	82.14	MH33	37.12

ES34	40.44	AB34	30.67	MH34	30.28
ES35	71.03	AB35	63.27	MH35	36.87
ES36	36.72	AB36	89.11	MH36	36.33